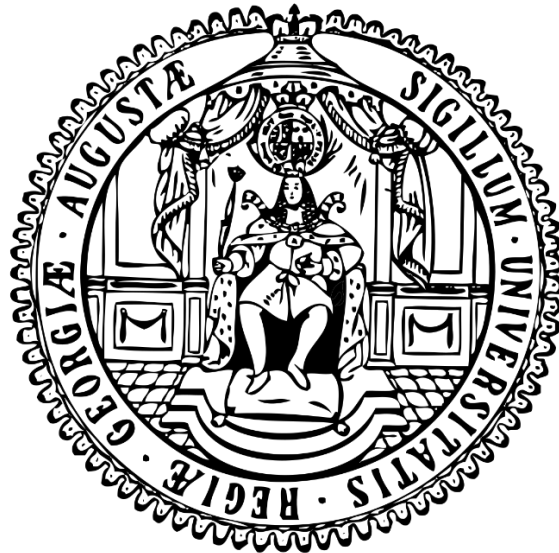


# The importance of homotypic interactions of unphosphorylated STAT proteins in cytokine-induced signal transduction



Dissertation

for the award of the degree

“Doctor rerum naturalium” (Dr. rer. nat.)

of the Georg-August-Universität Göttingen

within the doctoral program “Molecular Medicine”

of the Georg-August University School of Science (GAUSS)

submitted by

**Priyanka Rajeev Menon**

born in Vadodara, India

Göttingen, 2021

## **Members of the Thesis Committee**

### **Prof. Dr. mult. Thomas Meyer (1st Reviewer)**

Department of Psychosomatic Medicine and Psychotherapy, University Medical Center  
Göttingen

### **Prof. Dr. Oliver Wirths (2nd Reviewer)**

Department of Psychiatry and Psychotherapy, University Medical Center Göttingen

### **Prof. Dr. Carsten Lüder**

Department of Medical Microbiology, University Medical Center Göttingen

## **Members of the Examination Board**

### **Prof. Dr. Susanne Lutz**

Institute of Pharmacology and Toxicology, University Medical Center Göttingen

### **Prof. Dr. Frauke Alves**

Department of Hematology and Medical Oncology, University Medical Center Göttingen,  
Max-Planck-Institute of Experimental Medicine

### **Prof. Dr. Dieter Kube**

Department of Hematology and Medical Oncology, University Medical Center Göttingen

**Date of Disputation: 25-02-2021**

# **AFFIDAVIT**

Here I declare that my doctoral thesis entitled

**“The importance of homotypic interactions of unphosphorylated STAT proteins in cytokine-induced signal transduction”** has been written independently with no other sources and aids than quoted.

Priyanka Rajeev Menon

Göttingen, January 2021

---

## Table of Contents

List of Abbreviations .....	4
Amino acids .....	7
Acknowledgements.....	8
Abstract.....	10
1. Introduction.....	12
1.1 STATs and the JAK-STAT pathway .....	12
1.2 JAK-STAT signalling in disease.....	18
1.3 Biology of STAT1.....	20
1.4 Biology of STAT3.....	24
1.5 Crosstalk between STAT1 and STAT3.....	28
1.6 Objectives.....	31
2. Materials and Methods.....	33
2.1 Materials.....	33
2.1.1 Cell lines .....	33
2.1.2 Chemicals and reagents .....	33
2.1.3 Culture media.....	36
2.1.4 Kits.....	36
2.1.5 Equipment.....	37
2.1.6 Disposables .....	38
2.1.7 Water.....	38
2.1.8 Sterilization of material .....	39
2.1.9 Oligonucleotides and primers .....	39
2.1.10 Enzymes and recombinant proteins .....	42
2.1.11 Antibodies.....	43
2.1.12 Plasmids and constructs .....	44
2.1.13 Bacterial strains and media .....	47
2.2 Methods.....	48
2.2.1 Cell culture.....	48
2.2.1.1 Cultivation of mammalian cells .....	48
2.2.1.2 Transfection .....	49
2.2.1.3 Stimulation of cells with cytokines and inhibitors.....	49
2.2.2 Molecular biology methods .....	49
2.2.2.1 Mutagenesis .....	49
2.2.2.2 Production of chemically competent bacteria.....	50

---

2.2.2.3 Transformation of plasmid DNA into competent bacteria .....	50
2.2.2.4 Isolation of plasmid DNA from bacteria .....	50
2.2.2.5 Sequencing .....	51
2.2.2.6 Determination of the concentration of DNA .....	51
2.2.2.7 Production of cell extracts .....	51
2.2.2.8 SDS polyacrylamide gel electrophoresis (SDS-PAGE) .....	52
2.2.2.9 Western blot and immunochemical protein detection .....	53
2.2.2.10 Immunocytochemistry and fluorescence microscopy.....	53
2.2.2.11 Reporter gene assay .....	54
2.2.2.12 Dephosphorylation assay .....	55
2.2.2.13 <i>In vitro</i> phosphorylation assay .....	56
2.2.2.14 Gel retardation experiments (Electrophoretic Mobility Shift Assay, EMSA) .....	56
2.2.2.15 RNA isolation .....	57
2.2.2.16 cDNA synthesis .....	58
2.2.2.17 Real-time PCR .....	58
2.2.3 Statistics .....	58
3. Results.....	60
3.1 The relevance of the anti-parallel, unphosphorylated dimer interface in STAT3.....	60
3.1.1 Identification of potentially destabilizing mutations in the NTD and CCD of STAT3 .....	60
3.1.2 Prominent nuclear localization of STAT3-V77A and STAT3-F174A mutants.....	61
3.1.3 Both STAT3 mutants show elevated levels of phosphorylation.....	68
3.1.4 STAT3-V77A and -F174A show increased fractions of DNA-bound molecules with unaltered specificity to DNA .....	72
3.1.5 STAT3 mutants show increased reporter activity and differential transcriptional response .....	74
3.1.6 STAT3 mutants show unaltered kinetics of <i>in vitro</i> phosphorylation and dephosphorylation.....	78
3.1.7 DNA binding influences the dephosphorylation kinetics of STAT3-F174A .....	80
3.2 The impact of unphosphorylated STAT1 on the activities of canonical JAK-STAT1 signalling .....	83
3.2.1 Identification of mutations that disrupt phosphorylation and dimerization of STAT1 .....	83
3.2.2 Cytoplasmic retention and unobservable phosphorylation of co-expressed WT in IFN $\gamma$ -stimulated cells expressing R602L/Y701F-GFP .....	84
3.2.3 Disruption of parallel and anti-parallel interactions in mutant STAT1 did not rescue the invisibility of co-expressed, phosphorylated WT .....	86

---

---

3.2.4 STAT1 mutants do not affect activation-inactivation of co-expressed WT, but impair the visibility of tyrosine-phosphorylation in cells .....	88
3.2.5 Unphosphorylated mutant STAT1 does not impact the DNA specificity and transcriptional response of co-expressed P-STAT1.....	90
3.2.6 Unphosphorylated STAT1 proteins with critically impaired DNA binding do not enable the detection of co-expressed WT .....	95
3.2.7 Deletion of the N-terminus or disruption of the NLS in mutant U-STAT1 restores the visibility of co-expressed phosphorylated WT .....	97
4. Discussion.....	101
4.1 The anti-parallel dimer interface is relevant in STAT3, the disruption of which manifests unique features that are similar yet distinct from STAT1.....	101
4.2 Unphosphorylated STAT1 affects the localization of phosphorylated STAT1 in a concentration-dependent manner .....	106
5. References.....	115
Curriculum vitae .....	133

**List of Abbreviations**

<b>A</b>	Adenine
<b>APCs</b>	Antigen-presenting cells
<b>APS</b>	Ammonium persulphate
<b>APRF</b>	Acute-phase response factor
<b>ATP</b>	Adenosine triphosphate
<b>BSA</b>	Bovine serum albumin
<b>C</b>	Cytosine
<b>CCD</b>	Coiled-coil domain
<b>CCL2</b>	C-C Motif Chemokine Ligand 2
<b>cDNA</b>	Complementary deoxyribonucleic acid
<b>CIS</b>	Cytokine-inducible SH2-containing protein
<b>CMC</b>	Chronic mucocutaneous candidiasis
<b>CRM</b>	Chromosome region maintenance
<b>CXCL10</b>	C-X-C Motif Chemokine Ligand 10
<b>Cy</b>	Cyanine
<b>DBD</b>	DNA-binding domain
<b>DMEM</b>	Dulbecco's Modified Eagle Medium
<b>DMSO</b>	Dimethyl sulphoxide
<b>DNA</b>	Deoxyribonucleic acid
<b>dsRNA</b>	Double-stranded ribonucleic acid
<b>DTT</b>	Dithiothreitol
<b>EDTA</b>	Ethylenediaminetetraacetic acid
<b>EGF</b>	Epidermal growth factor
<b>EMSA</b>	Electrophoretic mobility shift assay
<b>EGTA</b>	Ethylene glycol-bis( $\beta$ -aminoethyl ether)-N,N,N',N'-tetraacetic acid
<b>FRET</b>	Fluorescence resonance energy transfer
<b>G</b>	Guanine
<b>GAF</b>	Gamma-activated factor
<b>GAS</b>	Gamma-interferon activated site
<b>GBP1</b>	Guanylate-binding protein 1
<b>GDP</b>	Guanosine diphosphate

<b>GFP</b>	Green fluorescent protein
<b>GOF</b>	Gain-of-function
<b>GTP</b>	Guanosine triphosphate
<b>HEPES</b>	4-(2-Hydroxyethyl)-1-piperazineethanesulphonic acid
<b>HDACi</b>	Histone deacetylase inhibitor
<b>HP1</b>	Heterochromatin protein 1
<b>Hyper-IgE</b>	Hyper-immunoglobulin E
<b>IFN</b>	Interferon
<b>IFNAR</b>	Interferon-alpha receptor
<b>IFNGR</b>	Interferon-gamma receptor
<b>IHCA</b>	Inflammatory hepatocellular adenoma
<b>IL</b>	Interleukin
<b>IRF</b>	Interferon regulatory factor
<b>IRIS</b>	Interferon response inhibitory sequence
<b>ISGF3</b>	Interferon-stimulated gene factor 3
<b>ISRE</b>	Interferon-stimulated response element
<b>JAK</b>	Janus kinase
<b>LD</b>	Linker domain
<b>LIF</b>	Leukaemia inhibitory factor
<b>LMB</b>	Leptomycin B
<b>LOF</b>	Loss-of-function
<b>LPS</b>	Lipopolysaccharide
<b>MCP1</b>	Monocyte chemotactic protein 1
<b>MGF</b>	Mammary gland factor
<b>MHC</b>	Major histocompatibility complex
<b>MIG</b>	Monokine-induced by gamma interferon
<b>NES</b>	Nuclear export signal
<b>NF-<math>\kappa</math>B</b>	Nuclear factor kappa B
<b>NLS</b>	Nuclear localization signal
<b>NPC</b>	Nuclear pore complex
<b>NTD</b>	N-terminal domain
<b>PAGE</b>	Polyacrylamide gel electrophoresis
<b>P-STAT</b>	Phosphorylated STAT



<b>PIAS</b>	Protein inhibitor of activated STAT
<b>PVDF</b>	Polyvinylidene fluoride
<b>QM</b>	Quadruple mutant
<b>qPCR</b>	Quantitative polymerase chain reaction
<b>RNA</b>	Ribonucleic acid
<b>RT</b>	Room temperature
<b>SCID</b>	Severe combined immunodeficiency
<b>SDS</b>	Sodium dodecyl sulphate
<b>SH2</b>	Src-homology 2 domain
<b>SOCS</b>	Suppressor of cytokine signalling
<b>STAT</b>	Signal transducer and activator of transcription
<b>SUMO</b>	Small ubiquitin-like modifier
<b>T</b>	Thymine
<b>TAD</b>	Transactivation domain
<b>TBS-T</b>	Tris-buffered saline-Tween 20
<b>TC-PTP</b>	T-cell protein tyrosine phosphatase
<b>TE</b>	Tris-EDTA buffer
<b>TEMED</b>	Tetramethylethylenediamine
<b>Th</b>	T helper
<b>T-LGL</b>	T-cell large granular lymphocyte leukaemia
<b>TNF<math>\alpha</math></b>	Tumour necrosis factor alpha
<b>U-STAT</b>	Unphosphorylated STAT
<b>WT</b>	Wild-type

## Amino acids

When referring to amino acids the one letter code is used.

<b>Amino Acid</b>	<b>Three letter code</b>	<b>One letter code</b>
Alanine	Ala	A
Arginine	Arg	R
Asparagine	Asn	N
Aspartic acid	Asp	D
Cysteine	Cys	C
Glutamic acid	Glu	E
Glutamine	Gln	Q
Glycine	Gly	G
Histidine	His	H
Isoleucine	Ile	I
Leucine	Leu	L
Lysine	Lys	K
Methionine	Met	M
Phenylalanine	Phe	F
Proline	Pro	P
Serine	Ser	S
Threonine	Thr	T
Tryptophan	Trp	W
Tyrosine	Tyr	Y
Valine	Val	V

## Acknowledgements

At this juncture in my time as a doctoral student, I would like to acknowledge certain individuals without whom this work would not have come to fruition. The contributions of the persons mentioned below are immeasurable, and I would carry their advice and the memories made with them, throughout my professional and personal journey.

I would like to extend my endless gratitude to and sincerely acknowledge the guidance of my supervisor Prof. Dr. mult. Thomas Meyer. His sound counsel has been fundamental to this work, and his words of support have helped me overcome several moments of self-doubt, both in my doctoral research and in my personal life. He inspired me to question everything I know, encouraged me to enjoy making mistakes and taught me that any problem can be effectively tackled by reapproaching it from different directions; especially by interspersing these deliberations with short breaks of black tea.

The contribution of Dr. Julia Staab in providing me with bright scientific inputs and in helping me organize the results in the course of this work cannot be effectively acknowledged. She has been a grounding influence in my scientific discussions with Prof. Meyer and I will cherish these debates and the time I spent with her, very dearly.

I learnt most of the laboratory skills employed in this project from our technician Anke Gregus, who has significantly contributed to this work by performing several of the mutagenesis experiments required for investigation. I would like to profusely thank her for being an effective teacher and providing me with robust, technical assistance. She warmly shared with me, tips and tricks from her vast experience in the laboratory and always lent a patient ear to my technical questions.

My thesis advisory committee members Prof. Dr. Oliver Wirths and Prof. Dr. Carsten Lüder have been instrumental in providing a direction and prioritizing experiments at important points in this project, and I deeply appreciate their valuable comments and suggestions which have helped me improve the quality of this work.

When I joined as a new PhD student, Dr. Asmma Doudin who was then in the middle of her doctoral studies, immensely helped me find a foothold in the new scientific environment. She strongly believed in me and my friendship with her cushioned the challenges I faced, in the formative years as a doctoral candidate. The cheerful company I had in the laboratory with students Till, Sabine, Louisa, Ruvini, Melissa, Abdallah, Isabel, Daniella, Chris and Niklas

have been encouraging at various points in this work. I found an encouraging colleague and wonderful friend in medical student Lena Behrendsen and she has made the final year of my doctoral studies immensely memorable with her presence.

I would like to specially thank current PhD student Sana Sheikh for being so accommodative of my time schedule and high-priority experiments. Her witty banter has calmed me down on several occasions and I wish her the best for her doctoral studies.

In addition, I would like to thank all the members of the Department of Experimental Neurodegeneration headed by Prof. Dr. Tiago Outeiro, especially Dr. Ellen Gerhardt and Christiane Fahlbusch, for training me on the usage of their facilities, and Daniela Proto for offering me with sound advice on several IT issues. I would like to extend my immense gratitude to the Göttingen Graduate Center for Neurosciences, Biophysics, and Molecular Biosciences (GGNB) at the University of Göttingen for providing me with their GGNB Bridging Fund stipend for last three months of my PhD project. I would also like to thank the members of the GGNB office, the Molecular Medicine program office and the International Office at the University of Göttingen for their help throughout my transition from master to doctoral studies.

I have had the unconditional support of my parents Sudha and Rajeev Menon, and my brother Hrishi through all my professional endeavours including my doctoral studies and their patient hearing and warm conversations have helped me overcome several stressful situations. My father's unflinching faith in my abilities and his practical advice has played a crucial role in shaping my scientific career.

My friends Aisha Ahmad and Amara Khan have been two strong pillars of support throughout my time in Göttingen both as a master and doctoral student and I will forever cherish our dinners, movie nights and all the countless times they have been by my side, when I needed them.

I would like to sincerely acknowledge the contribution of Dr. Juliana Usher at the Department of Psychosomatic Medicine and Robin Schaeffer at the Psychosoziale Beratung of the Studentenwerk Göttingen in helping me manage and improve my personal life without affecting my performance in scientific research.

Finally, I would like to thank my extended family and friends for their wishes and encouragement.

## Abstract

Several cytokines mediate cellular responses via the family of transcription factors called signal transducers and activators of transcription (STAT). Though phosphorylated STATs (P-STAT) form the active and extensively studied component of STAT-mediated signal transduction, recent studies report novel physiological roles for unphosphorylated STATs (U-STAT). However, the interactions within U-STATs and between P-STATs and U-STATs are not very well understood. This project investigates how U-STATs interact with themselves and other P-STATs and the impact of this interaction on cytokine-induced signal transduction. While the U-STAT anti-parallel dimer interface has been reported and studied in STAT1, despite of high sequence homology, a similar interface has not been examined in STAT3. Through site-directed mutagenesis, two STAT3 point mutations V77A in the amino-terminal domain and F174A in the coiled-coil domain have been studied to determine the relevance of the anti-parallel dimer in STAT3-mediated signal transduction. Both V77A and F174A displayed a predominant nuclear accumulation in resting cells and cytokine stimulation led to slight increase in nuclear accumulation. The STAT3 mutants showed elevated levels of cytokine-stimulated tyrosine phosphorylation, while the affinity of mutant P-STAT3 bound to *in vitro* GAS sites was unaltered. The high concentration of mutant P-STAT3 in V77A- and F174A-expressing cells resulted in an elevated transcription of reporter constructs and endogenous target genes containing one-and-a-half GAS sites in their promoter region, but did not affect other genes with a single GAS promoter. Both V77A and F174A behaved similar to the wild-type (WT) in *in vitro* phosphorylation and dephosphorylation assays, but showed a resistance to *in vivo* dephosphorylation induced by the kinase inhibitor staurosporine. By an addition of GAS sequences to *in vitro* dephosphorylation assays, it was confirmed that increased nuclear presence and binding to DNA drove the hyper-phosphorylated status of these mutants. These results provide the evidence of an anti-parallel dimer interface in STAT3, the disruption of which leads to STAT3 hyperactivity. Constitutively active STAT3 has been implicated to drive several cancers, and these results present the anti-parallel dimer of U-STATs as an important mechanism to regulate STAT3 signalling. Though U-STATs have been recently identified to have their distinct gene activation pattern, whether U-STATs have an impact on P-STAT-mediated signal transduction is unknown. Therefore, the unphosphorylated and dimerization-deficient double mutant R602L/Y701F was generated in STAT1, to identify any possible interactions between U-STAT1 and P-STAT1. This double mutant, when co-expressed in cells with WT STAT1, lead to an inhibition of the IFN $\alpha$ - and IFN $\gamma$ -induced nuclear import of

STAT1. Additionally, mutating residues involved in the anti-parallel dimer interface in mutant U-STAT1 did not abolish the import block of P-STAT1. Experiments revealed that dimerization-deficient U-STAT1 inhibited the nuclear import of co-expressed P-STAT1 in a concentration-dependent manner with no major changes in the DNA binding and transcriptional activities of P-STAT1. The co-expressed WT molecule phosphorylated and dephosphorylated similarly in the presence and absence of mutant U-STAT1, but its nuclear import was blocked. Through mutagenesis and deletion experiments, the interaction between mutant U-STAT1 and P-STAT1 was identified to the amino-terminus of the mutant protein. Therefore, a transient import block mediated by high cellular concentration of U-STAT1 is proposed, wherein the assembly of the import structure of P-STAT1 is disrupted by interaction via the amino-terminus of U-STAT1. This STAT1 nuclear import block structure, that does not completely inhibit STAT1-mediated signal transduction in the nucleus, can be used to promote intracellular STAT1-mediated processes other than cytokine signalling, in cells primed with IFN $\gamma$ .

# 1. Introduction

## 1.1 STATs and the JAK-STAT pathway

The discovery of STAT (signal transducers and activators of transcription) proteins originated from the curiosity of Darnell and colleagues, behind the remarkably short duration required to elicit a transcriptional response from cells treated with type I & II interferons (IFNs) (Darnell et al., 1994). This led to the identification of a family of DNA-binding proteins which transduced ligand-receptor interactions occurring at the cell surface as a signal, which could be transferred to the nucleus to initiate a pattern of gene transcription, as a cellular response to this external stimulus. These transcription factors, termed as signal transducers and activators of transcription or STATs, have since then been extensively studied to be important mediators of inflammation, apoptosis, proliferation, differentiation and survival. STATs respond to a wide variety of secretory signalling proteins or cytokines such as IFNs or interleukins (ILs), which are secreted by immune cells to prime neighbouring cells against bacterial and viral infections, thereby requiring a faster induction within minutes (Darnell et al., 1994). Some of these ligands are also growth factors, like epidermal growth factor (EGF) or leukaemia inhibitory factor (LIF), which are cytokine subsets involved in cell growth and differentiation, thereby requiring a gradual and prolonged induction pattern (Cartwright et al., 2005; David et al., 1996). To maintain signal sensitivity and retain this complexity of transcriptional machinery across all species, the STAT family is evolutionarily highly conserved (Levy & Darnell, 2002).

STAT proteins were believed to have risen in the early evolution of multicellular organisms and have been studied in invertebrates, like the slime mould *Dictyostelium discoideum* and the fruit fly *Drosophila melanogaster*, to play important roles in their development and differentiation. There are seven mammalian STAT members, namely STAT1, STAT2, STAT3, STAT4, STAT5a, STAT5b and STAT6 in the sequence of their identification. All STATs are approximately 750-850 amino acids long, have a molecular weight between 80-113 kDa, and are identically organized into six functional domains based on their polypeptide secondary structures. The common STAT modular organization comprises of an amino (NH<sub>2</sub>)-terminal domain (NTD), a coiled-coil domain (CCD), a DNA-binding domain (DBD), a linker domain (LD), an Src homology 2 domain (SH2) and a carboxy (COOH)-terminal transactivation domain (TAD) (Figure 1, zoom box). The TAD of STATs contains a highly conserved tyrosine residue, which is phosphorylated upon cytokine stimulation and is essential for its transcriptional activity (Levy & Darnell, 2002). The STATs also contain a conserved serine

residue in the TAD, which provides another site for phosphorylation, that ensures maximal transcriptional efficiency (Decker & Kovarik, 2000). The STAT functional domains are further divided into three mobile structural elements: the NTD, the STAT core fragment comprising of the CCD/DBD/LD/SH2 and the TAD (Decker & Müller, 2012). Both the NTD and TAD are connected to the core fragment via short, flexible linkers. Out of the different functional domains, the SH2 and NTD are highly conserved among the STATs, while the TAD is the least conserved and confers specificity among the STAT family members via binding to transcriptional cofactors.

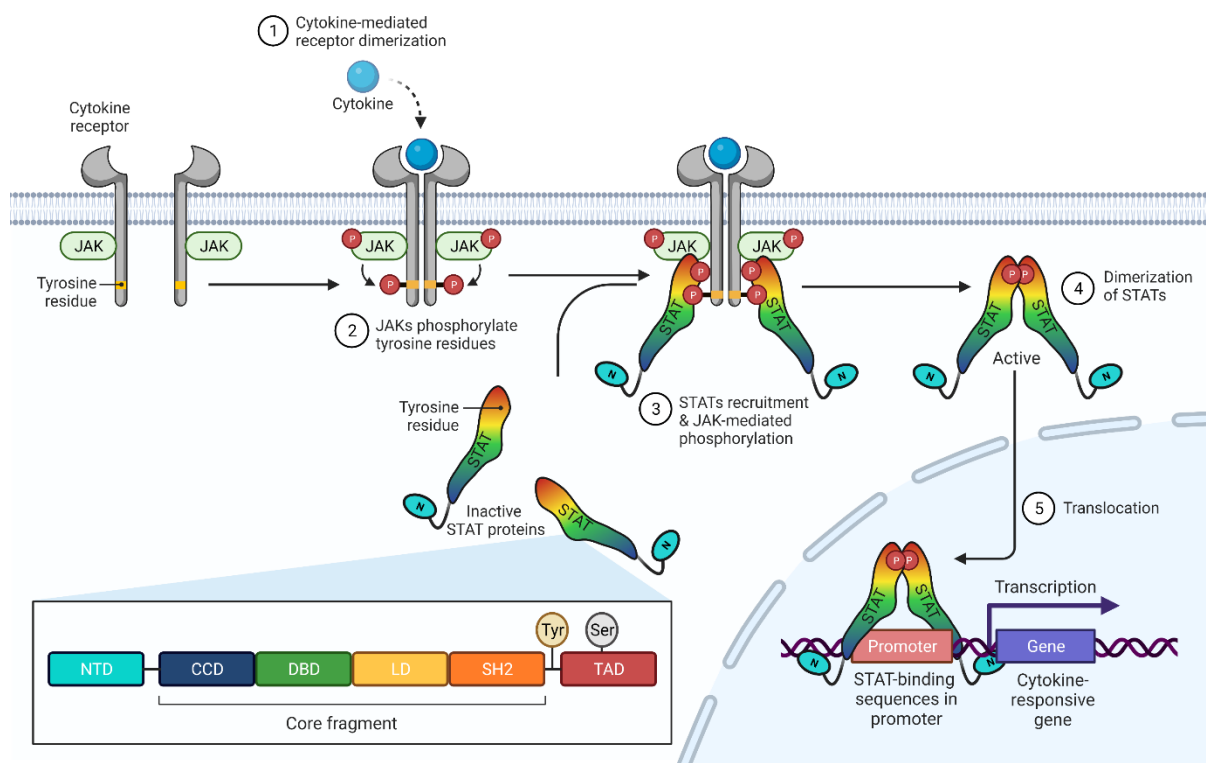


**Figure 1: STAT structure and JAK-STAT pathway.**

Described here in the zoom-in box is the modular STAT structure organized into six domains, namely the NTD, CCD, DBD, LD, SH2 and TAD with critical tyrosine and serine residues which form phosphorylation sites in the active, full-length STAT protein. JAK-STAT signalling has been illustrated in the background, wherein activities starting with ligand binding of cognate receptor to transcription of genes in response to ligand binding have been described.

The founding member of the STAT family, STAT1 was first described to be a 91 kDa associated protein in the IFN $\alpha$ -induced interferon-stimulated gene factor 3 (ISGF3), and to constitute the gamma-activated factor (GAF), which mediated IFN $\gamma$  signalling (Fu et al., 1992; Schindler et al., 1992; Shuai et al., 1992). STAT2 was also discovered along with STAT1 as the other 113 kDa constituent of the ISGF3 which is phosphorylated independent of STAT1



and is critical to IFN $\alpha$  signalling (Improta et al., 1994a; Leung et al., 1995). STAT3, initially referred to as acute-phase response factor (APRF), was found as a 92 kDa protein activated by IL-6 and EGF in acute inflammation (Lütticken et al., 1994; Wegenka et al., 1994; Zhong et al., 1994a). Restricted in its tissue distribution, STAT4 was discovered to be highly expressed in myeloid cells and testes and is activated by IL-12 to regulate T-cell differentiation (Bacon et al., 1995; Cho et al., 1996; Yamamoto et al., 1994; Zhong et al., 1994b). STAT5, previously known as prolactin-induced mammary gland factor (MGF), was discovered in the mammary epithelium of lactating animals and was later investigated to have two isoforms of similar weight encoded by two closely related but separate genes: *STAT5A* and *STAT5B* (Azam et al., 1995; Gouilleux et al., 1994). STAT5 is activated by IL-3 family of cytokines and regulates myeloid growth and hematopoiesis (Mui et al., 1995). Lastly, STAT6 was identified as a mediator of IL-4 signalling which contributes to T-lymphocyte proliferation and differentiation of T helper 2 cells (Th2) (Hou et al., 1994; Kotanides & Reich, 1993; Schindler et al., 1994)

As mentioned earlier, all STATs are activated by the binding of one or more cytokines to their corresponding transmembrane receptors. The phosphorylation of a critical tyrosine residue in the TAD of STATs is catalysed by kinases belonging to the Janus kinase family (JAK), and these two components together make up the JAK-STAT pathway (Levy & Darnell, 2002). Three out of the four mammalian JAK members: JAK1, JAK2, TYK2 are ubiquitously expressed, except of JAK3 which is reserved to haematopoietic cells (Leonard & O'Shea, 1998). JAKs are constitutively and non-covalently bound to the cytoplasmic domain of cytokine receptors. As is typical for protein tyrosine kinases, JAKs harbour an activation loop made up of tandem tyrosine residues. Upon ligand binding, these cytokine receptors homo- or heterodimerize, bringing the receptor-associated JAKs in close proximity to facilitate transphosphorylation of reciprocal activation loops, thereby enhancing their catalytic activity. Auto-phosphorylated JAKs subsequently phosphorylate tyrosine residues in the cytoplasmic tails of these cytokine receptors, which then act as docking sites for unphosphorylated STATs (U-STATs) to bind via their SH2 domains (Darnell, 1997). U-STATs are then activated to phosphorylated STATs (P-STATs) by JAK-mediated tyrosine phosphorylation. Activated STATs form homo- or heterodimers and translocate to the nucleus in a process that requires an intracellular RanGTP/GDP gradient, metabolic energy and a family of carrier proteins called importins (Meyer & Vinkemeier, 2004). Importins recognize basic amino acids, such as arginine/lysine-rich sequences within the STAT core fragment, called a nuclear localization

signal (NLS) and subsequent nuclear accumulation happens within minutes (Begitt et al., 2000; Fagerlund et al., 2002; Meyer & Vinkemeier, 2004).

Inside the nucleus, the DBD of STATs can recognize two types of high-affinity STAT response elements in the promoter/enhancer region of STAT target genes. One of these elements, first discovered in IFN $\gamma$ -stimulated genes, is a palindromic sequence TTCN<sub>x</sub>GAA called gamma-interferon activated site (GAS), wherein X=3 binds all STATs while X=4 is reserved for STAT6 (Decker et al., 1997). The second element is a consensus sequence 5'-TTTCNNTTTC-3' flanked by AG at the 5' end and pyrimidine bases at the 3' end and is called interferon-stimulated response element (ISRE). The ISRE exclusively binds the ISGF3 complex containing STAT1, STAT2 and interferon regulatory factor 9 (IRF9) in response to IFN $\alpha/\beta$  or Type I IFN signalling (Darnell, 1997; Levy et al., 1988). Recognition and binding of STATs to these high-affinity STAT-specific sites initiates the induction of cytokine-responsive target genes (Darnell et al., 1994). In this way, cytokine binding triggers a signal transduction cascade, facilitated by activated STATs, that leads to changes in the gene expression profile within the cell. This cascade which originates with ligand binding at the cell surface and culminates with ligand-stimulated gene transcription in the nucleus, forms the activation cycle of the JAK-STAT pathway (Figure 1).

Prior to cytokine-dependent activation and participation in the JAK-STAT pathway, monomeric U-STAT1 can dimerize or exist in higher-order structures within the cytoplasm (Ndubuisi et al., 1999; Ota et al., 2004). STAT dimers adopt two possible orientations which involves a rearrangement of their structural domains and a change in the direction of monomer alignment (Figure 2). One conformation is that of an anti-parallel dimer, wherein the core fragments of aligned monomers run anti-parallel to each other, such that their TADs lie in opposite directions. This anti-parallel STAT dimer is formed by reciprocal interactions between the NTDs of the participating monomers as well as associations between the CCD and the DBD of the respective core fragments (Zhong et al., 2005). The other possible orientation involves a parallel alignment of both core fragments such that their TADs lie on the same side and are in close proximity to allow reciprocal interactions between the SH2 and TADs of the corresponding monomers, thereby forming the STAT parallel dimer. P-STATs adopt the parallel dimer conformation since they contain a phosphotyrosine residue in their TADs that constitutes this interaction with the SH2 domain of another activated STAT monomer (Shuai et al., 1994). On the other hand, U-STATs exist as monomers or preformed, anti-parallel dimers in the cytoplasm (Mao et al., 2005; Neculai et al., 2005). Therefore, via constant dissociation

and reassociation reactions, monomeric STATs tend to oscillate between anti-parallel and parallel dimeric states, and the selective proportion of a given dimer conformation is determined by the level of STAT tyrosine phosphorylation (Wenta et al., 2008).

Upon cytokine stimulation, the conformation of STAT dimers shifts from the predominant U-STAT anti-parallel dimers to a high concentration of P-STAT parallel dimers which can participate in the activation cycle of the JAK-STAT pathway. This conformational switch between the anti-parallel and parallel dimer has also been proposed to occur around the NTD-NTD interactions within a dimer, without the need for a dissociation-reassociation cycle (Mertens et al., 2006). While monomeric U-STATs constitutively shuttle between the cytoplasm and the nucleus in a carrier-free, energy-independent manner via direct interactions with the proteins of the nuclear pore complex (NPC) channel that facilitates entry into the nucleus, a rapid nuclear accumulation in response to cytokine binding cannot occur without a conformational switch (Meyer et al., 2002; Martincuks et al., 2016). This is ensured by the anti-parallel conformation of U-STAT dimers which masks the NLS, enabling them to be selectively cytoplasmic and available for cytokine-dependent activation. Only through tyrosine phosphorylation and reciprocal SH2 interactions between two P-STAT monomers does a conformational change around the NTD take place, rendering the parallel P-STAT dimer-specific NLS freely accessible to importins (Zhong et al., 2005).

Once imported into the nucleus, activated STATs bind to DNA and are retained in the nucleus until they dissociate from DNA and are dephosphorylated by nuclear phosphatases (Haspel et al., 1996; Haspel & Darnell, 1999). However, after dissociation from DNA, dephosphorylation of STATs requires a second conformation change from a parallel DNA-bound dimer to an anti-parallel dimer. This switch in dimeric states serves two essential functions. Switching to the anti-parallel conformation after dissociation from DNA masks the STAT DBD thereby preventing reassociation of the dimer to DNA. Furthermore, the anti-parallel dimer disrupts the phosphotyrosine-SH2 interactions and exposes these phosphotyrosine residues, moving them to the dimeric exterior and increasing accessibility to the phosphatase (Mertens et al., 2006). Following dephosphorylation, STATs are exported from the nucleus via binding to CRM-1 (chromosome region maintenance) export protein, which recognizes short stretches rich in hydrophobic residues, predominantly leucines as nuclear export signals (NES) (Begitt et al., 2000; Bhattacharya & Schindler, 2003). Just like constitutive import, export can also proceed via direct interactions between monomeric U-STATs and NPC proteins, as can be seen from only a partial blockage of STAT1 nuclear export by the CRM-1 inhibitor leptomycin B (LMB)

(Begitt et al., 2000; Kudo et al., 1999). On the other hand, CRM-1 mediated nuclear export is energy-dependent and requires high nuclear RanGTP/GDP levels (Fornerod et al., 1997). Therefore, the activities which make up the dissociation of DNA-bound STATs and their export from the nucleus constitute the inactivation cycle of the JAK-STAT pathway (Figure 1, Figure 2).

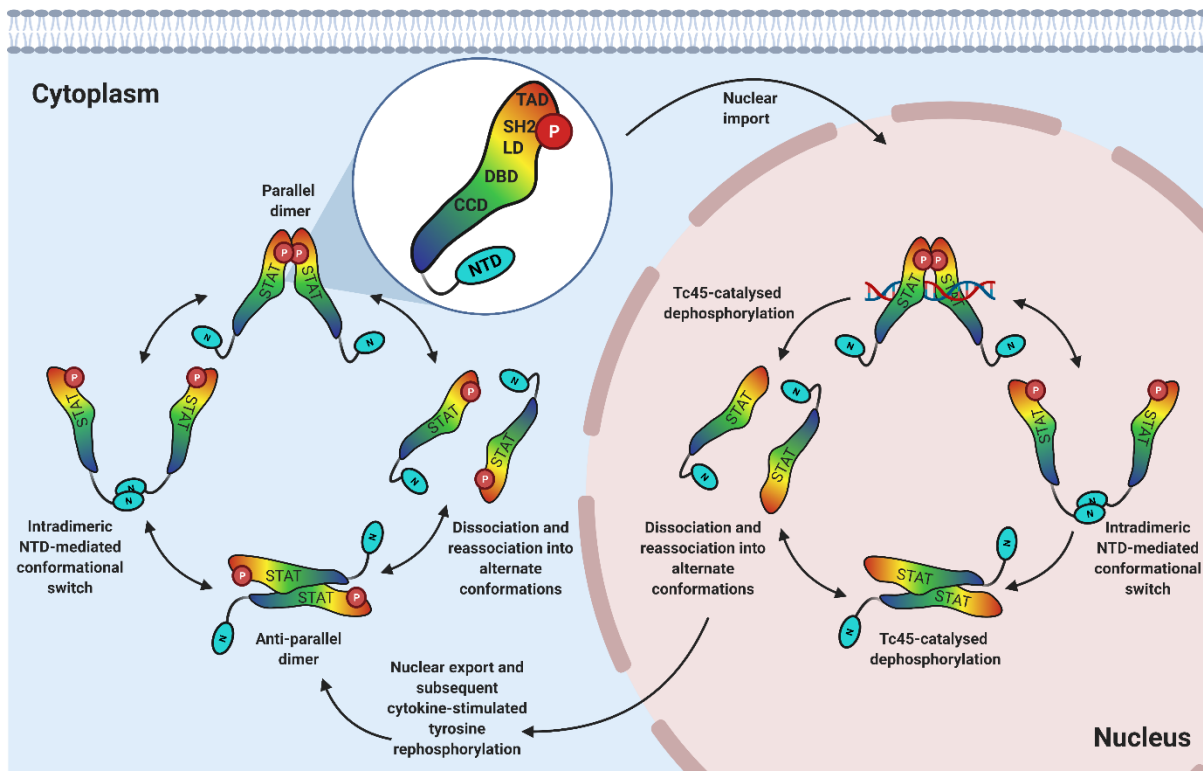


**Figure 2: STAT dimeric conformations**

This figure describes the rearrangements that occur within the STAT dimer in consecutive cycles of phosphorylation and dephosphorylation. Upon phosphorylation at the critical tyrosine residue in the TAD, STATs shift from a monomeric or anti-parallel state to form parallel dimers stabilized by reciprocal interactions between the phosphotyrosine and SH2 domain and exposing NLSs which enable nuclear import (McBride et al., 2002; Melén et al., 2001; Shuai et al., 1994). For phosphorylated dimers to be dephosphorylated by nuclear Tc45 phosphatase, the parallel phospho-dimers reorient into anti-parallel dimers such that their phosphotyrosine residues are exposed for dephosphorylation. The STAT NTD may play a crucial role in acting as a tether around which this reorientation takes place and/or stabilizing the corresponding anti-parallel dimeric state (Mertens et al., 2006; Zhong et al., 2005).

Since persistent gene activation or dysregulation can lead to several auto-immune diseases and cancer, the JAK-STAT pathway harbours several inherent inactivation mechanisms mediated by cytoplasmic and nuclear phosphatases, suppressors of cytokine signalling (SOCS) proteins and protein inhibitors of activated STAT (PIAS). These proteins necessary for deactivation are

often under the transcriptional regulation of STATs (Levy & Darnell, 2002; Starr & Hilton, 1999). The SOCS proteins 1-7, which also includes cytokine-inducible SH2-domain-containing protein or CIS, are inhibitors that suppress STAT activation at the receptor, via the binding of SOCS to the catalytic region of the JAKs. This prevents JAK auto-phosphorylation and inhibits the phosphorylation of STAT proteins on the conserved tyrosine residue. CIS-mediated inactivation takes place through binding to the phosphorylated receptor tail. Therefore, STATs and CIS compete for docking sites (Rawlings et al., 2004; Starr & Hilton, 1999). While SOCS proteins function as latent cytoplasmic inhibitors, nuclear activated STATs are inhibited by several PIAS proteins by interacting with STAT dimers and preventing DNA binding and subsequent transcription. PIAS1 has been identified as an interaction partner of STAT1, whereas PIAS3 binds to STAT3.

## **1.2 JAK-STAT signalling in disease**

Over 25 years since the discovery of JAK-STAT pathway in the pursuit of studying interferon-mediated gene induction, this evolutionarily conserved signal transduction cascade is now known to be universally utilized by various cytokines, interferons, growth factors, and other related extracellular molecules to modulate gene expression (Stark & Darnell, 2012).

An effective tool for the cell to sense its surroundings and decode environmental signals into adaptive cellular processes, the JAK-STAT pathway is a critical component of immunity, and errors in both JAKs and STATs manifest as immunodeficiencies, auto-immune diseases and malignancies (Villarino et al., 2015).

Severe combined immunodeficiency (SCID) patients, who exhibit markedly impaired development and function of lymphocytes, have been investigated to harbour mutations in JAK3, which associates with the gamma-c chain cytokine receptor causing abnormalities in JAK-STAT signalling associated with IL-2 (O'Shea et al., 2013). Acute myeloid leukaemia patients have been found to harbour mutations in JAK1, while JAK2 mutations have been studied to cause myeloproliferative neoplasms in humans. A patient mutation in TYK2 has been associated with causing atopic dermatitis and increasing susceptibility to viral, bacterial and fungal infections.

Hyper-immunoglobulin E (hyper-IgE) syndrome, a multisystem disorder characterized by severe cyst-forming pneumonias, chronic dermatitis, elevated serum IgE levels and connective tissue abnormalities, has been studied to be associated to mutations in STAT3 (Holland et al.,

2007). Several STAT1 gain-of-function (GOF) mutations have been found in patients with chronic mucocutaneous candidiasis (CMC), which manifests as persistent infections of skin, nails and oral mucosa with *Candida albicans* (O'Shea et al., 2013, 2015). While loss-of-function (LOF) or dominant negative mutations in STAT1 have been studied to cause recurrent mycobacterial infections mediated by impaired IFN $\gamma$  (type II IFN) signalling, a complete deficiency of STAT1 blocks both type I and type II IFN signalling leading to a combined loss of viral and bacterial immunity.

Autosomal recessive mutations in STAT5B result in dwarfism due to a loss of growth hormone signalling, and immunodeficiency and autoimmunity caused by impaired response to IL-2. Constitutively active STAT3 via sequence mutations or abnormal cytokine signalling, increase tumour cell proliferation and survival, while suppressing anti-tumour immunity in many types of solid and haematological malignancies (O'Shea et al., 2013, 2015).

Given the broad involvement of the JAK-STAT pathway in cancer and immune disorders, JAKs and STATs have become important therapeutic targets in the mitigation of several infections and controlling tumour growth. JAK inhibitor tofacitinib has been effective in treating patients with psoriasis, while another potent JAK inhibitor ruxolitinib reduced oral thrush and improved general health in a patient with STAT1 GOF mutation-mediated CMC (Mössner et al., 2016; O'Shea et al., 2015). The homology between STAT molecules poses a challenge in the development of specific STAT inhibitors, as most of the strategies targeting STAT inhibition involve disrupting dimerization and phosphorylation by binding to the SH2 domain and/or inhibit DNA binding. STA-21 and Stattic, small molecule inhibitors that bind to the STAT3 SH2 domain and inhibit dimerization, have been found to be effective in inducing apoptosis in breast cancer cells and alleviating inflammation in experimental rheumatoid arthritis (Miklossy et al., 2013). Intrabodies or intracellular antibodies, engineered against the phosphotyrosine residue of STAT3 have been shown to block its downstream signalling without affecting the activities of U-STAT3 or STAT3 serine phosphorylation. Pravastatin, a small molecule inhibitor of STAT1, has been reported to be effective in a murine model of atherosclerosis. Silencing of STATs via siRNA or the employment of decoy oligonucleotides binding and masking the STAT DBD have shown efficacy in *in vivo* cancer models.

Apart from synthetic molecules, several naturally occurring compounds such as curcumin and capsaicin have been investigated to abolish STAT activity in several cancer models (Miklossy et al., 2013; O'Shea et al., 2015). However, the efficacy of JAK-STAT therapeutic targeting is

still limited mainly to *in vitro* studies and its expansion to clinical medicine is often difficult due the lack of specificity of these targeting strategies. This evolutionarily conserved pathway is a point of cross-talk between several cytokines and signalling molecules, and a precise dissection of the similarities and differences between its components, namely the different JAKs and STATs, is required to develop novel therapies against aberrant JAK-STAT signalling with a high degree of specificity and less off-target effects.

### **1.3 Biology of STAT1**

The founding member of the STAT family, STAT1, is a major transcription factor activated mainly by type I and type II interferons to initiate immune responses mediating anti-fungal, anti-bacterial, anti-parasitic and anti-viral immunity. It directly activates several immune effector genes that are involved in promoting microbicidal functions of macrophages, establishing an antiviral state in IFN $\alpha$ -stimulated cells, and mediating antigen processing and presentation via major histocompatibility complexes (MHCs) (Najjar & Fagard, 2010).

Cytoplasmic expression of caspases or proteases, that mediate apoptosis by sequential cleavage in response to stimuli such as TNF $\alpha$ , requires STAT1 (Kumar et al., 1997). In line with its prominent role in promoting apoptosis, STAT1 also regulates genes involved in cell-cycle arrest and represses genes that promote proliferation. Combining its pro-apoptotic and anti-proliferative effect with its negative regulation of angiogenesis, tumorigenesis and invasion makes STAT1 function as a tumour suppressor in cancer models (Huang et al., 2002; Kaplan et al., 1998).

Being the first STAT to discovered, the interactions between the STAT1 functional domains and the arrangement of its mobile structural elements have been extensively studied over the years. The first crystal structure of a STAT protein was that of a DNA-bound, tyrosine-phosphorylated STAT1 dimer, lacking the NTD and a partial TAD owing to a highly flexible sequence linking them to the core fragment, that hampered crystallization (Chen et al., 1998). This structure, wherein the two STAT1 core fragments were aligned parallel to each other, formed the basis of the parallel STAT dimeric conformation stabilized by reciprocal interactions between the phosphotyrosine and the SH2 domains. Further studies resolved the structure of an unphosphorylated STAT1 dimer along with the NTD and determined two binding interfaces, one involving NTD interactions and the other with reciprocal interactions between the CCD and DBD of the protomers (Mao et al., 2005). The highly conserved NTD

of 135 amino acids is of primary importance to the STAT1 structure due to its ability to mediate protein-protein interactions, which is imperative for dimerization and NTD-associated cooperative DNA binding. Tetramerization or oligomerization of STATs stabilizes DNA binding on weak promoters (John et al., 1999). The NTDs of STAT1 dimers facilitate cooperativity on DNA, as can be seen from a mutation at a conserved phenylalanine residue in position 77 of the STAT1 NTD that disrupts tetramerization on DNA and dephosphorylation of P-STAT1 (Meyer et al., 2004). The role of the NTD in facilitating a rearrangement between the parallel and anti-parallel dimer was proposed from the observation that the STAT1 F77A mutation showed elevated levels of tyrosine phosphorylation due to defective dephosphorylation and a prolonged nuclear retention in cytokine-stimulated cells, despite the withdrawal of cytokine stimulation or the subsequent presence of a kinase inhibitor (Mertens et al., 2006; Meyer et al., 2004).

The linker from 116-142 amino acids between the NTD and CCD of STAT1 is also crucial to the conformational shift, as it was proposed that the rearrangement occurs around this length (Mertens et al., 2006).

The CCD or four-helix bundle of STAT1 consists of 181 amino acids (136-317) and contributes to intradimeric interactions by binding to the DBD of the STAT1 partner monomer. The mutation of residues involved in this binding interface (Q340, L383, G384, T385, H406, Q408 of the STAT1 DBD and critically F172 in the STAT1 CCD) leads to the destabilization of the anti-parallel conformation, resulting in hyper-phosphorylation (Mao et al., 2005; Mertens et al., 2006). A mutation at residue F172 showed a prolonged nuclear accumulation even after the withdrawal of cytokine stimulation and conferred a resistance to Tc45-catalysed dephosphorylation *in vitro*, which further confirmed that a switch from the parallel to the anti-parallel dimer conformation is necessary for dephosphorylation and nuclear export (Staab et al., 2013; Zhong et al., 2005). The CCD of STAT1 harbours a nuclear export signal and is known to interact with p48 from the IRF family of proteins to form the IFN $\alpha$ -induced ISGF3 complex (Bromberg & Darnell, 2000). A mutation at a CCD residue R274 has been found in patients with CMC, and both mutations at R274 and the adjacent Q275 have been identified as STAT1 GOF mutations which are dephosphorylation-sensitive but show a premature nuclear accumulation which drives their hyperactivity (Mössner et al., 2016; Petersen et al., 2019).

The DNA-binding domain of STAT1 has the primary function of binding to GAS sites on DNA and is arranged in an immunoglobulin-like structure as a series of  $\beta$ -sheets interconnected via



loops (Chen et al., 1998). The STAT1 DBD is similar to the DBDs of other transcription factors such as NF- $\kappa$ B and p53, wherein loops between the immunoglobulin-like folds form the segment that physically associates with the DNA. DBD residues K336 and N460 in these loops contact the major groove of DNA, while E421 protrudes into the minor groove. The DBD interacts with DNA in a manner, such that one monomer binds to half of a palindromic GAS site and vice versa (Chen et al., 1998). DBD mutations alter the specificity of DNA binding, as can be seen from the behaviour of mutations at residues contacting the phosphate backbone of DNA, T327H, V426H and T427H collectively termed as the DNA<sup>plus</sup> mutant, wherein the parent amino acids have been replaced with positively charged residues (Meyer et al., 2003). These mutants showed non-specific DNA binding at sequences weakly resembling GAS sites, prolonged cytokine-induced tyrosine phosphorylation and nuclear accumulation, but did not activate STAT1 target genes like the wild-type (WT). Moreover, a mutant that weakened DNA binding, by the replacement of these residues with negatively charged amino acids V426D and T427D (DNA<sup>minus</sup>) lost its DNA binding capacity and subsequent nuclear accumulation (Meyer et al., 2003). The DBD residue T385, which is critical to the anti-parallel dimeric interface and interacts with F172 in the CCD of the opposite protomer, when mutated resists dephosphorylation and shows prolonged nuclear accumulation due to its inability to stabilize the anti-parallel conformation (Staab et al., 2013). Two negatively-charged glutamic acid residues, E411 and E421, in the DBD have been reported to be involved in liberating the STAT1 dimer from DNA, characterized by high dissociation rates from non-GAS elements and representing a mechanism for minimizing nuclear retention at transcriptionally inert sites on DNA (Koch et al., 2012). The DBD has also been investigated to harbor an NLS which is recognized by importin  $\alpha$ 5, thereby mediating the nuclear import of STAT1 (Fagerlund et al., 2002; McBride et al., 2002; Meyer et al., 2002)

The STAT1 linker domain spanning 489-576 amino acids connects the DBD to the SH2 domain (Chen et al., 1998). The STAT1 LD has been studied to couple the phosphotyrosine binding site with the DBD, establishing a structural rigidity yet retaining an optimal flexibility between these two domains, that determines the binding and residence time of STAT1 on DNA (Yang et al., 2002). Mutations at LD residues K544 and E545 result in a higher dissociation rate of STAT1 from DNA, due to an alteration in the flexibility between the DBD and SH2 domain (Yang et al., 1999, 2002). The LD also harbors a conserved motif containing a lysine residue K567, which is involved in the recognition of GAS sites, and the two glutamic acid residues E559 and E563, which mediate the alignment to DNA and dissociation from low-

affinity sites (Hüntelmann et al., 2014). In addition, the STAT1 LD has also been reported to interact with NPC proteins and regulate the nucleocytoplasmic translocation of STAT1 (Marg et al., 2004).

Being the most highly conserved domain of STATs, the SH2 domain has the dual function of recruiting monomeric STAT1 to phosphorylated docking sites on the cytoplasmic tails of membrane-bound cytokine receptors thereby facilitating tyrosine phosphorylation of STAT1, and the subsequent stabilization of activated homo- and heterodimers of STAT1 via reciprocal SH2-phosphotyrosine interactions between monomers (Chen et al., 1998; Shuai, et al., 1993; Shuai et al., 1994). A conserved arginine residue at position 602 in SH2 recognizes the critical phosphotyrosine residue at position 701 of the opposite protomer in an interaction mediated by the residues adjacent to the phosphotyrosine (701-708) and a K584 in the SH2 domain. The strong mutual interaction between the phosphotyrosine and the SH2 R602 and surrounding TAD residues lead to the formation of highly stable, parallel homodimers of STAT1. Therefore, upon the disruption of R602, the dimerization ability and cytokine-induced nuclear import of STAT1 is lost (Chen et al., 1998; McBride et al., 2000; Shuai et al., 1994). Furthermore, the SH2 domain has been studied to contribute to nuclear import by providing a theoretical binding site between residues 651-666 in a proposed model of P-STAT1 bound to importin  $\alpha 5$  (Nardozi et al., 2010).

The transactivation domain varying between 40-200 amino acids is the least conserved domain of the STAT proteins and is probably responsible for the divergence in target gene specificity among the STATs (Paulson et al., 1999). The STAT1 TAD of 67 amino acids contains the critical tyrosine residue at 701, which is phosphorylated by JAKs and is key to its transcriptional activity (Schindler et al., 1992; Shuai et al., 1992). In addition to the Y701, the TAD also contains a conserved serine residue in position 727, which is important for maximum transcriptional activity (Wen et al., 1995). STAT1 $\beta$ , which is the naturally occurring splice variant of STAT1 lacking the S727 residue, can dimerize, translocate to the nucleus and bind to DNA. Due to the absence of complete transcriptional activity of full-length STAT1 $\alpha$ , STAT1 $\beta$  was initially understood to be a negative regulator of STAT1 (Darnell, 1997; Darnell et al., 1994). However, a recent study reports STAT1 $\beta$  to show residual transcriptional activity in a model of STAT1 $\alpha$ -deficient mice selectively expressing STAT1 $\beta$  (Semper et al., 2014). Apart from harbouring critical residues that confer transcriptional activity, the STAT1 TAD also plays a major role in the recruitment of transcriptional coactivators (Parrini et al., 2018).

Unphosphorylated STAT1 also functions as a transcription factor with its own distinct gene induction pattern and a capacity to prolong the gene activation of interferon-induced P-STAT1, establishing a non-canonical STAT signalling as opposed to the canonical P-STAT1 signal transduction (Cheon & Stark, 2009; Majoros et al., 2017; Yang & Stark, 2008). One of the prominent roles of U-STAT1 is mediating apoptosis via influencing caspase expression, wherein STAT1-deficient U3A cells are resistant to apoptosis. This is rescued by reconstituting these cells with WT-STAT1 or the Y701F mutant of STAT1, which shows that the role of STAT1 in facilitating TNF $\alpha$ -mediated apoptosis is independent of its tyrosine phosphorylation. U-STAT1 also has been reported to interact with heterochromatin protein 1 (HP1) and maintain the stability of transcriptionally repressed heterochromatin (Brown & Zeidler, 2008; Li, 2008). A part of this project aims at investigating the influence of U-STAT1 on the nucleocytoplasmic distribution and transcriptional control of P-STAT1.

#### **1.4 Biology of STAT3**

One of the most important STAT members, STAT3, was discovered in liver cells as a transcription factor activated by IL-6 family of cytokines that function via the gp130 receptor and was initially termed as APRF based on its induction of acute phase response genes. Due to its high homology with the other members of the protein family constituting the ISGF3 and GAF, it was renamed as STAT3 and was studied to be additionally responsive to IFNs (Raz et al., 1994; Wegenka et al., 1994; Zhong et al., 1994a). STAT3, activated via IL-6-type cytokines, mediates several distinct cellular responses, including induction of acute phase response in liver inflammation, stimulation of proliferation and differentiation in lymphocytes, maintenance of pluripotency of embryonic stem cells, expression of survival genes and inhibition of apoptosis. STAT3 is indispensable for embryogenesis and early development which can be deciphered from early embryonic lethality caused by ablation of STAT3 in mice. As a result of catering to majority of the cytokines and growth factors signalling via the gp130 receptor, STAT3 shows pleiotropic effects in different cells, including skin, thymic epithelium, lymphocytes, mammary gland, liver, nervous system, and bone marrow (Levy & Lee, 2002). Due to its prominent role in promoting survival of cells and evading apoptosis, constitutively active STAT3 drives several hallmarks of cancer and helps maintain cultured cells in a transformed state, thereby functioning as a protooncogene (Bromberg et al., 1999).

The earliest crystal structure of STAT3 was that of a phosphorylated STAT3 $\beta$  DNA bound-homodimer (136-716 amino acids) lacking the NTD and a part of the TAD, wherein the two

P-STAT3 $\beta$  protomers were oriented parallel to each other gripping the DNA like a pair of pliers, similar to STAT1 (Becker et al., 1998; Chen et al., 1998). The crystal structure of unphosphorylated STAT3 exists both as a monomer lacking the NTD and TAD and as an unphosphorylated STAT3 $\beta$  dimer complexed on DNA, similar to the phosphorylated STAT3 $\beta$  DNA-bound parallel dimer (Nkansah et al., 2013; Ren et al., 2008). Unphosphorylated STAT3 also has significant transcriptional control and this was explained by the crystallization of DNA-bound U-STAT3 dimer. However, there is significant debate over the oligomerization of STAT3 prior to cytokine stimulation and in the absence DNA, wherein certain studies report STAT3 to be monomeric while others show that unphosphorylated STAT3 contains preformed dimers (Haan et al., 2000; Kretzschmar et al., 2004; Ren et al., 2008). While the orientation of the promoters in these preformed dimers is unclear, the relevance or impact of the STAT1 anti-parallel dimeric interface and the conformational switch between the dimeric states has been scarcely investigated in STAT3. One of the objectives of this work is to study the importance of the previously reported STAT1 anti-parallel binding interface in STAT3.

The STAT3 NTD of 138 amino acids is critical in mediating cooperative DNA binding of activated STAT3 dimers via tetramerization on tandem weaker sites in gene promoters (Hu et al., 2015). This helps in expanding the STAT3 gene pool, which probably drives some of its pleiotropic effects. The STAT3 NTD also mediates dimerization, DNA binding and nuclear accumulation of U-STAT3 and through post-translational modifications, assists in forming STAT3 complexes with other transcriptional cofactors. The crystal structure of the STAT3 NTD was resolved to be similar to STAT1 and STAT4, containing eight  $\alpha$ -helices folded into a triangular hook wherein two binding interfaces were determined between the NTDs. While one interface constituted interactions with residues V77 and L78, the other binding interface was mediated by W37. Therefore, a deletion of the NTD lead to a loss of DNA-dependant cooperativity and significant downregulation of STAT3 target genes, while point mutations at W37, V77 and L78 behaved similarly, but to a lesser degree. The inflammatory hepatocellular adenoma (IHCA)-causing L78 mutation has been characterized via FRET experiments to disrupt dimerization of U-STAT3 independently and in combination with V77A as a double mutant, suggesting that homotypic NTD interactions occur in the unphosphorylated STAT3 dimer (Domoszlai et al., 2014; Vogt et al., 2011). However, whether the STAT3 NTD mediates a conformational switch between anti-parallel and parallel dimers is unclear. Despite of similarities in the roles of the STAT1 and STAT3 NTDs in dimerization and cooperative DNA binding as can be seen from deletion studies and the point mutation at STAT3-L78, the

behaviour of the STAT3-V77 residue which is homologous to F77 in STAT1 has not been independently studied. This work investigates the impact of a mutated V77 residue in the STAT3 NTD on the phosphorylation and the activities constituting signal transduction by STAT3.

Similar to STAT1, the coiled-coil domain of STAT3 is arranged as four anti-parallel  $\alpha$ -helices and contains several basic sequences that serve as NLSs, thereby playing an important role in STAT3 nuclear translocation (Becker et al., 1998; Vogt et al., 2011). Since the STATs have a high sequence homology, mutations at homologous residues in STAT1 and STAT3 CCD should display similar effects on the functioning of the total protein, as can be seen from NTD deletions of the two transcription factors. This extrapolation is under debate, as two contradictory studies exist which involve the phenotype of the F174 residue in the STAT3 CCD (homologous to STAT1 F172). A mutation F174S was reported in a patient with T-cell large granular lymphocyte (T-LGL) leukaemia to be hyper-phosphorylated, with a high inducibility of STAT3 target genes, which is consistent with the behaviour of STAT1 F172W (Andersson et al., 2016; Staab et al., 2013; Zhong et al., 2005). However, a different study by Ren et al (2008) reported the same residue mutation F174W as being similar to the WT protein, claiming that a binding interface between the CCD and DBD from the STAT1 anti-parallel dimer did not exist in STAT3, as it did not alter the phenotype of their mutant (Ren et al., 2008). One of the main objectives of this study is to investigate a mutation at this critical CCD residue F174 in STAT3, whose STAT1 homologue stabilizes the anti-parallel STAT1 dimer upon a shift in conformational states.

The DBD of STAT3 is made of consecutive  $\beta$ -sheets, wherein the loops interconnecting the sheets, contact the DNA sugar backbone and phosphate group via several residues (Becker et al., 1998). The residue N466 (homologous to N460 in STAT1) is of particular importance in identifying potential GAS sites. Similar to STAT1, mutations in the DBD affect the DNA binding activity in STAT3. Mutations within two conserved motifs of the STAT3 DBD, EE434/435AA and VVV461/462/463AAA did not alter the phosphorylation or dimerization of STAT3 but lead to a marked disruption of DNA binding (Horvath et al., 1995). The STAT3 DBD was also reported to contain an arginine-rich NLS R414/417 that cooperates with the NLS R214/215 in the STAT3 CCD to facilitate nuclear translocation (Ma et al., 2003). However, in Ren et al (2008) the STAT3 DBD residues which interact with the side chain of F174 in a pocket structure, when mutated also show an unaltered phenotype as opposed to their

STAT1 homologues (Mao et al., 2005; Mertens et al., 2006; Ren et al., 2008). Therefore, the existence and importance of the anti-parallel dimer binding interface between the CCD and DBD of STAT, is a question that needs to be investigated.

The STAT3 DBD is connected to the SH2 domain via a connector called the linker domain. The STAT3 LD has been studied to cooperate with the DBD in effectively recognizing and binding to DNA, as can be seen from the mutation at LD residue K551 (homologous to K544 in STAT1) resulting in low transcriptional activation and high dissociation rate from DNA (Mertens et al., 2015). An additional mutation at STAT3 LD residue W546 lead to a similar phenotype and elucidated a functional interaction with K551 and DBD residue E434, underlining the impact of the STAT3 LD in assisting DNA binding. This study also identified a residue W564 which, when mutated, reduced the stability of the STAT3 protein, and another mutation in the distal region of the LD, D570K which exhibited a hyper-active phenotype (Mertens et al., 2015). Apart from merely connecting the DBD and SH2, the impact of these mutations confers a more critical role of the LD in the association-dissociation kinetics of STAT3 and DNA.

The SH2 domain of STAT3 is responsible for phosphorylation and homo- or hetero-dimerization, wherein R609 and the surrounding residues form a hydrophobic pocket that directly interacts with the phosphotyrosine 705 of another STAT3 protein, or recruits STAT3 to the phosphotyrosine residues at receptor docking sites prior to activation. A mutation at R609 (homologous to R602 in STAT1) abolished tyrosine phosphorylation, nuclear accumulation and dimerization of STAT3 (Kretzschmar et al., 2004; Martincuks et al 2016). The oncogenic potential of STAT3 was discovered upon the mutation of the SH2 domain residues A661 and N661 to cysteine, thereby facilitating sulfhydryl bonds between monomers to allow for a phosphorylation-independent constitutive dimer. Several STAT3 SH2 domain mutations, particularly Y640F and V637M, have been identified in patients with T-LGL leukaemia, hyper-IgE syndrome and various other malignancies (de Araujo et al., 2019). This makes the SH2 domain a prominent target for the design of small molecular STAT3 inhibitors, wherein the potential disruption of dimerization leads to an inhibition of STAT3 signal transduction (Miklossy et al., 2013).

The STAT3 TAD is an intrinsically disordered structure harbouring the critical conserved tyrosine residue at position 705 (in STAT1 the homologous position is Y701) and a serine residue at position 727 (in STAT1 also S727), which are phosphorylated upon cytokine

---

stimulation. Similar to STAT1, the phosphorylation of S727 maximizes STAT3 phosphotyrosine-mediated transcription (Becker et al., 1998; Wen et al., 1995). STAT3 $\beta$  is a STAT3 isoform which differs from full-length STAT3 $\alpha$  by a TAD truncation of 50 amino acids including the S727 residue, which is replaced by 7 specific residues and acts as a negative regulator of STAT3 (Caldenhoven et al., 1996). However, the expression of STAT3 $\beta$  rescues embryonic lethality of STAT3 $\alpha$ -deficient mice, suggesting a distinct role and transcriptional profile of STAT3 $\beta$  (Zhang et al., 2019). A mutation of Y705 abolishes cytokine-stimulated phosphorylation, nuclear accumulation, and signal transduction of STAT3, thereby exhibiting a dominant-negative effect on wild-type STAT3 (Kaptein et al., 1996; Kretzschmar et al., 2004). Therefore, the STAT3 TAD with both Y705 and S727, is essential to ensure the integrity of STAT3-dependent transcription.

Unphosphorylated STAT3 leads the transcription of a distinct subset of genes independent of P-STAT3, by forming complexes with unphosphorylated NF- $\kappa$ B. Since STAT3 is its own target gene, IL-6-induced P-STAT3 activates and increases the concentration of U-STAT3 that drives late cytokine-dependent signalling (Yang et al., 2007). While in lung cancer cells, U-STAT3 has been reported to promote heterochromatin formation and combat the oncogenic role of P-STAT3, persistent nuclear accumulation of U-STAT3 has been studied to promote angiotensin II type 1 receptor-induced cardiac hypertrophy and heart failure (Dutta et al., 2020; Yue et al., 2010). However, the structure of the U-STAT3 dimer is not clear as studies claim U-STAT3 to be both predominantly monomeric and oligomeric. The other part of this project investigates whether the anti-parallel dimer of unphosphorylated STAT1, can be found in STAT3.

## **1.5 Crosstalk between STAT1 and STAT3**

What forms an interesting aspect of the JAK-STAT pathway, are the contradictory roles of STAT1 and STAT3 in physiology and disease (Avalle et al., 2012). While STAT1 signalling mediates innate and adaptive immunity, arrests cell growth and favours apoptosis, STAT3 promotes immunosuppression, survival signals and cell proliferation. Notwithstanding their high sequence similarity and transduction of signals from a common pool of receptors and cytokines, the activities of STAT1 and STAT3 are under reciprocal regulation. Any fluctuations in their expression or phosphorylation could drive the cell to entirely opposite fates, which can be consequential in homeostasis and pathophysiology.

As described previously, type I/II IFN signalling via IFN-receptors (IFNAR for  $\text{INF}\alpha$ /IFNGR for  $\text{INF}\gamma$ ) centrally activates STAT1 which mediates anti-viral immunity and immune responses against other pathogens via phosphorylation, nuclear accumulation, ISRE/GAS binding and induction of genes under the transcriptional control of IFNs (Darnell et al., 1994). On the other hand, STAT3 is the key activator of IL-6 family of cytokines and growth factors which function via the dimerization of gp130 receptors and other specific growth factor receptors leading to similar activities of STAT3 (Zhong et al., 1994a) (Figure 3). Both interferons and interleukins lead to transient cross-activation of STAT3 and STAT1, respectively. *In vitro* dimerization of phosphorylated STAT1 and STAT3 and the binding of the activated STAT1-STAT3 heterodimers to DNA is possible. However, *in vivo* conditions enforce a more stringent ligand bias, and the distinct nature of their target gene repertoire might warrant the need for additional transcriptional coactivators (Avalle et al., 2012; Regis et al., 2008).

The direction of cellular fate towards survival or apoptosis in diverse contexts such a development and tumorigenesis, depends on the equilibrium between the contrasting signals received from extracellular cytokines and growth factors (Avalle et al., 2012; Regis et al., 2008; Stephanou & Latchman, 2005). STAT1 drives apoptosis via the expression of death receptors and ligands, caspases, inducible nitric oxide (iNOS), cyclin dependent (CDK) kinase inhibitors and by direct interactions with tumour suppressors like p53. STAT1 negatively regulates proliferative genes like *c-Myc* and cyclins and anti-apoptotic genes like *Bcl2* and *Bcl-xl*. In contrast, constitutive activation of STAT3 induces transformation of cells, and promotes the expression of proliferative and anti-apoptotic genes in a cell-type specific manner. Apart from inducing apoptosis, STAT1 also triggers inflammation via the upregulation of proinflammatory genes like *ICAM1* and *CXCL10*, mediating the recruitment and adhesion of immune cells to the site of inflammation. STAT1 triggers the production of pro-inflammatory mediators like reactive oxygen/nitrogen species that promote vasodilation leading to immune infiltration and enhances antigen presentation via increased expression of MHC class I and class II molecules. This is opposed by the ability of STAT3 to repress these pro-inflammatory genes and facilitate immune evasion via the inhibition of antigen presentation and T-cell responses (Avalle et al., 2012; Najjar & Fagard, 2010; Regis et al., 2008; Stephanou & Latchman, 2005).

However, the crosstalk between STAT1 and STAT3 has significant physiological implications as both STATs are their own target genes. An imbalance of STAT expression can be triggered



by external stimuli or by the maturation process within a cell type. In macrophages precultured with IFNs, the anti-inflammatory cytokine IL-10 that predominantly functions via activated STAT3, displays a pro-inflammatory effect. This is facilitated by the high number of STAT1 molecules in these IFN-primed cells that can interact with STAT3 and form STAT1-STAT3 heterodimers thereby reducing activated STAT3 which classically homodimerize to mediate the anti-inflammatory effect of IL-10. Similarly, in STAT1-deficient macrophages, T-lymphocytes or MEF cells, IFN $\gamma$  switches from its pro-apoptotic role to induce proliferation via the activation of STAT3-mediated transcription. Therefore, the relative abundance of STAT1 or STAT3 can cross-regulate their cognate cytokine-dependent signal transduction, thereby manifesting as opposing cellular responses (Avalle et al., 2012; Regis et al., 2008).

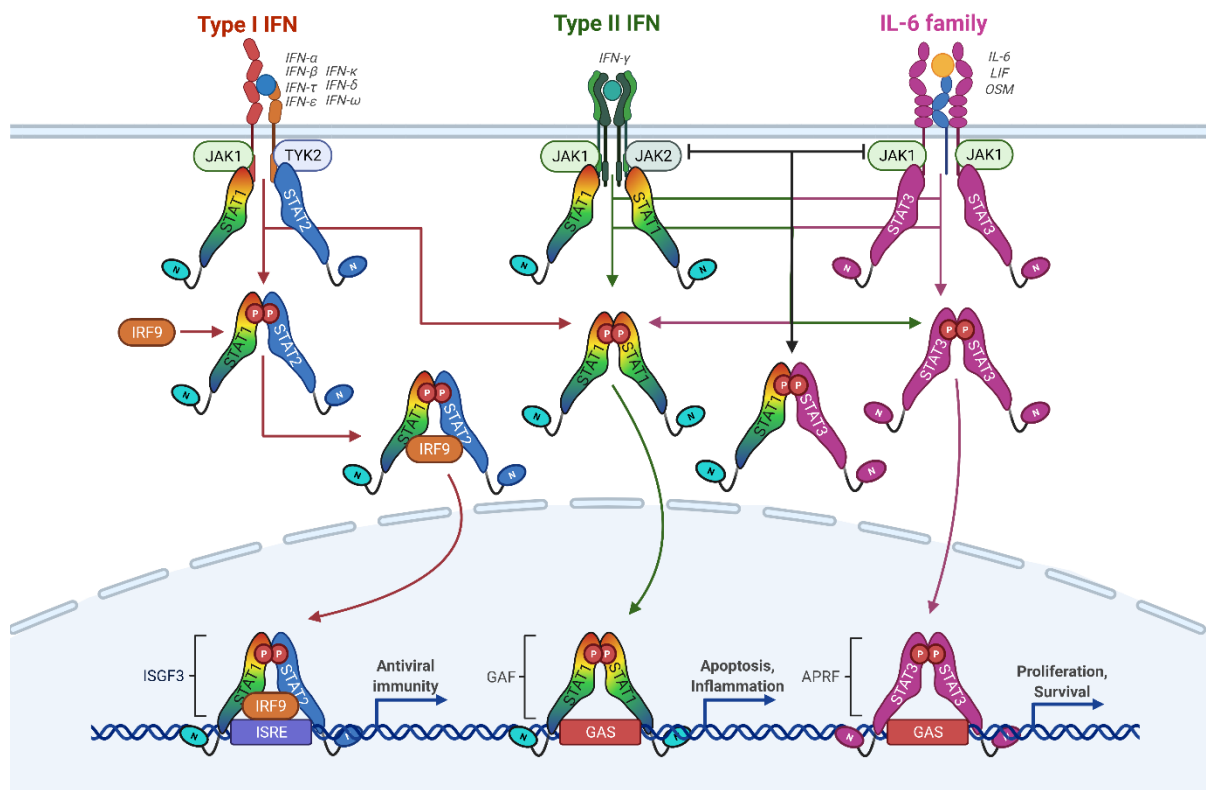


**Figure 3: Cross-talk within STATs.**

Since multiple STATs can be phosphorylated by a cytokine to varying degrees, there are many ways through which STATs can cross-interact, some of which have been illustrated in this figure. While STAT1 homodimerizes in response to IFN $\gamma$ , STAT1 and STAT2 dimerize to form the ISGF3 with IRF9 (Improta et al., 1994b; Shuai et al., 1992). On the other hand, STAT3 homodimers are formed upon stimulation with IL-6, but heterodimers of STAT1 and STAT3 have been reported with a proposed inhibitory function on their respective cytokine responses (Ho & Ivashkiv, 2006; Wegenka et al., 1994).

The note-worthy and central component of this crosstalk mechanism is the STAT1-STAT3 heterodimer. *In vitro* experiments studying the inhibitory effect of STAT3 on IFN $\alpha$  signalling

or IL-6-stimulated transient activation of STAT1 has helped isolate this STAT1-STAT3 heterodimer (Haan et al., 2005; Ho & Ivashkiv, 2006). These studies report the STAT1-STAT3 heterodimer to be formed only upon the cytokine-stimulated phosphorylation of both contributing STAT species. The STAT1-STAT3 heterodimer can possibly sequester a particular STAT (e.g. STAT1) and remove it from the pool available for homodimerization, thereby reducing the signal transduction efficiency of the sequestered STAT (Delgoffe & Vignali, 2013). Other roles of the STAT heterodimer could include binding to sequences other than those recognized by either of their STAT contributors and/or recruiting cofactors which cannot bind to either of the STAT homodimers. While the precise role of the STAT1-STAT3 heterodimer in the signal transduction pathway of STAT1 and STAT3 is unclear, a resolution of the STAT1-STAT3 heterodimer crystal structure with the relative orientation of the contributing STATs could provide some answers to the questions surrounding the cross-interactions of STAT1 and STAT3. Another approach which could provide clues to the pattern of heterodimerization between STAT1 and STAT3, is to study the behaviour of the functional domain residues and intradimeric interactions within STAT3 in comparison to STAT1, which has been employed in this project.

## **1.6 Objectives**

This project aims at studying the role of unphosphorylated STATs and their binding interfaces, via a site-directed mutagenesis approach in STAT1 and STAT3. As has been described in the previous sections, the tyrosine phosphorylated STAT3 dimer bound to DNA has been reported to adopt a parallel conformation like STAT1, whereas the structure of the unphosphorylated STAT3 dimer is unclear due to contradictory studies on the behaviour of homologous STAT3 residues from the well-characterised STAT1 anti-parallel dimer interface (Andersson et al., 2016; Becker et al., 1998; Ren et al., 2008) Therefore, the first part of this project characterizes two mutations which have been mentioned in literature and clinical data, to determine the relevance of the anti-parallel dimer interface in STAT3. The first mutation is the V77A (F77 in STAT1) in the STAT3 NTD hand-shake interface, to study whether homotypic amino-terminal interactions that assist in facilitating a conformational switch between parallel and anti-parallel dimeric states in STAT1, are indeed present in STAT3 (Mertens et al., 2006). The second mutation F174A (homologous to F172 in STAT1) has been introduced in the STAT3 coiled-coil domain to determine whether the relevance of an anti-parallel binding interaction established in STAT1, can be extended to STAT3 (Zhong et al., 2005). In conjunction with the

above-mentioned mutations and WT STAT3, a double-mutation R609L/Y705F has been introduced in both the STAT3 SH2 domain and TAD to render a dimerization-deficient STAT3 construct, which is used as a negative control (Kaptein et al., 1996; Kretzschmar et al., 2004). These mutations have been studied to investigate the structural alterations undergone by U-STAT and P-STAT dimers in their activation-deactivation cycle and the subsequent effect of these conformations on cytokine-signalling.

The second part of the project investigates the function of unphosphorylated STAT on the JAK-STAT signal transduction cascade, focussing on the impact of a high concentration of unphosphorylated STAT1 on the nucleocytoplasmic shuttling of phosphorylated STAT. The strategy used to answer this question involves mutating the functional interaction surfaces of STAT1, to generate a construct that cannot be phosphorylated nor can dimerize. In a stepwise process, first the effects of an excess of the phosphorylation- and dimerization-deficient double mutant of STAT1, R602L/Y701F, have been studied on the nuclear import of co-expressed phosphorylated WT STAT1. In the next steps, a triple and quadruple mutant have been generated that disrupt known binding interfaces in both parallel and anti-parallel conformations of the STAT1 dimer, to study interactions with co-expressed WT STAT1 (Petersen et al., 2019; Staab et al., 2013). Based on literature, additional mutations and deletions have been introduced to render a STAT1 construct that is incapable of interacting with another co-expressed WT STAT1. The constructs generated in the second part of this study help determine the role of U-STATs on the cellular distribution and transcriptional activity of their phosphorylated counterparts.

## 2. Materials and Methods

### 2.1 Materials

#### 2.1.1 Cell lines

##### *human cell lines*

HeLa-S3	Human adherent epitheloid cervix carcinoma cell line; positive for HPV16 (Scherer et al., 1953); kind gift from Professor Uwe Vinkemeier, Nottingham
U3A	STAT1-deficient human adherent epitheloid fibrosarcoma line (McKendry et al., 1991); Kind gift from Professor Uwe Vinkemeier, Nottingham

#### 2.1.2 Chemicals and reagents

*Table 1: List of chemicals and reagents*

Name	Company
Agar	Carl Roth, Karlsruhe, Germany
Agarose	Biozym Scientific, Hessisch Oldendorf, Germany
Ampicillin	Sigma-Aldrich, Taufkirchen, Germany
Adenosine triphosphate (ATP)	Sigma-Aldrich
APS (ammonium persulphate)	Carl Roth
Boric acid	Amersham Pharmacia Biotech, Freiburg, Germany
Bromophenol blue	Fisher Bioreagents, Pittsburgh, USA
BSA (bovine serum albumin) Fraction V	Carl Roth
Complete Mini protease inhibitor cocktail	Roche, Rotkreuz, Switzerland
$\alpha$ -[ <sup>32</sup> P]-dATP (3000 Ci/mmol)	Perkin Elmer, Rodgau, Germany
DMSO (dimethyl sulfoxide)	Sigma-Aldrich
dNTP (deoxynucleotide triphosphates)	Carl Roth

DTT (dithiothreitol)	Applichem, Darmstadt, Germany
EDTA (ethylenediaminetetraacetic acid)	Sigma-Aldrich
EGTA (ethylene glycol-bis( $\beta$ -aminoethyl ether)-N,N,N',N'-tetraacetic acid)	Carl Roth
Ethanol, 99.8 %	Carl Roth
Ethidium bromide	Carl Roth
FBS (foetal bovine serum) Superior	Biochrom, Berlin, Germany
Ficoll-Paque Plus	Amersham Bioscience
Fluoromount G	Southern Biotech, Birmingham, USA
Formaldehyde solution, 37 %	Carl Roth
Glycine	Carl Roth
Glycyl-glycine	Sigma-Aldrich
Glycerin	Carl Roth
HEPES (N-2-hydroxyethylpiperazine-N-ethanesulfonic acid)	Carl Roth
HCl (hydrogen chloride)	Carl Roth
H <sub>2</sub> SO <sub>4</sub> (sulphuric acid)	Carl Roth
Hoechst 33258	Sigma-Aldrich
Igepal CA-360	Sigma-Aldrich
Kanamycin	Sigma-Aldrich
KCl (potassium chloride)	Merck Millipore, Germany
K <sub>2</sub> HPO <sub>4</sub> (potassium hydrogen phosphate)	Merck Millipore
MegaTran 2.0	Origene, Rockville, USA
$\beta$ -Mercaptoethanol	Sigma-Aldrich
Methanol	Merck Millipore
MgCl <sub>2</sub> (magnesium chloride)	Sigma-Aldrich
MgSO <sub>4</sub> (magnesium sulphate)	Carl Roth
MnCl <sub>2</sub> (manganese (II) chloride)	Carl Roth
NaCl (sodium chloride)	Carl Roth

NaCl, 0.9 %	B. Braun, Melsungen, Germany
Na <sub>2</sub> CO <sub>3</sub> (sodium carbonate)	Carl Roth
NaH <sub>2</sub> PO <sub>4</sub> (sodium phosphate monobasic)	Merck Millipore
Na <sub>2</sub> HPO <sub>4</sub> (sodium phosphate dibasic)	Merck Millipore
NaHCO <sub>3</sub> (sodium bicarbonate)	Carl Roth
NaN <sub>3</sub> (sodium azide)	Thermo Fischer
NaOH (sodium hydroxide)	Carl Roth
Na-Pyruvate (sodium pyruvate)	Thermo Fischer
Na <sub>3</sub> VO <sub>4</sub> (sodium orthovanadate)	Acros Organics, Geel, Belgium
ONPG (o-nitrophenyl-β-D-galactopyranoside)	Sigma-Aldrich
Pefabloc	Roche
PBS (phosphate-buffered saline), sterile	Life Technologies, Carlsbad, USA
Penicillin/streptomycin	Biochrom
Poly-dIdC (poly-deoxyinosinic-deoxycytidylic acid)	Sigma-Aldrich
Polyethyleneglycol 8000	Carl Roth
2-propanol (isopropanol)	Carl Roth
Puromycin	Sigma-Aldrich
Rotiphorese Gel 30 (Acrylamide/Bisacrylamide (37:5:1)- solution)	Carl Roth
Rotiphorese Gel 40 (Acrylamide/Bisacrylamide (29:1)- solution)	Carl Roth
Rotiphorese 10x SDS-PAGE	Carl Roth
SNAP-Cell TMR-Star	New England Biolabs, Massachusetts, USA
SDS (sodium dodecyl sulphate)	Carl Roth
Sodium acetate	Carl Roth
Sodium deoxycholate	Applichem
Staurosporine	Sigma-Aldrich
TEMED (tetramethylethylenediamine)	Carl Roth

Tris-base (Tris-(hydroxymethyl)-amino methane)	Carl Roth
Tris-HCl (Tris-hydrochloride)	Carl Roth
Triton X-100	Carl Roth
Tryptone	Carl Roth
Tween-20	Carl Roth
Yeast extract	Carl Roth

### 2.1.3 Culture media

*Table 2: List of media*

Name	Company
DMEM (Dulbecco's modified Eagle's medium) (Glucose 4.5 g/L, 580 mg/L L-glutamine, 110 mg/L Na-pyruvate)	Biochrom
LB medium (Luria/Miller)	Carl Roth
RPMI (Roswell Park Memeroial Institute medium) 1640	Lonza, Basel, Switzerland

### 2.1.4 Kits

*Table 3: List of kits*

Name	Company
Absolute Blue QPCR SYBR Green Mix	Thermo Fischer, Waltham, USA
Luciferase assay system	Promega Corporation, Mannheim, Germany
PeqGOLD total RNA Kit (S-line)	VWR Peqlab, Darmstadt, Germany
PeqGOLD Plasmid Mini Prep Kit I	VWR Peqlab
Qiagen Plasmid Maxi Kit	Qiagen, Hilden, Germany
QuikChange II Site-Directed Mutagenesis Kit	Stratagene, La Jolla, USA
Verso cDNA Synthesis Kit	Thermo Scientific

## 2.1.5 Equipment

**Table 4:** List of equipment

<b>Name</b>	<b>Company</b>
Biological safety cabinet class II, Herasafe KS 9	Thermo Fischer Scientific, Langenselbold, Germany
BioPhotometer plus	Eppendorf, Hamburg, Germany
Centrifuge 5804 R	Eppendorf
-20°C freezer	Liebherr, Germany
Incubator B 5061 EC-CO <sub>2</sub>	Heraeus, Hanau, Germany
Innova 42 bacterial incubator	New Brunswick Scientific, Eppendorf
Luminometer Centro-LB-960	Berthold Technologies, Bad Wildbad, Germany
Microcentrifuge 5415 R	Eppendorf
Microscope, inverted, Axiovert 40 CFL	Zeiss Oberkochen, Germany
Mini centrifuge ROTILABO	Carl Roth
Minispin plus centrifuge	Eppendorf
Nikon Eclipse Ti fluorescence microscope	Nikon Instruments, Amsterdam, Netherlands
Neubauer-modified counting chamber	Paul Marienfeld, Königshofen, Germany
Odyssey CLx imaging system	LI-COR, Bad Homburg, Germany
IKA Vortex 3, shaker	IKA-Werke, Staufen, Germany
pH meter	Sartorius, Göttingen, Germany
Pipettes, Type Research (P1000, P200, P100, P10, P2.5)	Eppendorf
ErgoOne Single-Channel pipettes (P1000, P200, P100, P20)	STARLAB, Hamburg, Germany
ErgoOne FAST Pipette Controller	STARLAB
Power supply unit	Biometra, Göttingen, Germany
Real-time cycler Mastercycler epgradient S	Eppendorf
Rocker Duomax 1030	Heidolph, Schwalbach, Germany
Semi-dry blotting cell	VWR Peqlab
SDS PAGE gel running system	Biometra



Thermo shaker TS1	Biometra
T3000 thermal cycler	Biometra
Waterbath GFL	Schuett biotecc, Göttingen, Germany
Lab balance	Sartorius

### 2.1.6 Disposables

*Table 5: List of disposables*

<b>Name</b>	<b>Company</b>
Cell culture flasks, T75	Sarstedt, Nümbrecht, Germany
Cell culture plates: 6-well, 48-well	Sarstedt
Cell scraper 24 cm	Sarstedt
Cryovials	Nunc, Roskilde, Denmark
Falcon tubes: 15 ml, 50 ml	Sarstedt
Glass cover slip	Thermo Fischer
Gloves, StarGuard Sensitive Nitrile Gloves, S	STARLAB
Micro-reaction tube: 0.2 ml, 1.5 ml, 2 ml	Eppendorf
Petri dishes, 10 cm	Corning, New York, USA
Pipette Tips (P1000, P100, P10)	Sarstedt
PVDF (polyvinylidene fluoride) membrane Immobilon-P	Merck Millipore
Round bottom tubes, 14 ml	BD Biosciences
Serological pipettes, 5 ml, 10 ml	Sarstedt, Nümbrecht, Germany

### 2.1.7 Water

Solutions mentioned in this study were produced using double-distilled H<sub>2</sub>O generated using the PURELAB Plus purification system (Elga Labwater, Celle, Germany) which produced water with a resistivity of 18.2 MΩ\*cm. When the protocol recommended the application of DNase-, RNase-, proteinase-free water, Molecular Biology Grade Water (5 Prime, Hilden, Germany) was used.

### 2.1.8 Sterilization of material

5075 ELV autoclave (Tuttnauer Europe B.V., Breda, Netherlands) was used to sterilize cell culture laboratory equipment and solutions.

### 2.1.9 Oligonucleotides and primers

All oligonucleotides and primer were purchased from Sigma-Aldrich. Primers were designed using Primer3Plus and NCBI Blast and reconstituted in TE buffer or DNase-, RNase-, proteinase-free water to be stored at -20 °C.

Primers for sequence-specific mutagenesis:

**Table 6:** List of sequence-specific mutagenesis primers

Name	Sequence
STAT1 W37F F	5'-CAG ACA GTA CCT GGC ACA GTT TTT AGA AAA GCA AGA CTG-3'
STAT1 W37F R	5'-CAG TCT TGC TTT TCT AAA AAC TGT GCC AGG TAC TGT CTG-3'
STAT1 F77A F	5'-TTC TTT GGA GAA TAA CGC CTT GCT ACA GCA TAA CAT A-3'
STAT1 F77A R	5'-TAT GTT ATG CTG TAG CAA GGC GTT ATT CTC CAA AGA A-3'
STAT1 R274W F	5'-GAG AGT CTG CAG CAA GTT TGG CAG CAG CTT AAA AAG TTG-3'
STAT1 R274W R	5'-CAA CTT TTT AAG CTG CTG CCA AAC TTG CTG CAG ACT CTC-3'
STAT1 T385A F	5'-GAA GTT CAA CAT TTT GGG CGC GCA CAC AAA AGT GAT GAA C-3'
STAT1 T385A R	5'-GTT CAT CAC TTT TGT GTG CGC GCC CAA AAT GTT GAA CTT C-3'
STAT1 L407A/L409A F	5'-GGC TGA ATT TCG GCA CGC GCA AGC GAA AGA ACA GAA AAA TGC CGA-3'
STAT1 L407A/L409A R	5'-GCA TTT TTC TGT TCT TTC GCT TGC GCG TGC CGA AAT TCA GCC-3'
STAT1 V426D/T427D F	5'-GAG GGT CCT CTC ATC GAT GAT GAA GAG CTT CAC TC-3'

STAT1 V426D/T427D R	5'-GAG TGA AGC TCT TCA TCA TCG ATG AGA GGA CCC TC-3'
STAT1 E524A F	5'-CTG AAC ATG TTG GGA GCG AAG CTT CTT GGT CCT AAC GCC-3'
STAT1 E524A R	5'-GGC GTT AGG ACC AAG AAG CTT CGC TCC CAA CAT GTT CAG-3'
STAT1 R586E F	5'-GGC TTC ATC AGC AAG GAG GAA GAG CGT GCC CTG TTG-3'
STAT1 R586E R	5'-CAA CAG GGC ACG CTC TTC CTC CTT GCT GAT GAA GCC-3'
STAT1 R602L F	5'-CCG GGG ACC TTC CTG CTG CTG TTC AGT GAG AGC TCC-3'
STAT1 R602L R	5'-GGA GCT CTC ACT GAA CAG CAG CAG GAA GGT CCC CGG-3'
STAT1 Y701F F	5'-GGC CTT AAA GGA ACT GGA TTT ATC AAG ACT GAG TTG-3'
STAT1 Y701F R	5'-CAA CTC AGT CTT GAT AAA TCC AGT TCC TTT AGG GCC-3'
STAT3 V77A F	5'-GCA AGA GTC CAA TGC CCT CTA TCA GCA CAA G-3'
STAT3 V77A R	5'-GTT GTG CTG ATA GAG GGC ATT GGA CTC TTG C-3'
STAT3 F174A F	5'-CTC CAG GAC GAC TTT GAT GCC AAC TAC AAA ACC CTC AAG-3'
STAT3 F174A R	5'-CTT GAG GGT TTT GTA GTT GGC ATC AAA GTC GTC CTG GAG-3'
STAT3 R609L F	5'-CCG GGC ACC TTC CTA CTG CTC TTC AGC GAG AGC AGC AA-3'
STAT3 R609L R	5'-TTG CTG CTC TCG CTG AAG AGC AGT AGG AAG GTG CCC-3'
STAT3 Y705F F	5'-GTA GTG CTG CCC CGT TTC TGA AGA CCA AGT TC-3'
STAT3 Y705F R	5'-GAA CTT GGT CTT CAG AAA CGG GGC AGC ACT AC-3'

Grade of purification: Desalted

Sequencing primers:

**Table 7:** List of sequencing primers

Name	Sequence
STAT1 171 R	5'-TCT GCA AGG TTT TGC ATT TG-3'
STAT1 312 F	5'-TTC AGA GCT CGT TTG TGG TG-3'
STAT1 484 F	5'-CCT TCT TCC TGA CTC CAC CA-3'
STAT1 611 R	5'-CTC CAC CCA TGT GAA TGT GA-3'
STAT3 51 F	5'-CAC ATG CCA CGT TGG TGT TTG-3'
STAT3 506 F	5'-CGA GGT GCT CAG CTG GCA G-3'
STAT3 682 F	5'-GGA GGA GGC ATT TGG AAA G-3'

Grade of purification: Desalted

Primers for quantitative real-time PCR (qRT-PCR):

**Table 8:** List of oligonucleotide primers for quantitative PCR (qRT-PCR)

Name	Sequence
<i>hCCL2</i> F	5'-GCA GCA AGT GTC CCA AAG AA-3'
<i>hCCL2</i> R	5'-CTG GGG AAA GCT AGG GGA AA-3'
<i>hCXCL10</i> F	5'-ATT CTG AGC CTA CAG CAG AG-3'
<i>hCXCL10</i> R	5'-GCT TGC AGG AAT AAT TTC AA-3'
<i>hC-MYC</i> F	5'-GGT CTT CCC CTA CCC TCT CAA CGA-3'
<i>hC-MYC</i> R	5'-GGC AGC AGG ATABGTC CTT CCG AGT-3'
<i>hGAPDH</i> F	5'-GAA GGT GAA GGT CGG AGT C-3'
<i>hGAPDH</i> R	5'-GAA GAT GGT GAT GGG ATT TC-3'
<i>hGBP1</i> F	5'-GGT CCA GTT GCT GAA ACA GC-3'
<i>hGBP1</i> R	5'-TGA CAG GAA GGC TCT GGT CT-3'
<i>hIRF1</i> F	5'-AGC TCA GCT GTG CGA GTG TA-3'
<i>hIRF1</i> R	5'-TAG CTG CTG TGG TCA TCA GG-3'
<i>hJUNB</i> F	5'-CCT TCT ACC ACG ACG ACT CA-3'
<i>hJUNB</i> R	5'-GCC CTG ACC AGA AAA GTA GC-3'
<i>hMIG1</i> F	5'-CCA CCG AGA TCC TTA TCG AA-3'
<i>hMIG1</i> R	5'-CTA ACC GAC TTG GCT GCT TC-3'
<i>hSOCS3</i> F	5'-AAG CAC AAG AAG CCA ACC AG-3'
<i>hSOCS3</i> R	5'-TTG TGG TTG CTA TCG TCC CA-3'

Grade of purification: HPLC

Hybridized oligonucleotides:

**Table 9:** List of hybridized oligonucleotides

Name	Sequence
2xGAS F	5'-AAG TCG TTT CCC CGA AAT TGA CGG ATT TCC CCG AAA C-3'
2xGAS R	5'-AAG TCG TTT CGG GGA AAT CCG TCA ATT TCG GGG AAA C-3'
M67 F	5'-ACG TCG ACA TTT CCC GTA AAT CTG-3'
M67 R	5'-CAG TCA GAT TTA CGG GAA ATG TCG-3'
GAS-nonGAS F	5'-ACG GCG TTT CCC CGA AAT TGA CGG ATT TAC CCC AAC-3'
GAS-nonGAS R	5'-CAG GGT TGG GGT AAA TCC GTC AAT TTC GGG GAA ACG-3'

Grade of purification: Desalted

### 2.1.10 Enzymes and recombinant proteins

**Table 10:** List of enzymes

Name	Company
DNA Polymerase I – (Klenow fragment)	New England Biolabs
<i>DpnI</i> endonuclease	Stratagene, La Jolla, USA
Jak2 (human recombinant, with N-terminal His-Tag, produced in baculovirus expression system)	Enzo Life Sciences, Farmingdale, USA
peqGOLD DNase I	VWR Peqlab
<i>PfuUltra</i> -HF-DNA-Polymerase	Stratagene, La Jolla, USA
T-cell-protein tyrosine phosphatase (human recombinant, C-terminal 11kDa deletion (TCΔC11) (aa 1-317) produced in <i>E.coli</i> )	Enzo Life Sciences
Trypsin	PAA, Pasching, Austria

**Table 11:** List of recombinant proteins

Name	Company
IFN- $\alpha$ , human, recombinant from <i>E. coli</i>	Biomol, Hamburg, Germany

IFN- $\gamma$ , human, recombinant from <i>E. coli</i>	Biomol
IL-6, human, recombinant from <i>E. coli</i>	Gibco, Thermo Scientific

### 2.1.11 Antibodies

**Table 12:** List of primary antibodies

Name	Company	Concentration ()
Monoclonal ANTI-FLAG M2, Clone M2	Sigma-Aldrich	1:1000
Stat1 (D1K9Y) rabbit monoclonal antibody	Cell Signaling Technology, Danvers, MA, USA	1:1000
Phospho-Stat1 (Tyr701) (58D6) rabbit monoclonal antibody	Cell Signaling Technology	1:1000
Stat3 (D1B2J) rabbit monoclonal antibody	Cell Signaling Technology	1:1000
Phospho-Stat3 (Tyr705) (D3A7) XP rabbit monoclonal antibody	Cell Signaling Technology	1:1000

All antibodies were diluted with 4% BSA in TBS-T for Western blotting or with 25% FBS in PBS in immunofluorescence experiments.

**Table 13:** List of secondary antibodies

Name	Company	Concentration
Donkey anti-rabbit secondary antibody, IRDye 800CW conjugated	LI-COR Biosciences, Bad Homburg, Germany	1:10000 (with 4% BSA in TBS-T for Western blotting)
Cy3-conjugated AffiniPure Goat Anti-Rabbit IgG (H+L)	Jackson Immunoresearch Laboratories, Philadelphia, USA	1:1000 (with 25% FCS in PBS for Immunofluorescence)

### 2.1.12 Plasmids and constructs

**Table 14:** List of plasmids and constructs

Name	Description	Reference
pEGFP-N1	Vector for expression of N-terminal GFP fusion plasmids in mammalian cells	Clontech, Mountain View, USA
pSTAT1 $\alpha$ -GFP <sup>1</sup> (STAT1 WT-GFP)	Human STAT1 $\alpha$ -cDNA (a.a. 1-746) cloned in pEGFP-N1	(Begitt et al., 2000)
pSTAT1 $\alpha$ (Y701F)-GFP <sup>2</sup>	Derived from <sup>1</sup> through sequence-specific mutagenesis using primer pair STAT1 Y701F F/R	For this thesis
pSTAT1 $\alpha$ (R602L/Y701F)-GFP <sup>3</sup>	Derived from <sup>2</sup> through sequence-specific mutagenesis using primer pair STAT1 R602L F/R	For this thesis
pSTAT1 $\alpha$ (R274W/R602L/Y701F)-GFP <sup>4</sup>	Derived from <sup>3</sup> through sequence-specific mutagenesis using primer pair STAT1 R274W F/R	For this thesis
pSTAT1 $\alpha$ (R274W/T385A/R602L/Y701F)-GFP <sup>5</sup>	Derived from <sup>4</sup> through sequence-specific mutagenesis using primer pair STAT1 T385A F/R	For this thesis
pSTAT1 $\alpha$ (R274W/T385A/V426D/T427D/R602L/Y701F)-GFP	Derived from <sup>5</sup> through sequence-specific mutagenesis using primer pair STAT1 V426D/T427D F/R	For this thesis
pSTAT1 $\alpha$ (F77A/R274W/T385A/R602L/Y701F)-GFP	Derived from <sup>5</sup> through sequence-specific mutagenesis using primer pair STAT1 F77A F/R	For this thesis
pSTAT1 $\alpha$ (W37F/R274W/T385A/R602L/Y701F)-GFP	Derived from <sup>5</sup> through sequence-specific mutagenesis using primer pair STAT1 W37F F/R	For this thesis
pSTAT1 $\alpha$ (E524A/R602L/Y701F)-GFP <sup>6</sup>	Derived from <sup>3</sup> through sequence-specific mutagenesis using primer pair STAT1 E524A F/R	For this thesis

pSTAT1 $\alpha$ (E524A/R586E/R602L/Y701F)- GFP	Derived from <sup>6</sup> through sequence-specific mutagenesis using primer pair STAT1 R586E F/R	For this thesis
pSTAT1 $\alpha$ ( $\Delta$ N)-GFP <sup>7</sup>	Human STAT1 $\alpha$ -cDNA (deletion of NTD) cloned in pEGFP-N1	A kind gift from Prof. Uwe Vinkemeier, Nottingham
pSTAT1 $\alpha$ ( $\Delta$ N/Y701F)-GFP <sup>8</sup>	Derived from <sup>7</sup> through sequence-specific mutagenesis using primer pair STAT1 Y701F F/R	For this thesis
pSTAT1 $\alpha$ ( $\Delta$ N/R602L/Y701F)- GFP	Derived from <sup>8</sup> through sequence-specific mutagenesis using primer pair STAT1 R602L F/R	For this thesis
pSTAT1 $\alpha$ (R274W/T385A/L407 A/L409A/R602L/Y701F)-GFP	Derived from <sup>5</sup> through sequence-specific mutagenesis using primer pair STAT1 L407A/L409A F/R	For this thesis
pSTAT1 $\alpha$ -Flag (WT-Flag)	Human STAT1 $\alpha$ -cDNA fused with a Flag tag	(Meyer et al., 2002)
pcDNA3.1-STAT1 $\alpha$ (Untagged STAT1)	Full-length human STAT1 $\alpha$ -cDNA cloned into the pcDNA3.1 mammalian expression vector (Invitrogen)	Prof. James E. Darnell, New York, USA (Meyer et al., 2002)
pbGal	$\beta$ -Galactosidase expression vector	Stratagene
pGAS3xLy6E	IFN $\gamma$ -dependent reporter gene vector	(Wen et al., 1995)
pcDNA FRT spez STAT3 GFP <sup>9</sup>	Full-length murine STAT3 $\alpha$ -cDNA cloned in pEGFP-N1	(Domoszlai et al., 2014); a kind gift from Prof. Gerhard Müller-Newen, Uniklinik RWTH Aachen



pSTAT3 $\alpha$ (V77A)-GFP	Derived from <sup>9</sup> through sequence-specific mutagenesis using primer pair STAT3 V77A F/R	For this thesis
pSTAT3 $\alpha$ (F174A)-GFP	Derived from <sup>9</sup> through sequence-specific mutagenesis using primer pair STAT3 F174A F/R	For this thesis
pSTAT3 $\alpha$ (R609L)-GFP	Derived from <sup>9</sup> through sequence-specific mutagenesis using primer pair STAT3 R609L F/R	For this thesis
pSTAT3 $\alpha$ (Y705F)-GFP <sup>10</sup>	Derived from <sup>9</sup> through sequence-specific mutagenesis using primer pair STAT3 Y705F F/R	For this thesis
pSTAT3 $\alpha$ (R609L/Y705F)-GFP	Derived from <sup>10</sup> through sequence-specific mutagenesis using primer pair STAT3 R609L F/R	For this thesis
pcDNA5 spez muSTAT3 SNAP HIS <sup>11</sup>	Full-length murine STAT3 $\alpha$ -cDNA cloned in pcDNA5/FRT/TO-SNAP-YFP	(Domoszlai et al., 2014); A kind gift from Prof. Gerhard Müller-Newen, Uniklinik RWTH Aachen
pSTAT3 $\alpha$ (V77A)-SNAP	Derived from <sup>11</sup> through sequence-specific mutagenesis using primer pair STAT3 V77A F/R	For this thesis
pSTAT3 $\alpha$ (F174A)-SNAP	Derived from <sup>11</sup> through sequence-specific mutagenesis using primer pair STAT3 F174A F/R	For this thesis
pSTAT3 $\alpha$ (R609L)-SNAP	Derived from <sup>11</sup> through sequence-specific mutagenesis	For this thesis

	using primer pair STAT3 R609L F/R	
pSTAT3 $\alpha$ (Y705F)-SNAP <sup>12</sup>	Derived from <sup>11</sup> through sequence-specific mutagenesis using primer pair STAT3 Y705F F/R	For this thesis
pSTAT3 $\alpha$ (R609L/Y705F)- SNAP	Derived from <sup>12</sup> through sequence-specific mutagenesis using primer pair STAT3 R609L F/R	For this thesis

### 2.1.13 Bacterial strains and media

#### *E.coli* DH5 $\alpha$ (Stratagene)

Genotype: *F- $\phi$ 80dlacZDM15 D(lacZYA-argF) U169 recA1 endA1 hsdR17(rk- mk+) phoA supE44  $\lambda$ thi-1 gyrA96 relA1*

#### *E.coli* XL1blue (Stratagene)

Genotype: *recA1 endA1 gyrA96 thi-1 hsdR17 supE44 relA1 lac [F'proAB lacIq ZAM15 Tn10 (Tetr )]*

Bacterial cultures were grown in either LB or SOC medium (Bioline, Luckenwalde, Germany) with appropriate additives. Antibiotic selection of bacterial colonies was done on LB agar plates.

LB medium

Composition: 10 g/L Bacto-Tryptone, 10 g/L NaCl, 5 g/L Yeast

The medium pH was adjusted to 7.0 with NaOH, and then autoclaved for 30 min at 121°C and 1.5 bar.

LB agar plates

15 g/L agar was added to the LB medium before autoclaving and antibiotic selection plates were made, after cooling the medium to ~55°C and adding kanamycin or ampicillin at a final concentration of 50  $\mu$ g/mL.

## 2.2 Methods

### 2.2.1 Cell culture

#### 2.2.1.1 Cultivation of mammalian cells

The cells used in this thesis (see 2.1.1) were cultured in their respective medium at 37 °C in a 5% CO<sub>2</sub> humidified atmosphere. The cell culture media used were as follows:

HeLa-S3	RPMI supplemented with 10% foetal calf serum (FBS) (Biochrom), 1% penicillin/streptomycin
U3A	DMEM supplemented with 10% foetal calf serum (FBS), 1% penicillin/streptomycin, 0.04 µg/mL puromycin (Sigma-Aldrich)

#### Passaging of cells in culture

Cells were passaged every 2 to 3 days. This was done by washing adherent cells with PBS (sterile, without Ca<sup>2+</sup> and Mg<sup>2+</sup>) and followed by incubation with trypsin/EDTA (0.05% trypsin, 0.2 g/L EDTA) for 3-4 min. Trypsin was subsequently inactivated by adding culture medium and cells were diluted to 1:8 – 1:10 before plating.

#### Freezing of cells for storage

Cells at a confluence of ~70% were washed with PBS and detached with trypsin. The cell suspension was collected and centrifuged at 800 rpm for 10 min at room temperature (RT). The resulting supernatant was discarded, the pellet resuspended in the respective freezing medium, and aliquots of 1.5 x 10<sup>6</sup> cells in 1 mL freezing medium were transferred to cryotubes. The tubes were transferred to a freezing container to facilitate gradual cooling to -80°C and were later stored at -80°C. The freezing medium comprised of the respective culture medium supplemented with 20% FBS and 7.5% DMSO.

#### Thawing of cells into culture

To thaw previously frozen cells, a cryovial of cells was taken from -80°C and immediately warmed in a water bath at 37°C. Upon melting of most of the cell suspension, the contents of the vial were added to 10 mL pre-warmed culture medium. The resulting larger suspension was then centrifuged at 800 rpm for 10 min at RT, to get rid of the remnants of DMSO and freezing medium from the cell suspension. The supernatant generated at this step was discarded and the pellet was resuspended in 10 mL pre-warmed culture medium and seeded into a T75 culture

flask. The cells were passaged upon confluence and media was changed in order to encourage cell growth.

### 2.2.1.2 Transfection

Depending on the suitability of the experiment, cells were cultured to a confluence of 50-70% in 6-well, 48-well or 8-chamber slides. Transfection of these cells with plasmid DNA was done using MegaTran 2.0 according to the manufacturer's instructions.

The protocol was optimized for the cell lines used as follows:

<u>Cell lines</u>	<u>DNA : MegaTran 2.0 ratio</u>
HeLa-S3	1:2 (media was replaced 30 mins prior to transfection)
U3A	1:3

<u>Well-type</u>	<u>DNA per well (<math>\mu\text{g}/\mu\text{L}</math>)</u>	<u>150 mM NaCl per well (<math>\mu\text{L}</math>)</u>
6-well plate	2 $\mu\text{g}$	200 $\mu\text{L}$
48-well plate	0.57 $\mu\text{g}$	50 $\mu\text{L}$
8-chamber slide	0.25 $\mu\text{g}$	30 $\mu\text{L}$

After transfection, cells were cultured for 24 h to allow for uptake and expression of the vector prior to stimulation.

### 2.2.1.3 Stimulation of cells with cytokines and inhibitors

In all experiments, unless otherwise stated, the cells were stimulated with 50 ng/mL human recombinant IFN $\gamma$ , 50 ng/mL human recombinant IFN $\alpha$  or 25 ng/mL human recombinant IL-6. All cytokines and inhibitors used were diluted directly in cell culture medium. The staurosporine treatment took place at a concentration of 1  $\mu\text{M}$ .

## 2.2.2 Molecular biology methods

### 2.2.2.1 Mutagenesis

Point mutations in STAT-encoding plasmids were introduced using the QuikChange II Site-Directed Mutagenesis Kit. For a PCR reaction mixture of 50  $\mu\text{L}$ , 25 ng template DNA, 125 ng each of the complementary primer pair, 5  $\mu\text{L}$  10x reaction buffer, 1  $\mu\text{L}$  dNTP mix and 2.5 units

PfuUltra HF DNA polymerase were used. The PCR protocol consisted of a 30 sec denaturation step at 95°C, followed by 16 repetitive cycles of 30 sec denaturation at 95°C, 1 min annealing step at 55°C and 14 min elongation step at 68°C. To remove the methylated parental DNA, the amplified plasmids were incubated with 10 units of *DpnI* endonuclease, for 1 hour at 37°C. For further transformation into XL1-blue super-competent *E. coli* cells, 2 µL of the unmethylated double-stranded DNA were used.

#### **2.2.2.2 Production of chemically competent bacteria**

To produce chemically competent bacteria, 50 mL of LB medium were inoculated with 500 µL of an *E. coli* DH5α overnight culture and cultivated at 37°C and 225 rpm up to an OD<sub>600</sub> of 0.2-0.5. The bacterial culture was cooled on ice for 10 min and centrifuged for 10 min at 3000 rpm and 4°C. The subsequent pellet obtained was then resuspended in 5 mL ice-cold TSS buffer (10% PEG 8000, 5% DMSO, 30 mM MgCl<sub>2</sub>, 1x LB). Aliquots of the resulting bacterial suspension (100 µL) were stored at -80 °C.

#### **2.2.2.3 Transformation of plasmid DNA into competent bacteria**

Plasmid DNA was transformed into competent bacteria using the heat shock method (Cohen et al., 1972). For this purpose, 100 µL competent *E. coli* DH5α bacterial cells or 50 µL super-competent XL1-blue *E. coli* cells were gradually thawed on ice and incubated on ice for 30 min with 10 ng of plasmid DNA or 1 µL of the mutagenesis product, respectively. Subsequent heat shock was done at 42°C and 30 sec for DH5α cells or 45 sec for XL1-blue cells. After a 2 min incubation on ice, the bacteria were added to pre-warmed 1 mL LB medium for DH5α cells or 500 µL SOC medium for XL1-blue cells and incubated at 37°C and 225 rpm for 1 h. Finally, 250 µL of the resulting bacterial suspension were then applied to an LB agar plate consisting of the appropriate selection antibiotic marker for the plasmid used and incubated at 37°C overnight.

#### **2.2.2.4 Isolation of plasmid DNA from bacteria**

##### Preparation of plasmid DNA for sequencing purposes

From the bacterial colonies grown on agar plates as described above, a bacterial colony was used to inoculate 5 mL LB medium with the appropriate selection antibiotic marker and incubated overnight at 37°C and 225 rpm. Subsequently, 2 mL of this overnight culture were pelleted at 13,000 rpm for 5 min. The plasmid DNA was isolated from the bacterial pellet using the peqGold Plasmid Miniprep Kit according to the manufacturer's instructions and used for sequencing.

### Preparation of plasmid DNA for experimental purposes

For preparative approaches, 100 mL of LB medium with the appropriate selection antibiotic marker were inoculated with a bacterial colony and incubated overnight at 37°C and 225 rpm. The bacterial suspension was then centrifuged at 6000 g for 15 min and plasmid DNA was isolated from the bacterial pellet using the QIAGEN Plasmid Plus Purification Kit. After the plasmid DNA was eluted with water, the concentration was determined, and the DNA was diluted to a working concentration of 1 µg/µL. The plasmid DNA was aliquoted to smaller volumes and stored at -20°C.

#### **2.2.2.5 Sequencing**

Sequencing was performed on all samples to check for the presence of point mutations. For this purpose, 1 µg of plasmid DNA was mixed with 40 pmol of the corresponding sequencing primer and made up to 15 µL with water. The samples were sequenced at SeqLab Sequencing Laboratories (Göttingen).

#### **2.2.2.6 Determination of the concentration of DNA**

The concentration of DNA was determined photometrically using quartz cuvettes at a wavelength of  $\lambda=260$  nm, wherein an OD<sub>260</sub> corresponds to 50 µg/mL DNA. The samples were measured using the BioPhotometer Plus (Eppendorf). The concentration was calculated using the following formula:

$$\text{DNA concentration } [\mu\text{g/mL}] = A_{260} \times 50 \times \text{dilution factor}$$

Contamination from proteins or other reagents was determined by measuring the absorption at  $\lambda=280$  nm and  $\lambda=230$  nm and forming the quotient  $A_{260}/A_{280}$  and  $A_{260}/A_{230}$ , respectively. Uncontaminated DNA samples generally had an  $A_{260}/A_{280}$  ratio of ~1.8 and an  $A_{260}/A_{230}$  ratio of ~2.1.

#### **2.2.2.7 Production of cell extracts**

Whole cell extracts were used for Western blot analyses, EMSA experiments, *in vitro* phosphorylation and *in vitro* dephosphorylation experiments. Towards this purpose, experimentally treated cells were washed first with sterile PBS, and then incubated with ice-cold cytosolic extraction buffer (20 mM HEPES, pH 7.4, 10 mM KCl, 10% (v/v) glycerol, 1 mM EDTA, 0.1 mM Na<sub>3</sub>VO<sub>4</sub>) freshly prepared by adding 0.1% IGEPAL-CA-360, 3 mM DTT, 0.4 mM Pefabloc and Complete mini protease inhibitors. The cells were incubated with the cytosolic extraction buffer for 5 min on ice, to induce cell lysis. The amount of buffer required

was based on the size of the cell culture dish and density of cell growth. For one well of a 6-well plate, 50-60  $\mu$ L of buffer were generally used.

After the incubation, the cells were scraped using a cell scraper, and collected in 1.5 mL reaction tubes. The lysates were centrifuged for 15 sec at 13,000 rpm and 4°C, to sediment the cell nuclei. The supernatants were transferred to new tubes and centrifuged again for 5 min at 11,000 rpm and 4°C. The cytosolic extracts thus obtained were mixed with an equal amount of nuclear extracts and, if not used directly, were frozen at -80°C for further experiments.

The pelleted cell nuclei were resuspended in nuclear extraction buffer (20 mM HEPES, pH 7.4, 420 mM KCl, 20% (v/v) glycerol, 1 mM EDTA, 0.1 mM Na<sub>3</sub>VO<sub>4</sub>) to which 3 mM DTT, 0.4 mM Pefabloc and Complete mini protease inhibitors were added, right before use. The amount of nuclear extraction buffer used was equal to the corresponding cytosolic extraction buffer. The tubes containing the resuspended nuclear pellet were incubated on ice for 30 min. After centrifugation at 13,000 rpm and 4°C for 15 minutes, the nuclear extracts were mixed with the same amount of cytosolic extracts and, if not used directly, stored at -80°C for further experiments. For Western blot experiments, the extracts were mixed with 6x SDS sample buffer (350 mM Tris-HCl, pH 6.8, 8% SDS, 30% glycerol, 10%  $\beta$ -mercaptoethanol, 0.04% bromophenol blue), denatured for 3 min at 95°C and stored at -20°C.

#### **2.2.2.8 SDS polyacrylamide gel electrophoresis (SDS-PAGE)**

In this thesis, STAT proteins were separated electrophoretically according to their size in a discontinuous polyacrylamide gel and then used for immunoblotting experiments. The vertical gel electrophoresis system Minigel-Twin (Biometra, Göttingen) was used for SDS-PAGE. The SDS-PAGE separation gels were made with 10% (v/v) Rotiphorese Gel 30 (acrylamide/bisacrylamide (37.5:1) solution) and 0.03% ammonium persulphate (APS) and 0.16% TEMED in 4x separation gel buffer (1.5 M Tris-Base, 0.4% SDS, pH 8.8). The stacking gel consisted of 5% Rotiphorese Gel 30, 0.06% APS, 0.2% TEMED in 4x stacking gel buffer (0.5 M Tris-HCl, 0.4% SDS, pH 6.8). The fresh or frozen protein lysates containing SDS sample buffer were reheated for 3 min at 95°C immediately before loading, and 16-20  $\mu$ L were loaded to the gel pockets. The electrophoresis was carried out at a constant current of 11 mA per gel in SDS running buffer (Rotiphorese 10x SDS-PAGE diluted 1x using distilled water).

### **2.2.2.9 Western blot and immunochemical protein detection**

The proteins separated by SDS-PAGE were transferred to a PVDF membrane (Millipore) for immunological detection. The electro-transfer was done according to a semi-dry method for 90 min at 80 mA per gel in the PerfectBlue Semi-Dry Sedec M blotter apparatus (VWR Peqlab). Prior to transfer, the membrane was hydrophilized in methanol for 5 min and then washed with transfer buffer (25 mM Tris base, 150 mM glycine, 10% methanol, pH 8.0) for at least 30 min. After the transfer, the free binding sites on the membrane were blocked using 4% BSA in TBS-T (Tris-buffered saline supplemented with Tween-20 (137 mM NaCl, 10 mM Tris-HCl, pH 7.4 and 0.1% Tween-20)) by shaking for 1 hour. The blots were then incubated overnight at 4°C by gentle shaking with the diluted primary antibody.

After washing five times for 5 min each with TBS-T, the membranes were incubated with the IRDye 800CW conjugated secondary antibody (LI-COR Biosciences) corresponding to the origin of the primary antibody, for 1 hour at RT with shaking in low-light conditions. The blots were given a 5 min wash for five times with TBS-T, followed by a last wash with TBS (without Tween-20). The proteins on the membrane were detected using the Odyssey CLx Near Infrared Fluorescence Imaging System (LI-COR Biosciences).

### **2.2.2.10 Immunocytochemistry and fluorescence microscopy**

For fluorescence microscopy analyses, cells were cultivated on 8-chamber LabTek chamber slides and transfected with STAT1 or STAT3 vectors. Cells expressing GFP-tagged STAT1 or STAT3 were stimulated 16-24 hours post-transfection, as indicated, and then fixed with 4% formaldehyde-PBS (37% formaldehyde stock diluted in non-sterile 1x PBS (137 mM NaCl, 2.7 mM KCl, 10 mM Na<sub>2</sub>HPO<sub>4</sub>, 1.8 mM KH<sub>2</sub>PO<sub>4</sub>, pH 7.4) for 15 min at RT with shaking. This was followed by two washing steps: with non-sterile PBS and distilled water, consecutively. Thereafter, the nuclei were stained with Hoechst 33258 (5 µg/mL in PBS, Sigma-Aldrich) for 10 min at RT with shaking. After washing again with non-sterile PBS and distilled water, the chamber slides were mounted with coverslips using Fluoromount-G mounting medium (Southern Biotech, Birmingham, USA).

For the labelling of SNAP-tagged STAT3 proteins, cells transfected with SNAP-tagged, STAT3-coding vectors were incubated with media containing red fluorescent substrate SNAP-Cell TMR-Star (New England Biolabs). For this purpose, the existing media on the cells were discarded and 60 µL per chamber of pre-warmed culture media containing SNAP-Cell TMR-Star at a concentration of 1:2000 were added and incubated for 30 min in a 37°C, 5% CO<sub>2</sub>



humidified incubator. Following the SNAP-tag labelling reaction, the cells were washed thrice with pre-warmed media and incubated in fresh culture media for an addition of 30 min. The cells were then stimulated, fixed and mounted, as described above.

For the immunocytochemical detection of endogenous/Flag-tagged STAT1 proteins, the cells were first fixed with methanol for 15 min at -20°C, before they were permeabilized with 1% Triton X-100 in PBS for 20 min. To saturate unspecific binding sites, the cells were treated with 25% FBS-PBS (25% FBS in PBS) for 45 minutes with shaking. This was followed by a 45 min incubation at RT while shaking with the primary antibody (1: 1000 in 25% FBS-PBS). Then the cells were washed thrice with PBS. To fluorescently detect the primary antibody, a Cy3-coupled anti-rabbit IgG secondary antibody from goat (1:1000 in 25% FBS-PBS) was added and incubated for 45 min at RT with shaking. The preparations were then washed thrice with PBS, and the nuclei were stained with Hoechst 33258 before mounting with coverslips, as described above.

The slides generated as a part of the fluorescence microscopy experiments were visualized using the Nikon Ti Eclipse fluorescence microscope. Fluorescence microscopic images were taken of the samples with a Nikon DS-Qi2 camera and processed using the associated software NIS elements (Nikon). GFP-coupled fusion proteins were visualized at an excitation wavelength of 480 nm, Cy3-coupled antibodies at 550 nm and Hoechst-stained cell nuclei at 280 nm. The further processing of the digitally stored data was done using image processing software Fiji (NIH) and CorelDRAW 2019 graphics suite (Corel Corporation, Ottawa, Canada).

#### **2.2.2.11 Reporter gene assay**

To analyse the promoter binding efficiency of STAT1 and STAT3 WT and mutant proteins, luciferase reporter gene assays were performed. For this purpose, a luciferase-coding reporter gene construct of the *Ly6E* gene was used, which has three IFN $\gamma$ -sensitive GAS binding sites in its promoter (Khan et al., 1993; Wen et al., 1995). For normalization purposes, a constitutively expressed  $\beta$ -galactosidase reporter was co-transfected and the  $\beta$ -galactosidase activity was determined from the same extracts.

U3A cells or HeLa cells were cultivated in 48-well culture dishes and each well was transfected with a mixture of 250 ng of a single or a combination of STAT-encoding plasmids, 200 ng of the  $\beta$ -galactosidase reporter and 70 ng of the 3xLy6E plasmid. On the next day 16-24 hours

after the transfection, the cells were either left untreated or stimulated with either IFN $\gamma$  or IL-6 for 6 hours. After the stimulation, the medium was aspirated, and the cells were washed once with sterile PBS. The cells were then lysed by adding 100  $\mu$ L per well of Triton-glycylglycine lysis buffer (25 mM glycylglycine, pH 7.8, 1% Triton X-100, 15 mM MgSO $_4$ , 4 mM EGTA), to which 3 mM DTT, 0.4 mM Pefabloc and Complete mini protease inhibitors were added right before use. The lysis reaction was carried out for 15 min at RT. The lysates were then transferred to 1.5 mL reaction tubes and centrifuged for 15 min at 13,000 rpm and 4°C. Then, 20  $\mu$ L of the supernatants were pipetted into a white 96-well plate (Nunc, Roskilde, Denmark) and the luciferase activity was measured upon adding 50  $\mu$ L luciferase assay system substrate solution (Promega) using Centro-LB-960 luminometer (Berthold Technologies, Bad Wildbad, Germany).

To quantify the transfection efficiency, 20  $\mu$ L of lysate were mixed with 280  $\mu$ L of a substrate solution consisting of 211  $\mu$ L of sodium phosphate buffer (10 mM, pH 7.2), 66  $\mu$ L of o-nitrophenyl- $\beta$ -D-galactopyranoside (ONPG, 4 mg/mL in 100 mM sodium phosphate buffer) and 3  $\mu$ L of a 100x magnesium solution (100 mM MgCl $_2$ , 4.5 mM  $\beta$ -mercaptoethanol). The enzymatic colour reaction was stopped after approximately 20 min with 500  $\mu$ L of a 0.5 M Na $_2$ CO $_3$  solution and the  $\beta$ -galactosidase activity was determined photometrically at 420 nm using Infinite 200 PRO plate reader (Tecan Life Sciences, Männedorf, Switzerland). Six measurements were done for each STAT construct and the normalization was performed by determining the quotient of luciferase activity and  $\beta$ -galactosidase expression.

#### **2.2.2.12 Dephosphorylation assay**

Cytokine-stimulated cells expressing the recombinant STAT protein of interest were used for total protein extraction. For the *in vitro* dephosphorylation, 10  $\mu$ L of dephosphorylation buffer (25 mM Tris-HCl, pH 7.5, 0.5 mg/mL BSA, 50 mM KCl, 5 mM EDTA) to which 20 mM DTT, Complete mini protease inhibitors and two units of T-cell protein tyrosine phosphatase (TC-PTP) (Enzo Life Sciences, USA) were added before using, was mixed with an equal volume (10  $\mu$ L) of total cell extract. In the case of dephosphorylation experiments done in the presence of DNA probes containing a GAS-binding site, 25 nM of a GAS-nonGAS DNA element were added to the dephosphorylation buffer before usage. The samples were incubated at 30°C for the indicated durations. The reaction was stopped by adding 6x SDS sample buffer and heating for 3 min at 95°C. The samples were analysed using polyacrylamide gel electrophoresis with subsequent Western blotting experiments.

For *in vivo* dephosphorylation, U3A cells were transfected in 6-well plates with STAT3-encoding plasmids and stimulated with IL-6 for 30 min. The cells were then washed once with sterile PBS and incubated with staurosporine for the indicated periods of time. Total cell extracts were prepared and the level of dephosphorylation was analysed by means of Western blotting experiments.

#### **2.2.2.13 *In vitro* phosphorylation assay**

Unstimulated cells expressing the STAT plasmid of interest were used for protein extraction. For *in vitro* phosphorylation, 10  $\mu$ L of total cell extract was mixed with 10  $\mu$ L of kinase buffer (50 mM HEPES, pH 7.4, 3 mM MgCl<sub>2</sub>, 3 mM MnCl<sub>2</sub>, 3  $\mu$ M Na<sub>3</sub>VO<sub>4</sub>, 0.1 mM ATP), to which 10 mM DTT and 4  $\mu$ g/mL Janus kinase 2 (JAK2) were added right before usage. The samples were incubated for the indicated times at 30°C. At the end of each incubation time, 6x SDS sample buffer was added and the mixture was heated at 95°C for 3 min to stop the reaction. The subsequent analysis was carried out using Western blotting.

#### **2.2.2.14 Gel retardation experiments (Electrophoretic Mobility Shift Assay, EMSA)**

Protein-DNA interactions were detected using EMSA experiments. For this purpose, radioactively-labelled probes with high-affinity STAT binding sites were incubated with total cell extracts from IFN $\gamma$ - or IL-6-stimulated cells transiently expressing the corresponding STAT1 or STAT3 derivatives. The protein-DNA complexes formed were separated from unbound DNA by means of a native polyacrylamide gel electrophoresis due to their reduced mobility and were detected by auto-radiography.

#### Hybridization reaction

Two different probes were used for EMSA experiments in this thesis. Towards this, the overhangs of complementary oligonucleotides with a single (M67) or double (2xGAS) STAT binding site were radioactively labelled. To produce the double-stranded probes, 50 pmol/mL of complementary oligonucleotides were added in oligo buffer (10 mM MgCl<sub>2</sub>, 50 mM KCl, 20 mM Tris-HCl, pH 7.5) and incubated for 5 minutes at 95°C and subjected to subsequent slow cooling to RT. The hybridized oligonucleotides were then stored at -20°C.

#### Radioactive labelling of double-stranded DNA

The radioactive labelling was carried out by filling the non-complementary 5'-overhanging ends of the hybridized oligonucleotide with radioactive nucleotides. For this purpose, 5 units of the Klenow fragment of *E. coli* DNA polymerase I, which has a 5'-3'-polymerase and a 3'-

5'-exonuclease (proof reading) activity, were added in 5  $\mu$ L 10x Eco-Pol buffer (New England Biolabs) to be mixed with 0.1 ng of double-stranded oligonucleotides and 8  $\mu$ L of [ $^{32}$ P]-labelled adenosine triphosphate (dATP). This mixture was then incubated for 25 min at RT. An excess of non-radioactive dATPs (6.5 mM) was then added for further 5 min and the reaction was stopped by adding 1  $\mu$ L of 0.5 M EDTA solution. Free nucleotides were separated by centrifugation for 3 min at 700 x g and RT with the aid of Illustra MicroSpin G-25 columns (GE Healthcare, Braunschweig, Germany).

#### Gel retardation

For the binding reaction, a mixture of 0.2  $\mu$ L radioactively-labelled DNA probe, 1  $\mu$ L poly-dIdC (2 mg/mL), 1.3  $\mu$ L DTT (100 mM), 3.5  $\mu$ L H<sub>2</sub>O and 2.5  $\mu$ L 5x gelshift buffer (100 mM HEPES, pH 7.9, 200 mM KCl, 5 mM MgCl<sub>2</sub>, 2.5 mM EDTA, 0.5 mM EGTA, 20% Ficoll) were incubated with 4.5  $\mu$ L cell extract for 15 min at RT. With smaller amounts of extract, the samples were made up to a total volume of 13  $\mu$ L with 1x PBS or cell extracts from untransfected U3A cells. In order to show that the resulting signal is the STAT1 or STAT3-DNA complex, 1.3  $\mu$ L of the STAT1 (D1K9Y) rabbit monoclonal antibody (Cell Signalling) or STAT3 (D1B2J) rabbit monoclonal antibody (Cell Signalling) was added to a reaction mixture. When unlabelled oligonucleotides were used as a competitor, 2  $\mu$ L of M67 oligonucleotide at a 750-fold excess were added to the reaction mixture and incubated for 10 min at RT.

Immediately after the reaction, the protein-DNA complexes formed were separated in a native, pre-equilibrated 4.8% TBE-polyacrylamide gel at 400 V and 4°C with 0.25x TBE running buffer for about 2.5 hours. To cast two gels, 12 mL Rotiphorese Gel 40 (acrylamide / bisacrylamide (29:1) solution) were mixed with 2.4 mL 10x TBE and 84 ml H<sub>2</sub>O. The gel was polymerized by adding 2 mL of 10% APS and 100  $\mu$ L of TEMED.

After the end of the electrophoresis, the gel was vacuum-dried at 80°C on Whatman paper (Albet LabScience, Dassel, Germany) and exposed on phosphor-imager film, at least overnight at RT. The films were scanned using the Fuji-BAS-1000 (Fuji, Düsseldorf) software and evaluated with ImageJ and Corel Draw.

#### **2.2.2.15 RNA isolation**

For the isolation of RNA, U3A cells were cultivated in 6-well plates and transfected with the corresponding STAT expression plasmids. The cells were transfected and cultivated overnight

in a medium containing 1% FBS (serum-starved). 24 hours post-transfection, cells were either left untreated or stimulated with 50 ng/mL IFN $\gamma$  (6 hours for STAT1 experiments) or 25 ng/mL IL-6 (3 hours for STAT3 experiments). After aspirating the medium, RNA was isolated using the peqGold Total RNA Kit according to the manufacturer's instructions. 50  $\mu$ L of RNase-free water were used to elute the RNA, and this was either used directly for cDNA synthesis or stored at -80°C.

#### **2.2.2.16 cDNA synthesis**

To produce the complementary DNA (cDNA) from RNA, reverse transcription was carried out using the Verso cDNA synthesis kit. In this reaction, 8  $\mu$ L of RNA were used per 20  $\mu$ L PCR mixture. The cDNA was stored at -20°C.

#### **2.2.2.17 Real-time PCR**

Examination of changes in endogenous gene expression between the different mutants of STAT1 and STAT3 was done by real-time RT-PCR using Absolute Blue QPCR SYBR Green Mix, according to the manufacturer's instructions. For this purpose, STAT1 and STAT3 target genes known from the literature were used and primers were designed using the program Primer3. Primers were obtained from Sigma-Aldrich and diluted to a working concentration of 5  $\mu$ mol/L. For each reaction, the master mix contained 10  $\mu$ L of SYBR green, 0.28  $\mu$ L of each primer and 9.44  $\mu$ L of H<sub>2</sub>O. A volume of 19  $\mu$ L was added to each cavity of a ThermoFast 96-well-plate, and 1  $\mu$ L of the cDNA solution was added to the reaction mix. All qPCR reactions were performed using the Real-time Mastercycler egradient S real-time cycler from Eppendorf. The software program Realplex ep was used to operate and adjust the settings for the real-time cycler. The following program was used: an initial step at 95°C for 15 min, followed by 45 cycles of denaturation at 95°C for 15 sec, annealing at 55°C for 30 sec, and extension at 72°C for 30 sec. *GAPDH* was used as the reference housekeeping gene. Duplicate determinations were carried out in each experiment. Data analysis was performed using the  $2^{-\Delta\Delta CT}$  method.

#### **2.2.3 Statistics**

Western blot analyses, immunocytochemistry, EMSA, dephosphorylation and phosphorylation assays were performed with independent transfections and reaction mixtures for a minimum of three times. Gene expression analyses were performed at least three times in independent transfections. For the reporter gene assays, a six-fold determination was made in each case, and at least three runs were performed for real-time RT-PCR. The mean values and the standard

deviations were determined from the results using Microsoft Office Excel and the statistics were performed on GraphPad PRISM. After checking for normal distribution of the unconnected samples and equality of the variances, the significance was calculated using Student t-test or Mann-Whitney rank sum test. In all tests, a p-value <0.05 was considered statistically significant. Crystallographic data were modified in PyMOL (Schrödinger, Mannheim, Germany). All schematic illustrations were created using BioRender (Toronto, Canada).

### 3. Results

#### 3.1 The relevance of the anti-parallel, unphosphorylated dimer interface in STAT3

##### 3.1.1 Identification of potentially destabilizing mutations in the NTD and CCD of STAT3

As described in the Introduction, STAT1 undergoes a conformational switch between the anti-parallel and parallel dimeric orientations in its activation-deactivation cycle (Mertens et al., 2006; Zhong et al., 2005). Therefore, mutations in the functional domains involved in either of the two conformations may confer an altered phenotype to the STAT1 protein, affecting one or more of its properties. To investigate whether this conformational switch also exists in STAT3, mutations were introduced from literature in the STAT3 functional domains and the resulting mutants were tested. One of the critical components that can enable this switch is a stable STAT3 anti-parallel dimer, the existence of which is under debate. Therefore, the first approach was to investigate STAT3 homologous residues from the anti-parallel CCD-DBD binding interface of STAT1.

Expression vectors encoding full-length murine STAT3 with a carboxy-terminal GFP (green fluorescent protein) or SNAP tag were used to investigate these questions. A mutation was introduced at position F174 in the STAT3 CCD, wherein the parent amino acid phenylalanine was mutated to alanine (Figure 4 B, C). The NTD of STAT1 has been reported to act as a tether, around which the STAT1 core-fragments undergo a reorientation (Mertens et al., 2006). In addition to F174A, a missense mutation was introduced in the STAT3 NTD at position V77, to determine whether this phenomenon can be extended to occur in STAT3 (Figure 4A). As a negative control, the double mutant R609L/Y705F was generated from a combination of the well-characterized mutations R609L and Y705F in the STAT3 SH2 and transactivation domain, respectively. Defective tyrosine phosphorylation and dimerization rendered the single point mutants to be insensitive to cytokine-induced nuclear accumulation, and the same was expected from the double mutant.

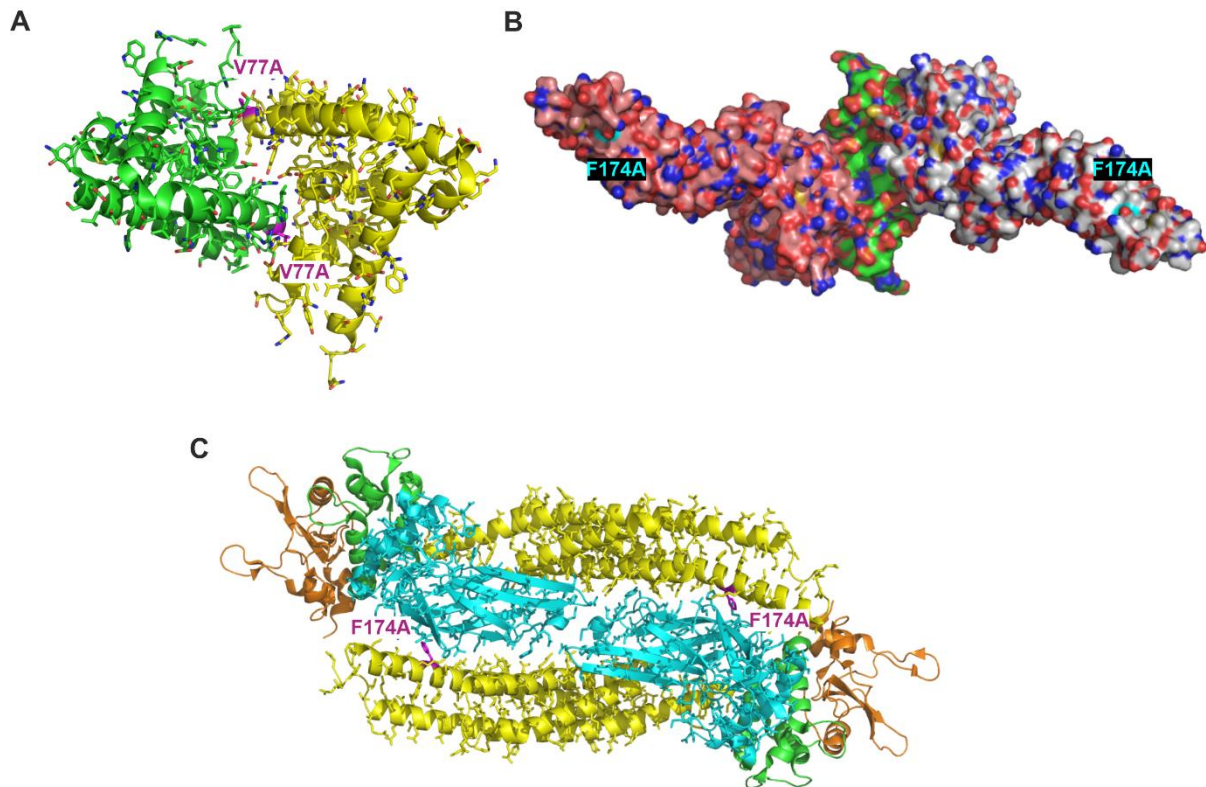


**Figure 4: Crystal structure of STAT3 containing the residues under investigation.**

(A) Shown is an NTD:NTD dimer of STAT3 harbouring the residue V77 (in pink). Mutation of V77 could potentially destabilize NTD interactions in the STAT3 protein. This structure has been created from the crystal structure of the murine STAT3 N-terminal domain (PDB: 4ZIA) (Hu et al., 2015). (B) A DNA-bound STAT3 parallel dimer with residue F174 labelled (in cyan), as revealed from the crystal structure of a murine STAT3 dimer bound to DNA (PDB: 1BG1) (Becker et al., 1998). (C) The localization of F174 (in pink) in an unphosphorylated, anti-parallel STAT3 dimer modified from the crystal structure of human STAT3 complexed with MS3-6 monobody (not shown) (la Sala et al., 2020). Mutation at F174 could potentially disrupt the anti-parallel dimer of STAT3.

### 3.1.2 Prominent nuclear localization of STAT3-V77A and STAT3-F174A mutants

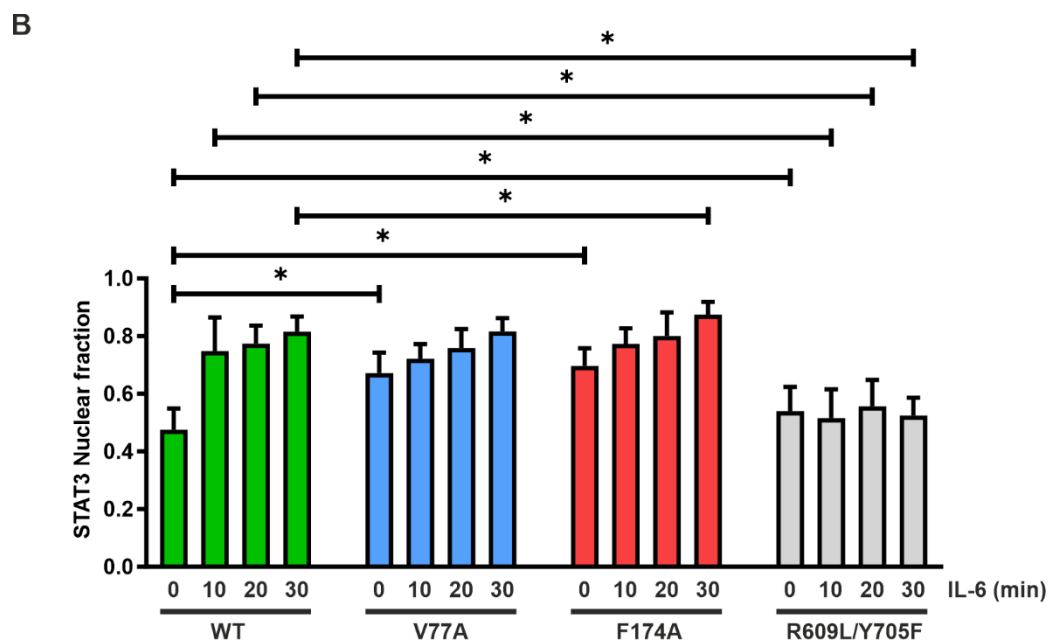
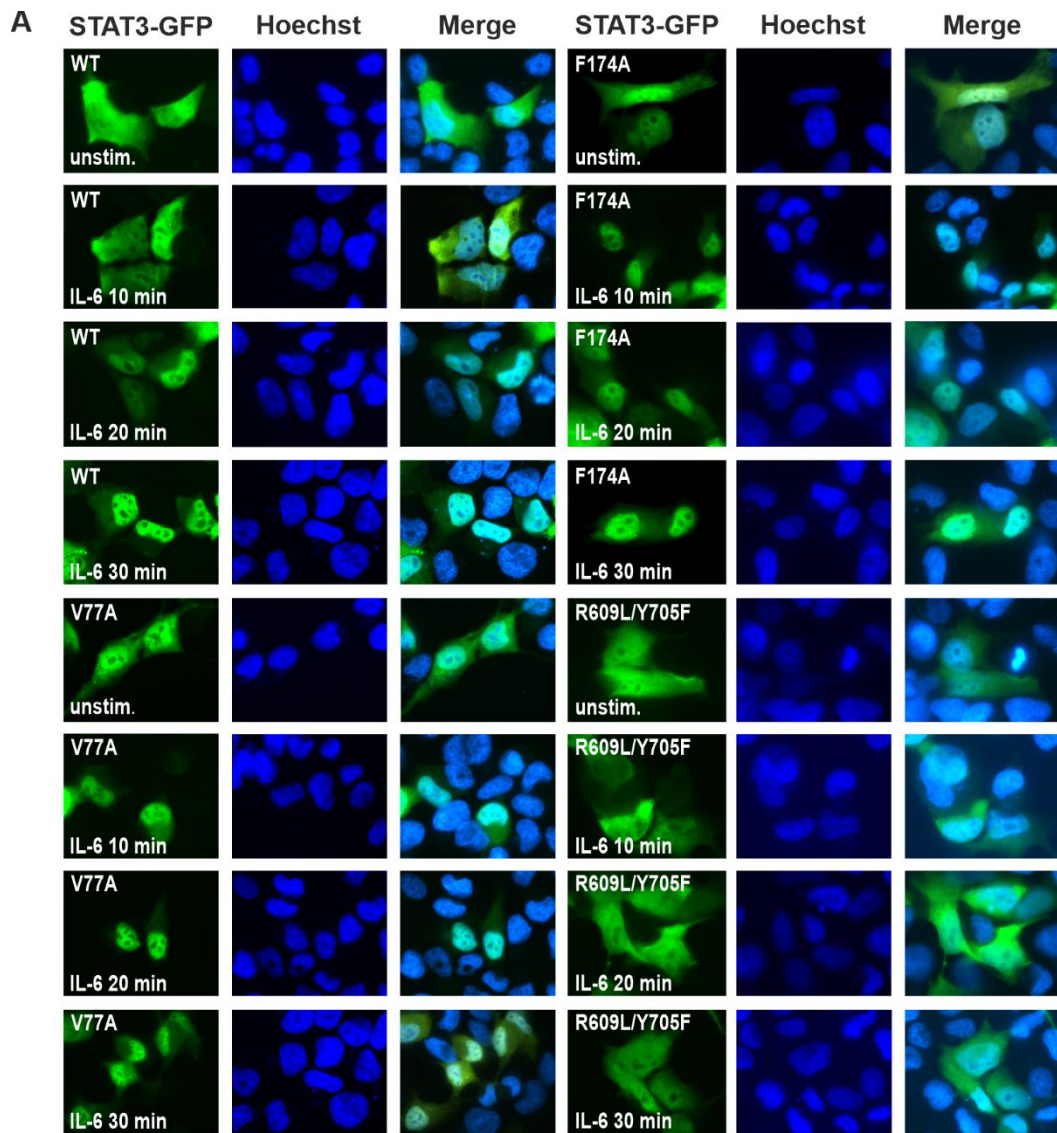
Through site-directed mutagenesis, the above-mentioned mutations were introduced in STAT3-GFP and STAT3-SNAP constructs. When expressed in cells, the localization of GFP-tagged proteins can be visualized from the GFP tag's emission wavelength at 511 nm, upon an excitation at 488 nm (Arpino et al., 2012). The SNAP tag is a mutant of the DNA repair protein O<sup>6</sup>-alkylguanine-DNA alkyltransferase that reacts specifically and rapidly with benzylguanine derivatives, leading to irreversible covalent labelling of the SNAP-tag with a synthetic probe (Keppler et al., 2004). After transfection, SNAP constructs were labelled using a SNAP-Cell TMR-Star substrate (New England Biolabs) that emits at 580 nm, upon excitation at 554 nm. The F77A mutation in the STAT1 NTD, which has been reported to abolish cooperative DNA



binding of STAT1, shows a prolonged nuclear accumulation upon IFN $\gamma$  stimulation (Meyer et al., 2004). Similarly, a mutation at position F172 in the CCD of STAT1, that interacts with residue T385 of the STAT1 DBD in the crystal structure of an anti-parallel STAT1 dimer and stabilizes it, also shows prolonged nuclear accumulation (Staab et al., 2013).

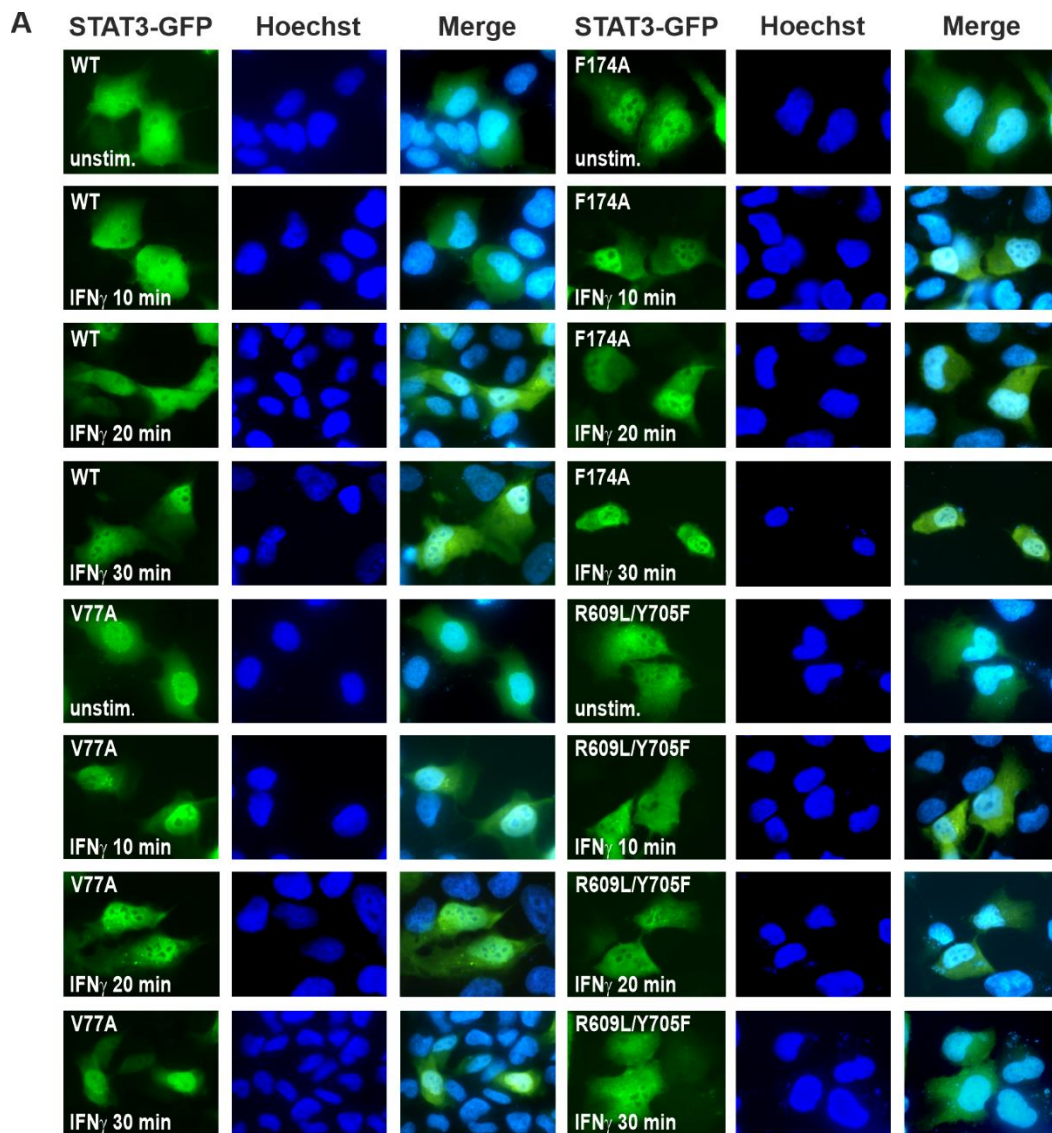
When transfected in STAT1-deficient U3A cells, as expected, both GFP-tagged mutants STAT3-V77A and -F174A, showed a strong nuclear accumulation upon stimulation with recombinant IL-6 (Figure 5 A, B). However, surprisingly both mutated proteins were predominantly nuclear even in the absence of cytokine stimulation. While the WT was predominantly cytoplasmic in unstimulated cells and translocated to the nucleus upon cytokine stimulation, both V77A and F174A showed a nuclear localization in resting cells even before treatment, which mildly increased upon stimulation with IL-6. As expected from the phenotype of the contributing single mutants, the double mutant R609L/Y705F displayed a pan-cellular distribution which did not change upon cytokine stimulation (Figure 5 A, B).

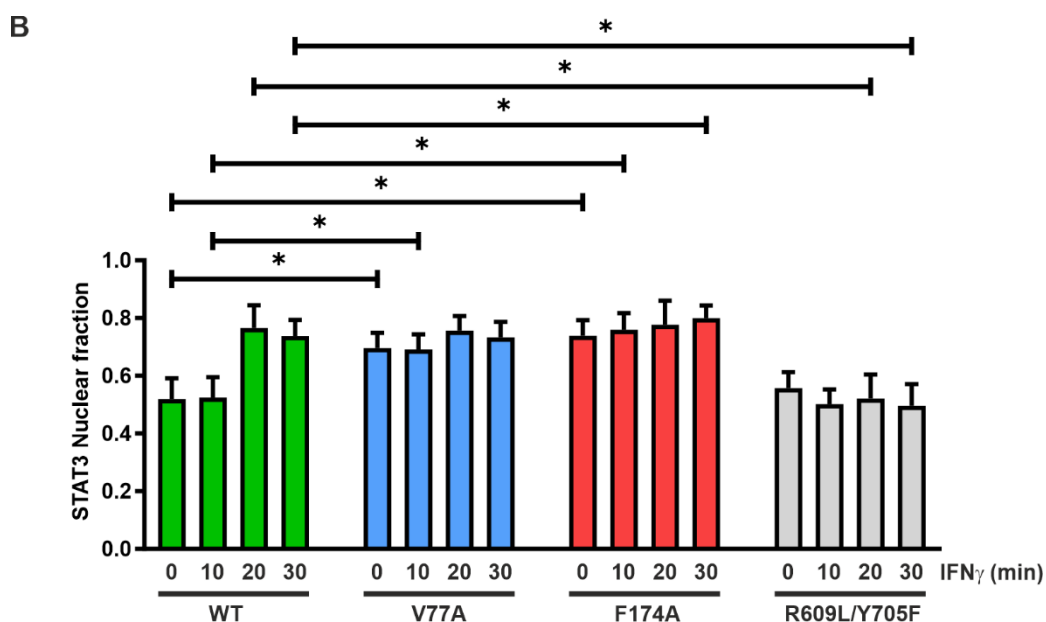
In order to explore these findings with a different cytokine, direct fluorescence microscopy experiments were performed after stimulation of U3A cells expressing the STAT3-GFP variants with recombinant IFN $\gamma$ . Both V77A and F174A proteins were nuclear even before the onset of IFN $\gamma$  stimulation (Figure 6 A, B). Again, the phosphorylation-deficient R609L/Y705F mutant showed no time-dependent changes in its intracellular distribution upon cytokine stimulation, confirming previous data for the single R609Q mutant (Martincuks et al., 2016) (Figure 6 A, B).



**Figure 5: Nuclear distribution of IL-6-stimulated cells expressing STAT3-GFP mutants**

STAT1-negative U3A cells were transfected with GFP-fusion proteins of WT or mutant STAT3 and treated with 25 ng/mL of recombinant IL-6 for the indicated times. (A) The fluorescence micrographs show the intracellular distribution of GFP-tagged STAT3 for the indicated variants as well as the localization of the corresponding Hoechst-stained nuclei (n=3 independent transfections). (B) Histograms demonstrate the nucleocytoplasmic STAT3-GFP distribution in untreated and IL-6-treated cells, as determined by the ratio of nuclear-to-total fluorescence intensity. Asterisks indicate significant differences between the WT protein and the respective mutants.

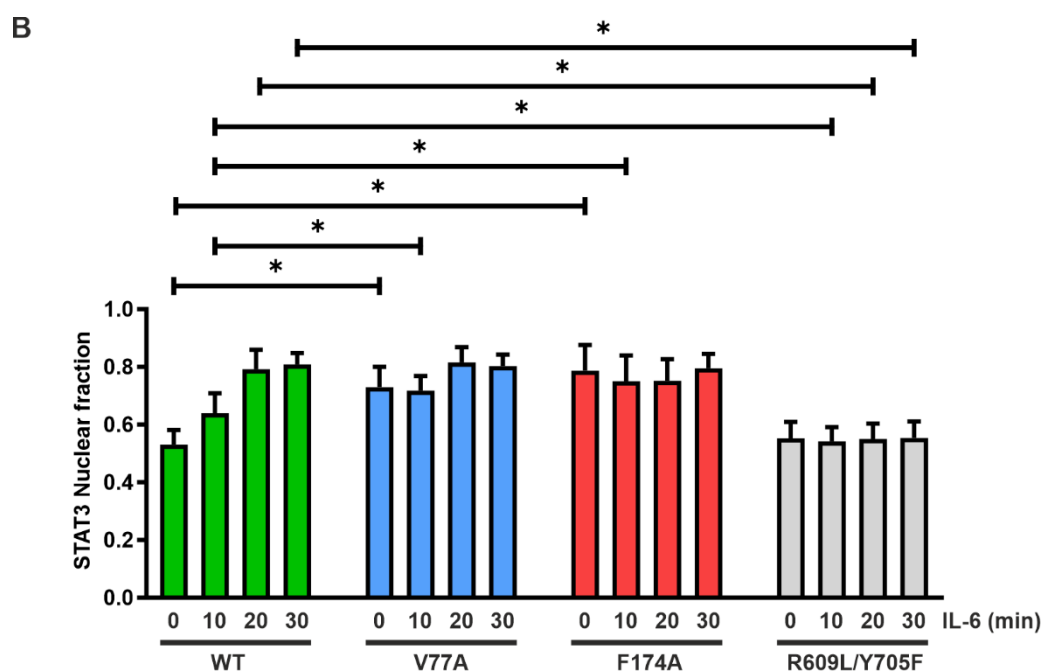
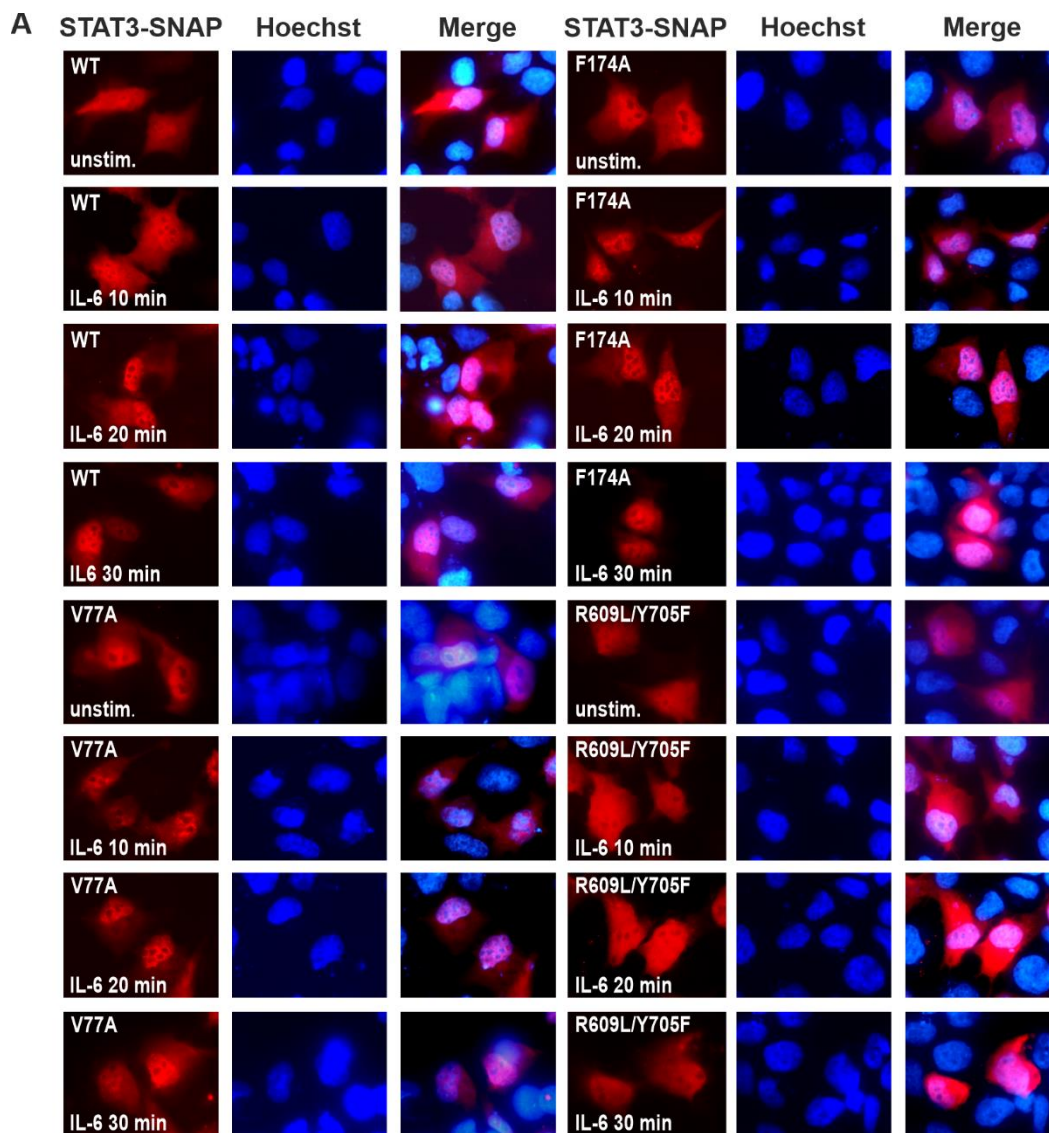




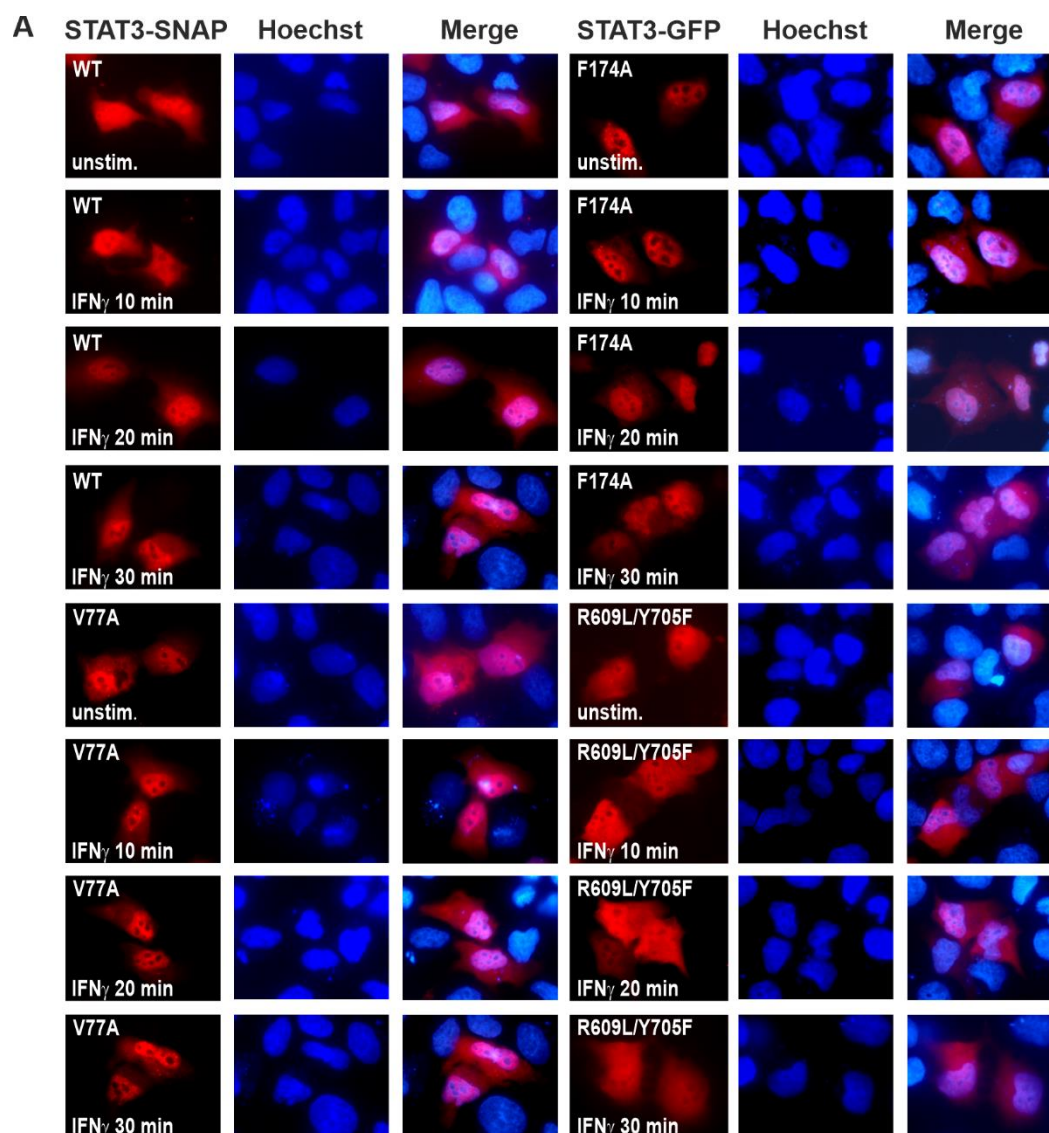
**Figure 6: Intracellular localization of STAT3-GFP mutants in IFN $\gamma$ -stimulated cells**

Transfected STAT1-negative U3A cells expressing GFP-fusion proteins of WT or mutant STAT3 were treated with 50 ng/mL of recombinant IFN $\gamma$  for the indicated times. (A) The fluorescence micrographs show time-dependent changes in the intracellular distribution of GFP-tagged STAT3 for the indicated variants as well as the localization of the corresponding Hoechst-stained nuclei (n=3 independent transfections). (B) Histograms demonstrate the nucleocytoplasmic STAT3-GFP distribution in untreated and IFN $\gamma$ -treated cells, as determined by the ratio of nuclear-to-total fluorescence intensity. Asterisks indicate significant differences between the WT protein and the respective mutants.

To further validate these observations, mutated SNAP-tagged STAT3 expression vectors were used in subsequent transfection experiments. Both V77A- and F174A-SNAP behaved in a similar fashion as their GFP-tagged counterparts with respect to stimulation with IL-6 or IFN $\gamma$  (Figure 7 A, B; Figure 8 A, B). Even before stimulation, the two mutated STAT3 proteins showed a higher concentration in the nucleus as compared to the cytosol. In contrast, no stimulation-dependent accumulation in the nucleus was observed for R609L/Y705F (Figure 7 A, B; Figure 8 A, B).



**Figure 7: Changes in the intracellular distribution of STAT3-SNAP mutants in IL-6-stimulated U3A cells**  
 U3A cells expressing SNAP-fusion proteins of WT or mutant STAT3 were treated with 25 ng/mL of recombinant IL-6 for the indicated times. (A) The fluorescence micrographs show the kinetics of intracellular redistribution of SNAP-tagged STAT3 for the indicated variants as well as the localization of the corresponding Hoechst-stained nuclei (n=3 independent transfections). (B) Histograms demonstrate the nucleocytoplasmic STAT3-SNAP distribution in untreated and IL-6-treated cells, as determined by the ratio of nuclear-to-total fluorescence intensity. Asterisks indicate significant differences between the WT protein and the respective mutants.



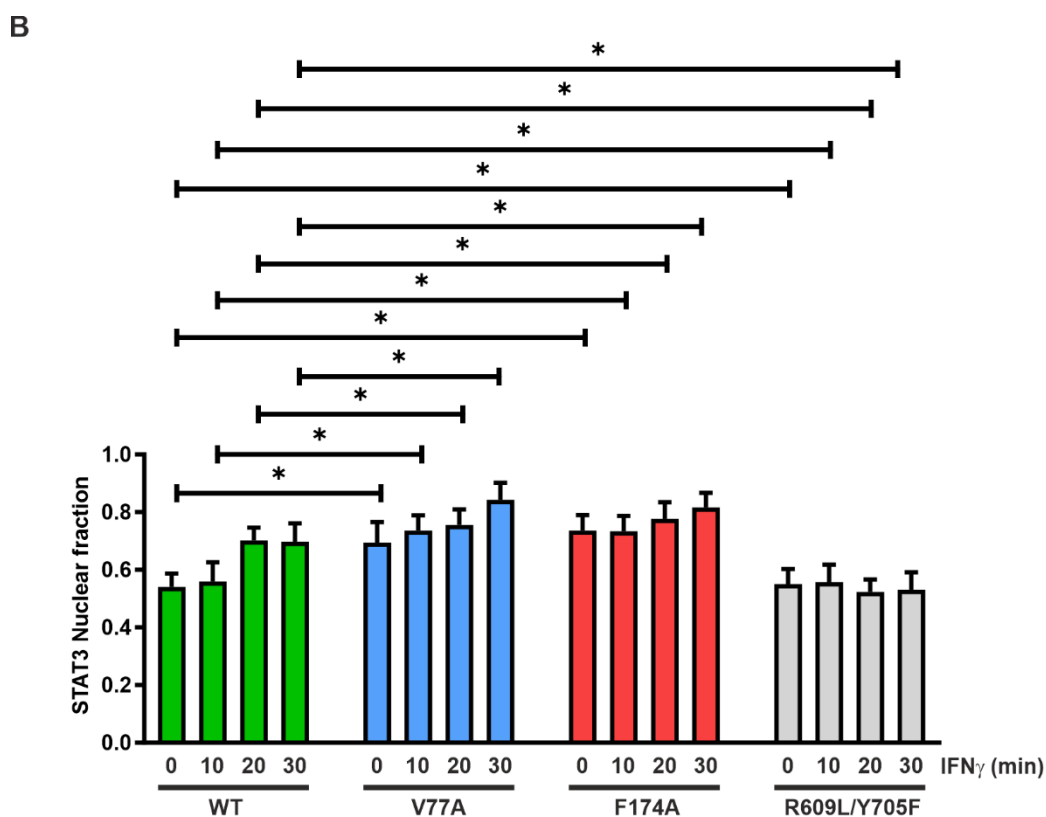


**Figure 8: Time kinetics of IFN $\gamma$ -induced nuclear accumulation of different STAT3-SNAP mutants**

U3A cells expressing SNAP-fusion proteins of WT or mutant STAT3 were treated with 50 ng/mL of recombinant IFN $\gamma$  for the indicated times. (A) The fluorescence micrographs show the intracellular distribution of SNAP-tagged STAT3 for the indicated variants and the localization of Hoechst-stained nuclei (n=3 independent transfections). (B) Histograms demonstrate the nucleocytoplasmic STAT3-SNAP distribution in untreated and IFN $\gamma$ -treated cells, as determined by the ratio of nuclear-to-total fluorescence intensity. Asterisks indicate significant differences between the WT protein and the respective mutants.

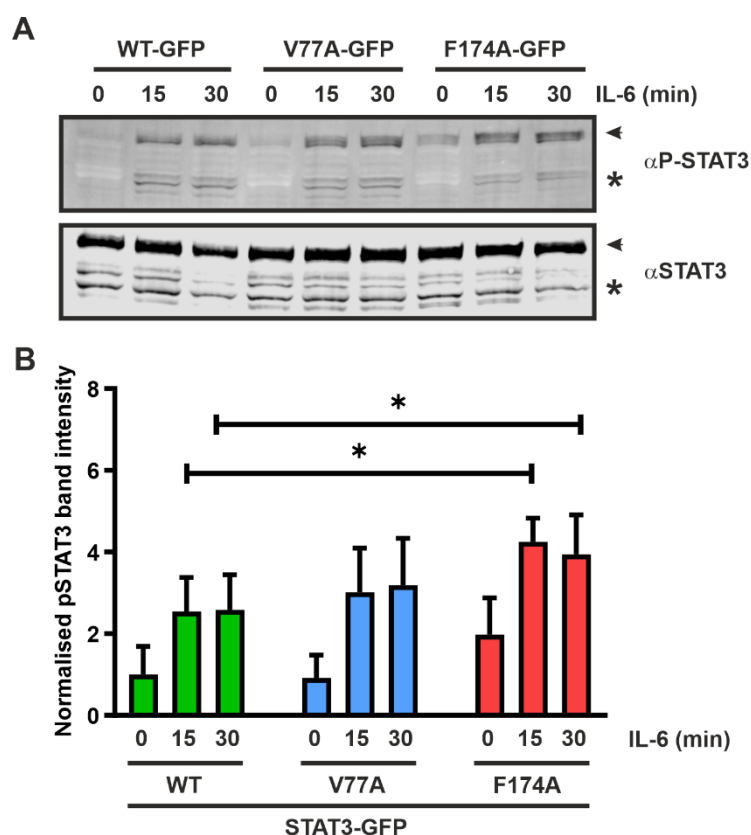
### 3.1.3 Both STAT3 mutants show elevated levels of phosphorylation

To investigate the effect of the NTD and CCD mutants on the levels of STAT3 tyrosine phosphorylation through a time course, U3A cells were transfected with GFP- and SNAP-tagged variants of STAT3. One day after transfection, cells were stimulated with either IL-6 or IFN $\gamma$ , as indicated, and total protein was extracted.

Immunoblotting data confirmed that both mutants demonstrated elevated levels of tyrosine phosphorylation as compared to the WT molecule (Figure 9 A, B; Figure 10 A, B; Figure 11 A, B; Figure 12 A, B). This was expected from the sequence homology and structural similarities between STAT1 and STAT3. The homologous STAT1 mutations F77A and F172W also showed higher levels of cytokine-stimulated tyrosine phosphorylation as

compared to WT STAT1 (Zhong et al., 2005). Therefore, STAT3 and STAT1 homologous mutations behaved similarly with respect to the kinetics of tyrosine phosphorylation.

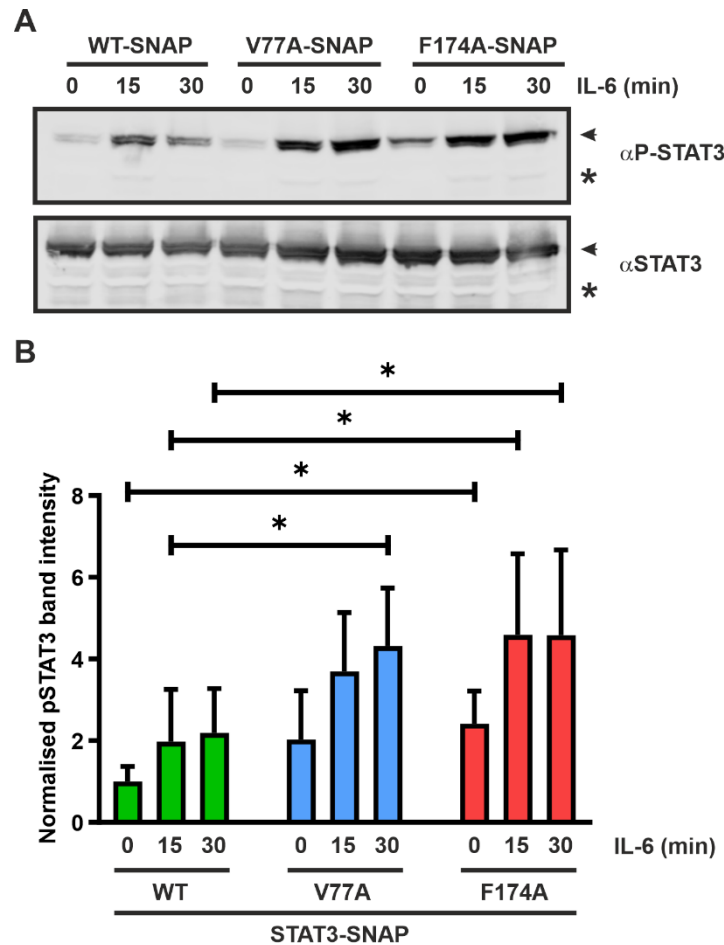
Interestingly, there was a detectable tyrosine phosphorylation for F174A, even in the absence of cytokine stimulation. This prominent hyperactivation and nuclear distribution of the STAT3 mutants even in resting cells presented a point at which the behaviour of STAT1 and STAT3 diverged.



**Figure 9: Elevated tyrosine phosphorylation levels of STAT3-GFP mutants in IL-6-treated cells**

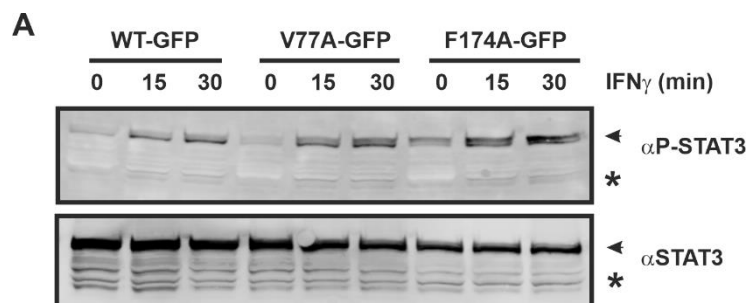
U3A cells expressing GFP fusion proteins of WT or mutant STAT3 were treated with 25 ng/mL of recombinant IL-6 for 0 min, 15 min and 30 min, respectively. (A) A representative Western blot result using whole cell extracts probed with a phosphotyrosine-specific STAT3 antibody ( $\alpha$ P-STAT3) and a pan-STAT3 antibody ( $\alpha$ STAT3). (B) Quantification of Western-Blot results from three independent transfection experiments, as shown in (A). Asterisks indicate significant differences between the WT protein and the respective missense mutants.





**Figure 10: Tyrosine phosphorylation in IL-6-stimulated cells expressing STAT3-SNAP mutants**

U3A cells expressing SNAP-fusion proteins of WT or mutant STAT3 were treated with 25 ng/mL of recombinant IL-6 for the indicated times. (A) Representative Western blot results from whole cell extracts probed with a phosphotyrosine-specific STAT3 antibody ( $\alpha$ P-STAT3) and a pan-STAT3 antibody ( $\alpha$ STAT3). (B) Quantification of Western-Blot results from three independent transfection experiments. Asterisks in (B) indicate significant differences between the WT protein and the respective mutants.



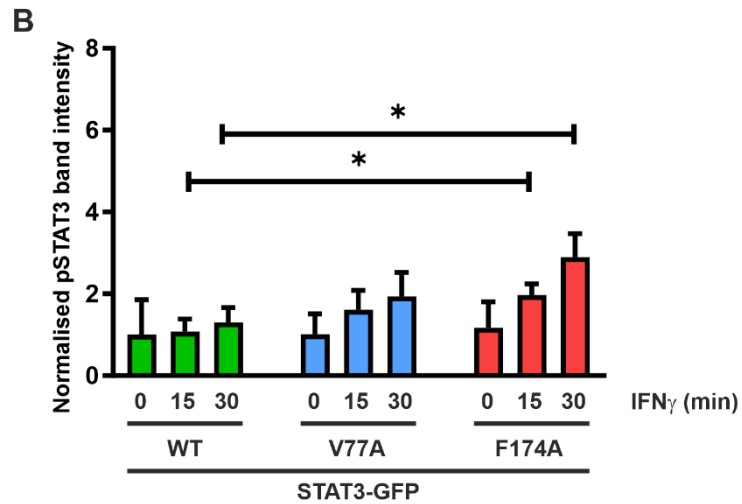


**Figure 11: Hyperphosphorylation of GFP-tagged STAT3-V77A and -F174A in IFN $\gamma$ -treated cells**

U3A cells expressing GFP-fusion proteins of WT or mutant STAT3 were treated with 50 ng/mL of recombinant IFN $\gamma$  for 0 to 30 min. (A) Representative Western blot results from whole cell extracts probed with a phosphotyrosine-specific STAT3 antibody ( $\alpha$ P-STAT3) and a pan-STAT3 antibody ( $\alpha$ STAT3). In (B) a quantification of these results from three independent experiments is shown. Asterisks in (B) indicate significant differences between the WT protein and the respective mutants.

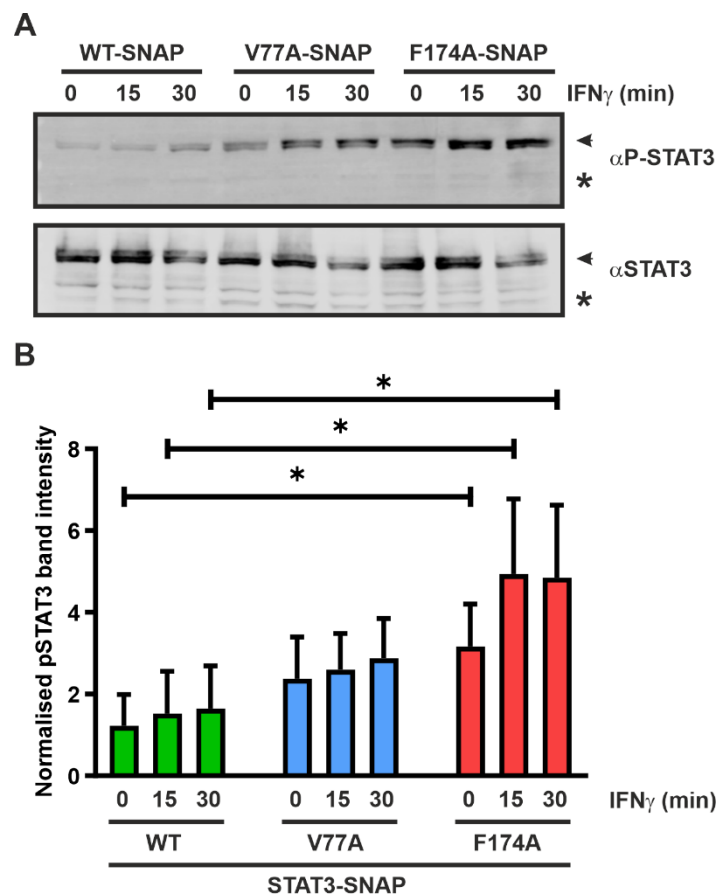


**Figure 12: Elevated tyrosine phosphorylation of the two STAT3-SNAP mutants**

U3A cells expressing SNAP-fusion proteins of WT or mutant STAT3, were treated with 50 ng/mL of recombinant IFN $\gamma$  for the indicated times. (A) Representative Western blot results from whole cell extracts probed with a

---

phosphotyrosine-specific STAT3 antibody ( $\alpha$ P-STAT3) and a pan-STAT3 antibody ( $\alpha$ STAT3). (B) Quantification of the Western-Blot results from three independent transfection experiments, as shown in (A). Asterisks indicate significant differences between the WT protein and the respective mutants.

### **3.1.4 STAT3-V77A and -F174A show increased fractions of DNA-bound molecules with unaltered specificity to DNA**

In subsequent experiments, the impact of disrupting STAT3 anti-parallel dimeric interactions, on the affinity and specificity to GAS sites of DNA was investigated. Using whole cell extracts from U3A cells transfected with the STAT3 variants, EMSA experiments were performed with the radioactively-labelled DNA probe M67 containing one GAS site.

A high number of phosphorylated V77A and F174A molecules were bound to the DNA probe containing a single GAS site than those of WT STAT3 (Figure 13 A, B). Interestingly, even extracts from unstimulated cells expressing F174A showed a detectable binding to GAS sites, while only extracts from cytokine-stimulated cells of the other variants exhibited prominent DNA binding activity (Lane 5, Figure 13A).

An increased DNA binding of the unstimulated F174A mutant could be a result of the elevated level of tyrosine-phosphorylated molecules in F174A-expressing cells, in the absence of cytokine stimulation, seen from Western blotting experiments in the previous section. A large number of activated STAT3 molecules existing as phosphorylated dimers in extracts from cells expressing V77A and F174A manifested as a higher fraction of DNA-bound STAT3 in the gelshift experiment. Similar results were obtained upon using SNAP-tagged constructs of the mutations in question and in either case, the negative control showed no GAS binding (Figure 13 C, D).

However, the increased fraction of GAS-bound molecules in V77A and F174A did not reflect a higher sequence-specific affinity to GAS sites. In competition experiments, a 750-fold molar excess of unlabelled GAS DNA was able to displace these GAS-bound mutant STAT3 molecules as efficiently as the WT (Figure 14 A, B). Therefore, both mutants showed unaltered DNA binding affinity, but significantly higher levels of tyrosine phosphorylation, which contributed to the high DNA-bound fraction of mutant STAT3 in these extracts as compared to the WT protein.

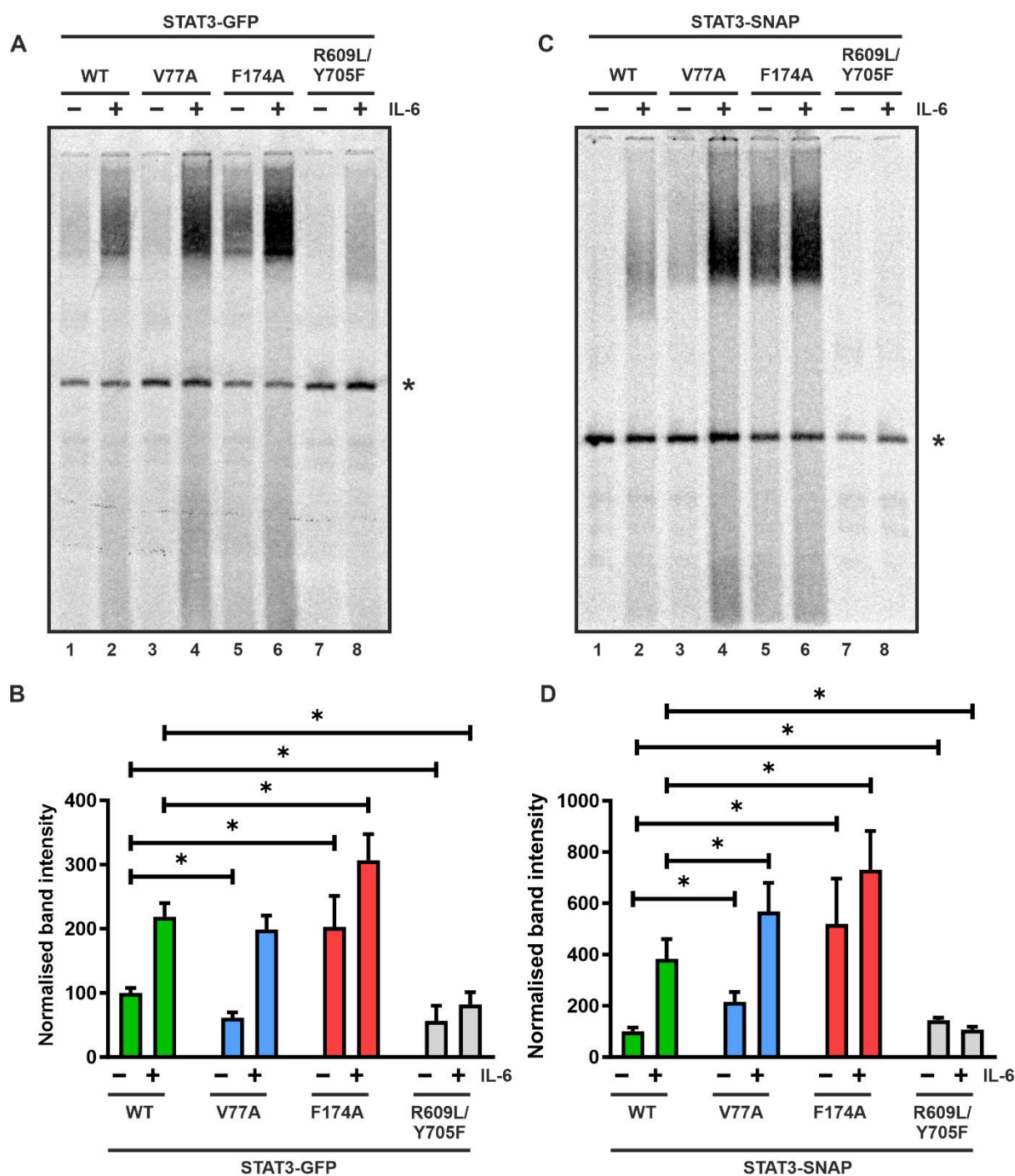


**Figure 13: Increased GAS binding in whole cell extracts from cells expressing V77A and F174A**

Electrophoretic mobility shift assay (EMSA) demonstrated increased binding of V77A- and F174A-GFP and their SNAP-tagged counterparts using whole cell extracts and a [ $^{33}$ P]-labelled M67 probe. In contrast, the double mutant R609L/Y705F mutant virtually showed no DNA-binding affinity as compared to the WT molecule. (A, C) Autoradiograms show representative EMSA results. Asterisks at the margin of the gels indicate unspecific binding. (B, D) Histograms depict the quantification thereof from three independent transfection experiments, with asterisks indicating differences between the WT protein and the respective mutant.

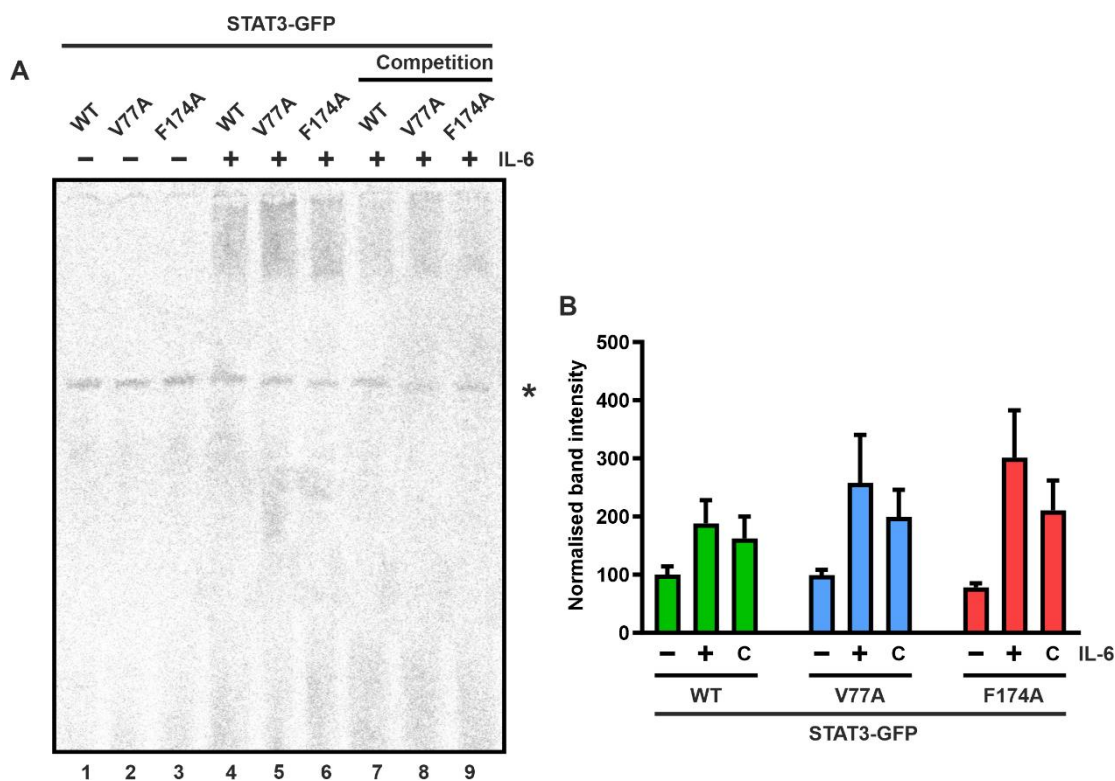


**Figure 14: Unaltered sequence-specificity of the V77A and F174A mutants to DNA.**

Unaltered dissociation kinetics from GAS sites for the tested STAT3 mutants, as demonstrated by means of a competition gelshift assay. Lysates from cells expressing the indicated tyrosine-phosphorylated STAT3 variants were equilibrated for 15 min with a radioactively-labelled high-affinity STAT-binding probe M67, before a 750-fold molar excess of unlabelled M67 was added for 10 min, and the reactions loaded on a non-denaturing gel. A representative autoradiogram of the competition gelshift is shown in (A), including the quantification from three independent experiments thereof (B).

### 3.1.5 STAT3 mutants show increased reporter activity and differential transcriptional response

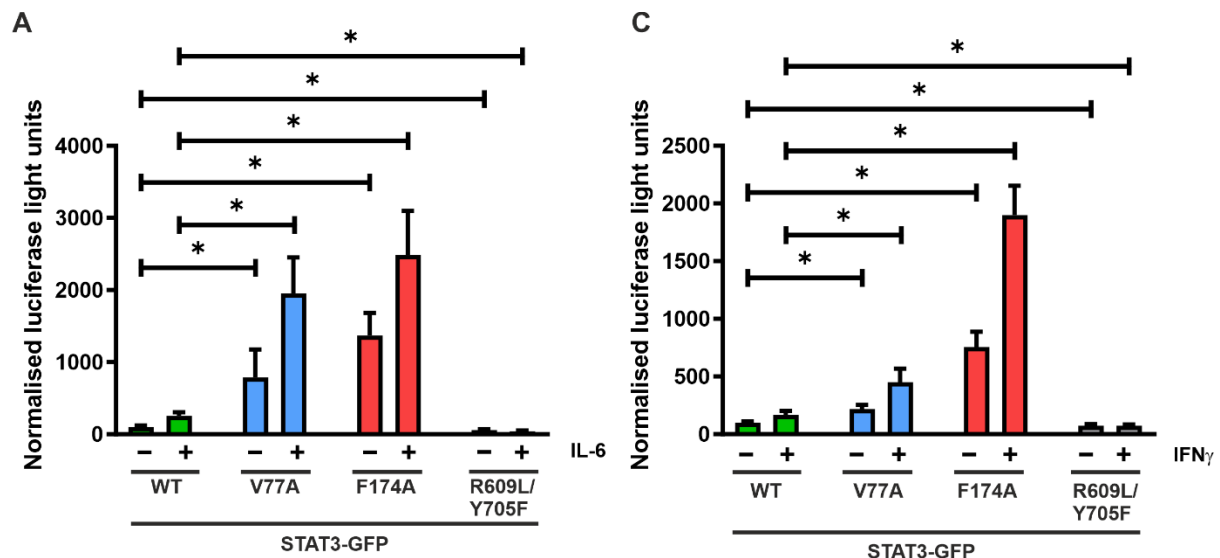
Upon observing high concentrations of GAS-bound STAT3 dimers in lysates from V77A- and F174A-expressing cells, subsequent experiments were performed to determine the ability of these mutations to initiate gene expression. In cells expressing STAT3 variants, the first step involved investigating the capacity of V77A and F174A to initiate transcription of a co-expressed luciferase reporter construct by binding to three GAS sites located in the IFN $\gamma$ -inducible promoter region of the luciferase gene (Khan et al., 1993; Wen et al., 1995).

Using U3A cells transfected with WT and mutant STAT3, reporter gene assays were performed wherein the luciferase activity was normalised to the  $\beta$ -galactosidase activity conferred by a co-transfected, constitutively expressed  $\beta$ -galactosidase gene. Both unstimulated and IL-6-stimulated U3A cells expressing the V77A and F174A mutants showed an increased luciferase activity as compared to the WT (Figure 15).

Additional data showed that IFN $\gamma$ -stimulated U3A cells expressing GFP- and SNAP-tagged STAT3 variants behaved similarly (Figure 16). In all cases, the R609L/Y705F negative control displayed no induction.

Interestingly, the V77A mutation in STAT3, which leads to a loss of NTD-dependent cooperative DNA binding to tandem GAS sites, showed an increase in reporter gene expression involving three tandem GAS sites. This increased transcriptional response resulting from the V77A mutation, despite of its unaltered GAS site affinity, can be explained by the hyperphosphorylation of this mutant.

The higher number of activated STAT3 dimers present in extracts from cells expressing this amino-terminal missense mutant resulted in an elevated ratio of GAS-bound STAT3 as compared to the total amount of STAT3 (Figure 13 A, B). The V77A mutant can occupy the triple GAS promoter in the reporter construct independently of interdimeric cooperativity. The sheer number of these activated mutant STAT3 dimers, which are available for cycles of binding to DNA and assisting transcription, compensate for any loss of amino-terminal mediated stabilizing interactions on DNA.



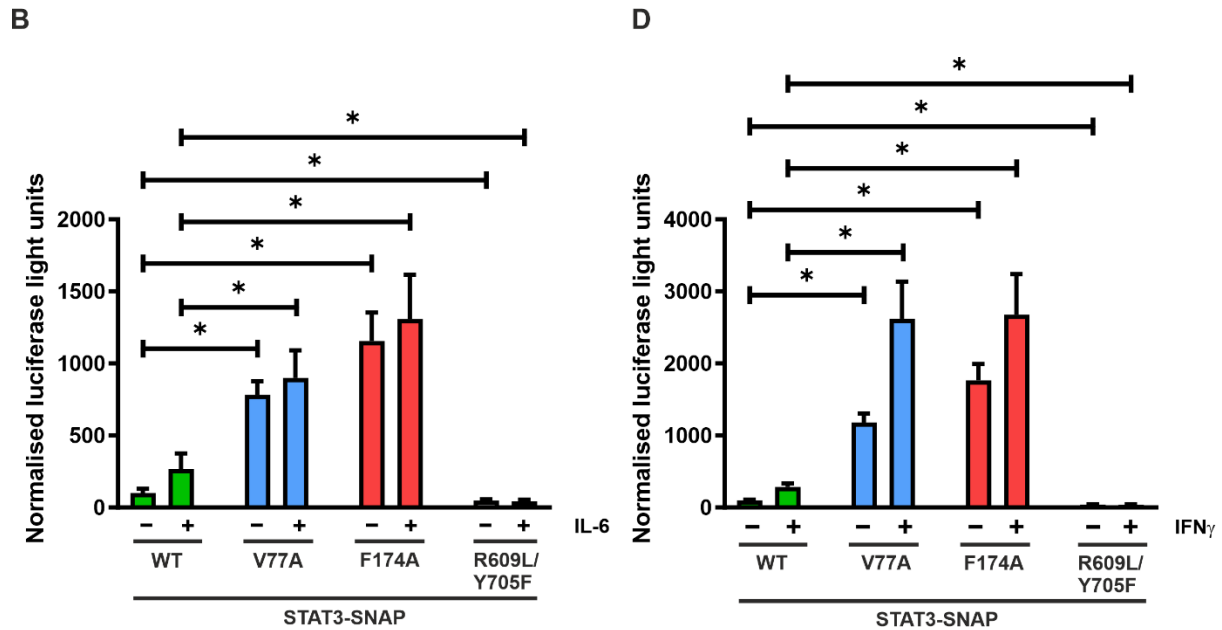


**Figure 15: V77A and F174A are hyper-active inducers of reporter constructs.**

Luciferase reporter gene assays in U3A cells expressing the indicated STAT3 variants normalized to the expression level of constitutively co-expressed  $\beta$ -galactosidase. The reporter constructs used in these experiments contained inserts of a triple GAS site from the *Ly6E* promoter (3xLy6E). Cells were either left untreated or stimulated for 6 h with 25 ng/mL of IL-6 or 50 ng/mL of IFN $\gamma$ , and in whole cell extracts, luciferase luminescence and the enzymatic activity of the co-expressed  $\beta$ -galactosidase were measured. The experiment was repeated in six independent transfections at least three times. Graphs representing cytokine-stimulated luciferase activity of GFP-tagged STAT3 (A, C) and SNAP-tagged STAT3 constructs (B, D). Asterisks indicate significant differences between the WT protein and the respective mutant.

The second approach involved testing the transcriptional activation of known STAT3 target genes by the mutants in this study. Four genes, namely *CCL2*, *SOCS3*, *JUNB* and *c-MYC* known to be under the transcriptional control of STAT3 in various oncogenic disease models, were selected to be tested via real-time PCR (qPCR) (Andersson et al., 2016; Carpenter & Lo, 2014). For this purpose, U3A cells expressing the indicated STAT3 variants were serum-starved for 18 hours prior to a 3-hour stimulation with IL-6 in serum-supplemented media. This was followed by RNA extraction from the cells, which was used for cDNA synthesis. Through qPCR analyses, it was observed that the inductive capacity of the STAT3 mutants was dependent on the gene in question, and specifically the promoter region of the gene. *CCL2*, also known as *MCPI*, is a key-member chemokine involved in chemotaxis and cell migration, making it a potent hallmark in inflammation and cancer models. The promoter region of the *CCL2/MCPI* gene has a unique composition, such that it harbours a GAS site preceded by a CT-rich sequence called interferon response-inhibitory sequence (IRIS) that has an inhibitory effect on the neighbouring GAS site in the absence of a strong cytokine response, but closely

resembles an ISRE sequence (Valente et al., 1998). Thus, in the presence of a high population of activated mutant STAT3 dimers, this unique promoter region presents one high affinity GAS site preceded by a partial affinity site to which activated STAT3 can bind manifesting as a high *CCL2* expression by the V77A and F174A mutants (Figure 16A). However, the three other genes showed a much lower inducibility (fold induction) and failed to be upregulated by the two mutants above the level of the WT protein upon cytokine treatment (Figure 16B).

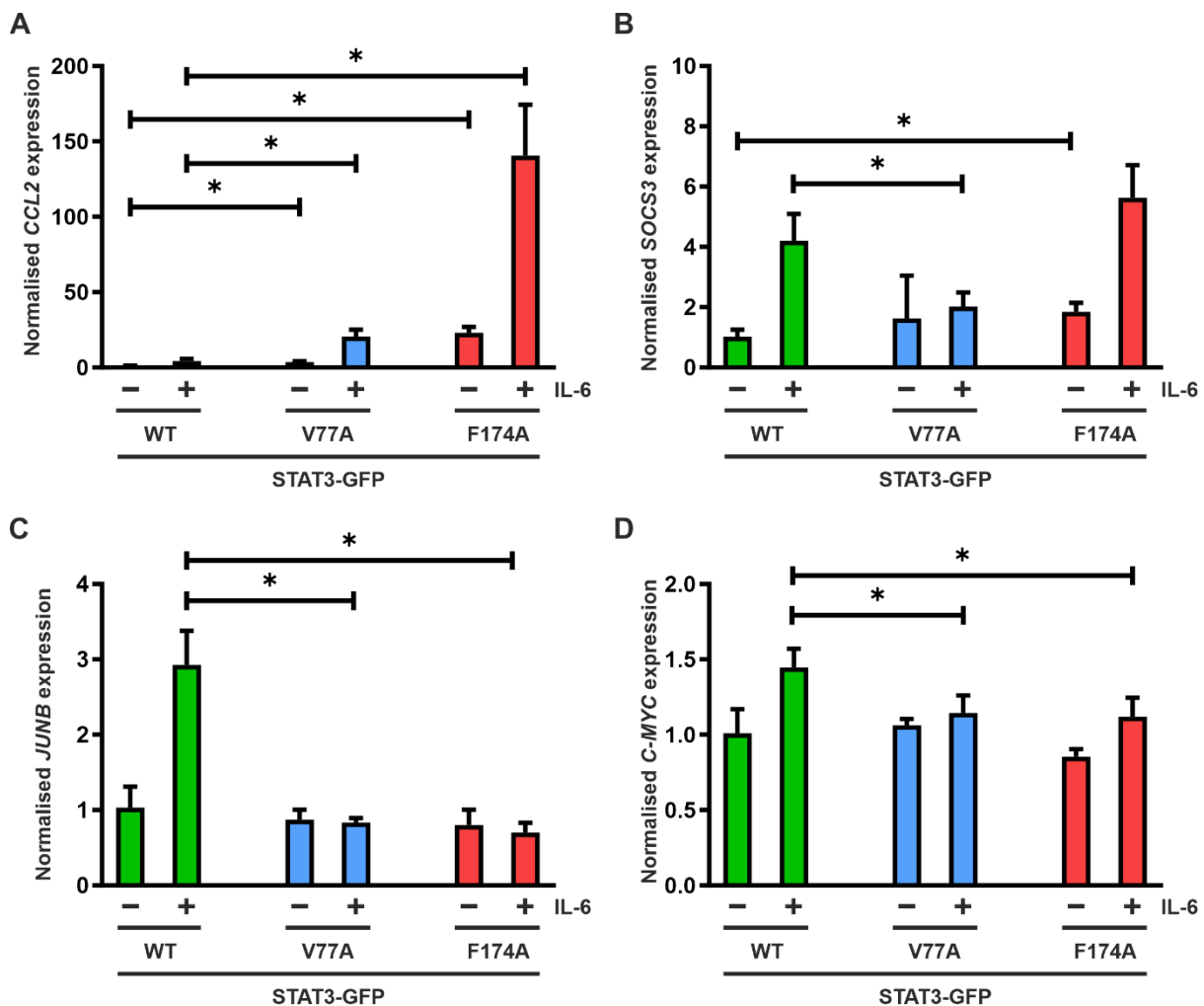


**Figure 16: Gene-specific expression pattern of V77A and F174A mutants.**

Endogenous gene expression by the indicated STAT3 mutants was determined by real-time RT-PCR assays. Histograms depict expression levels of *CCL2* (A), *SOCS3* (B), *JUNB* (C), *C-MYC* (D) gene before and after 3 h stimulation with IL-6. Gene induction was normalized to the expression of the house-keeping gene *GAPDH*. Histograms show means and standard deviations wherein significant differences for IL-6-stimulated variant samples in comparison to the WT protein are marked by bars and asterisks. The experiment was repeated three times in two independent transfections.

Genes such as *JUNB* and *C-MYC*, which are important mediators of cell cycle progression and proliferation, contain a single GAS element in their promoter region (Kojima et al., 1996;



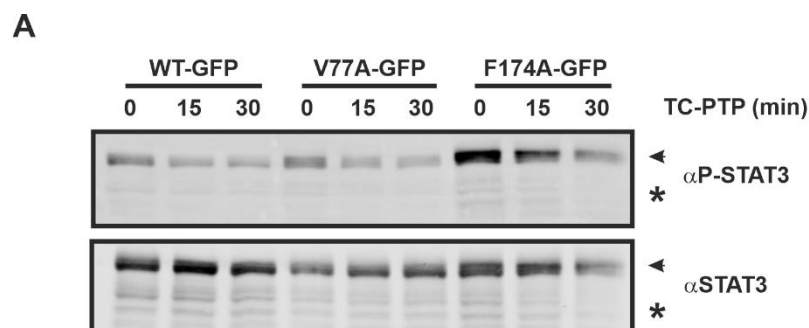
Ramana et al., 2000). A single or isolated GAS site, being available for occupancy, limits the inducibility of these genes, which can be seen from the insensitivity of these genes to transcriptional activation by the STAT3 mutants (Figure 16 C, D).

### 3.1.6 STAT3 mutants show unaltered kinetics of *in vitro* phosphorylation and dephosphorylation

Given the premature nuclear accumulation and elevated tyrosine phosphorylation of the V77A and F174A mutants, it was unclear whether the hyper-phosphorylated status of these mutants resulted from accelerated tyrosine phosphorylation by kinases and/or impaired dephosphorylation by phosphatases.

To answer this, the kinetics of phosphorylation and dephosphorylation of these mutants were examined in *in vitro* experiments. For the indicated times, extracts from unstimulated cells were incubated with the recombinant JAK2 enzyme and, alternatively, extracts from cytokine-stimulated cells were used with the recombinant TC-PTP phosphatase.

Western blot results from these reactions showed that the two hyper-active STAT3 variants V77A and F174A were phosphorylated or dephosphorylated in a similar manner as the WT protein, despite of the F174A mutant displaying higher levels of tyrosine-phosphorylation at the onset of the experiment (Figure 17, 18). It was inferred from this result that the mechanism driving the observed hyper-phosphorylation and predominant nuclear distribution of V77A and F174A consisted of factors other than an increased susceptibility to kinase activity or a reduced susceptibility to the TC-PTP phosphatase.



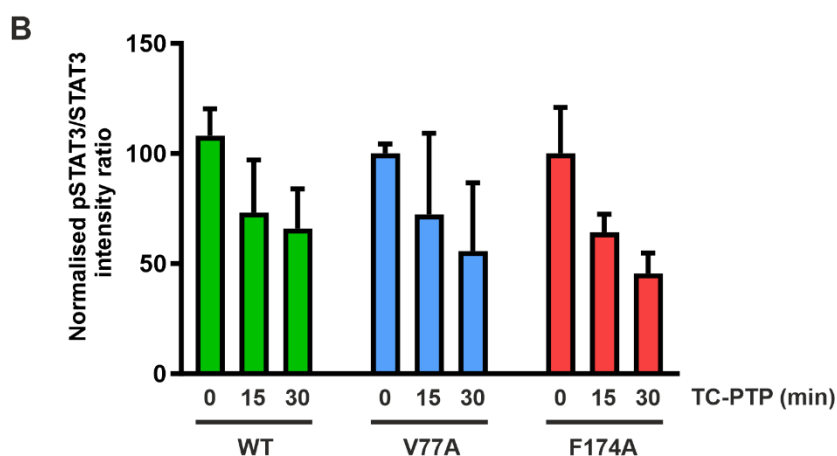


**Figure 17: STAT3 mutants display unaltered dephosphorylation kinetics *in vitro*.**

Results from an *in vitro* dephosphorylation assay using extracts from IL-6-prestimulated U3A cells (10  $\mu$ l each) incubated for 0, 15 and 30 min with 2 U of the STAT-specific TC-PTP phosphatase (n=3). Tyrosine dephosphorylation was followed by immunoblotting (A) including a quantitative analysis of the phosphotyrosine signal divided by the signal from total STAT3 (B).

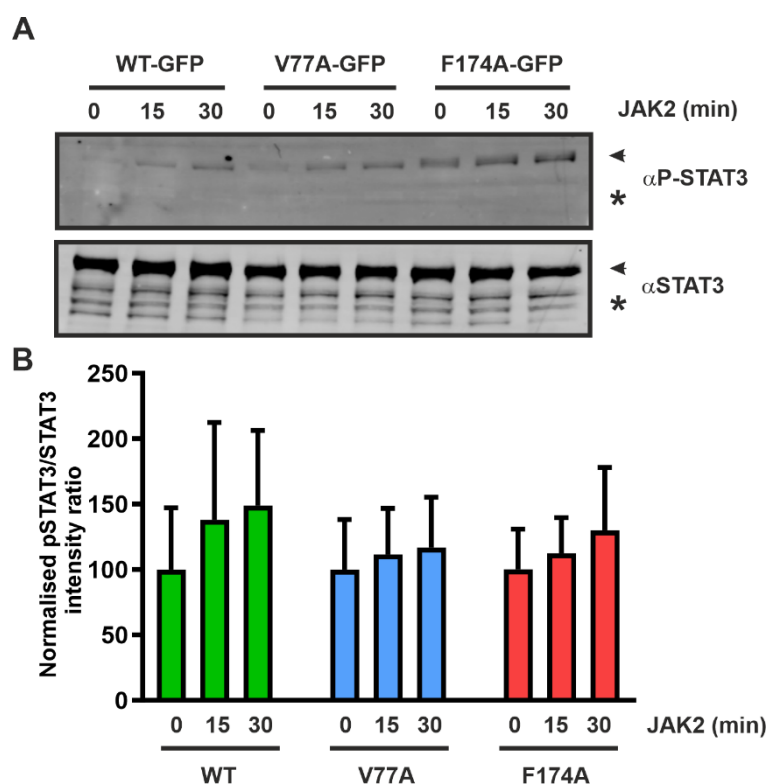


**Figure 18: STAT3 mutants exhibit unchanged *in vitro* phosphorylation kinetics.**

*In vitro* phosphorylation assay demonstrated no differences in tyrosine phosphorylation rates of the STAT3 variants by JAK2. Whole cell extracts from reconstituted U3A cells expressing STAT3 (10  $\mu$ l in each reaction) were incubated with 4  $\mu$ g/mL of recombinant JAK2 kinase and the levels of phospho-STAT3 were monitored over time by means of Western blotting (n=3) (A). Statistical analysis revealed no significant difference in the phosphorylation kinetics between WT and mutant STAT3 (B).

### 3.1.7 DNA binding influences the dephosphorylation kinetics of STAT3-F174A

The preceding experiments indicated that the two hyper-phosphorylated mutants V77A and F174A displayed a selectively nuclear localization in resting cells which was slightly pronounced upon cytokine stimulation and contained a higher number of activated molecules which showed normal GAS binding. Defective kinase or phosphatase activity as a driver of the hyper-phosphorylation could be ruled out, as these mutants showed unaltered phosphorylation and dephosphorylation kinetics *in vitro*. However, *in vitro* experiments with the phosphatase cannot fully encapsulate the activities involved in the phosphorylation-dephosphorylation kinetics within a cell. Therefore, an experiment was performed to determine any differences in the dephosphorylation of V77A and F174A *in vivo*. The potent kinase-inhibitor staurosporine was employed to inhibit kinase activity in a time-dependent manner in IL-6-prestimulated cells expressing the STAT3 variants.

Unexpectedly, the IL-6-induced phosphorylation of F174A was prolonged and did not diminish as fast as the WT, upon the addition of staurosporine (Figure 19). This observation provided a significant clue towards the mechanism driving the nuclear localization and hyper-phosphorylation of the F174A mutant. As has been described in STAT1, the phosphorylation-dephosphorylation cycle is dependent on the switching of states between parallel and anti-parallel dimers (Wenta et al., 2008). Therefore, a mutation at position F174 in the STAT3 CCD, that can potentially disrupt this conformational switch, should render this mutant resistant to dephosphorylation.

However, in *in vitro* experiments F174A had a similar response to recombinant TC-PTP phosphatase as the WT. This contradictory behaviour points to the impact DNA binding on the dephosphorylation of STATs. Dissociation from high-affinity GAS sites is crucial for the parallel/anti-parallel shift in STAT1 dimers (Riebeling et al., 2014). Therefore, a subsequent hypothesis was formulated wherein nuclear F174A molecules bound to DNA are protected from being dephosphorylated by nuclear Tc45 phosphatase, which manifests as a prolonged P-STAT3 signal, despite the staurosporine-mediated inhibition of kinase activity. Likewise, the V77A mutant, which cannot form homotypic NTD interactions, showed a slightly prolonged phosphorylation in response to staurosporine (Figure 19).

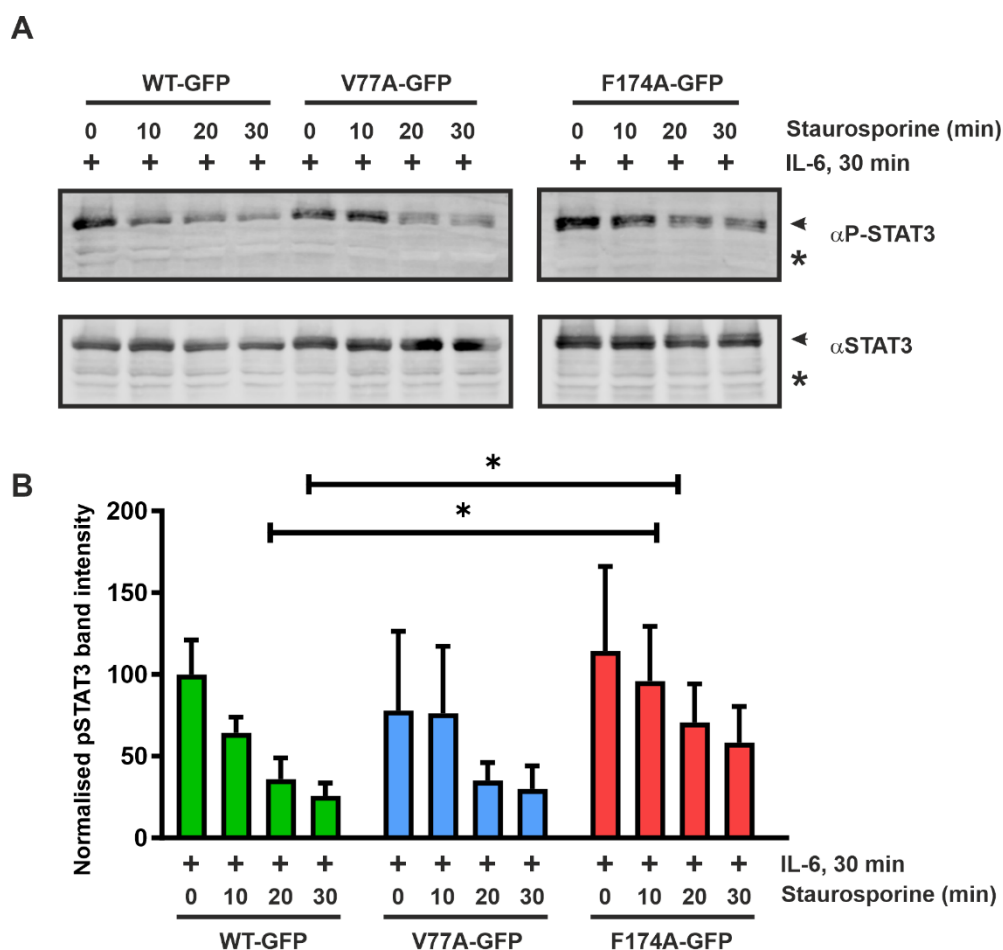


**Figure 19: Resistance to *in vivo* dephosphorylation of STAT3 mutants upon staurosporine treatment.**

U3A cells expressing GFP-fusion proteins of WT or mutant STAT3 were treated for 30 min with 25 ng/mL of recombinant IL-6, followed by incubation with kinase inhibitor staurosporine (1  $\mu$ M) for the indicated times up to 30 min. (A) Representative immunoblot from whole cell extracts and (B) the quantification of immunoblotting results from three independent transfection experiments, as shown in (A). Asterisks indicate significant differences between the WT protein and the respective mutant.

This hypothesis was tested by performing an *in vitro* dephosphorylation experiment with the addition of a GAS-nonGAS oligonucleotide in the reaction mixture. To this end, a double-stranded DNA element with a full GAS site followed by an adjacent partial GAS site was present in the *in vitro* dephosphorylation reaction. Two tandem GAS sites rarely occur in the genome and this sequence was chosen for a more effective representation of *in vivo* conditions. As shown in Figure 20, in the presence of DNA containing high-affinity binding sites, the mutant F174A protein partially resisted dephosphorylation induced by recombinant TC-PTP phosphatase. STAT3-V77A also showed resistance but to a lesser degree.

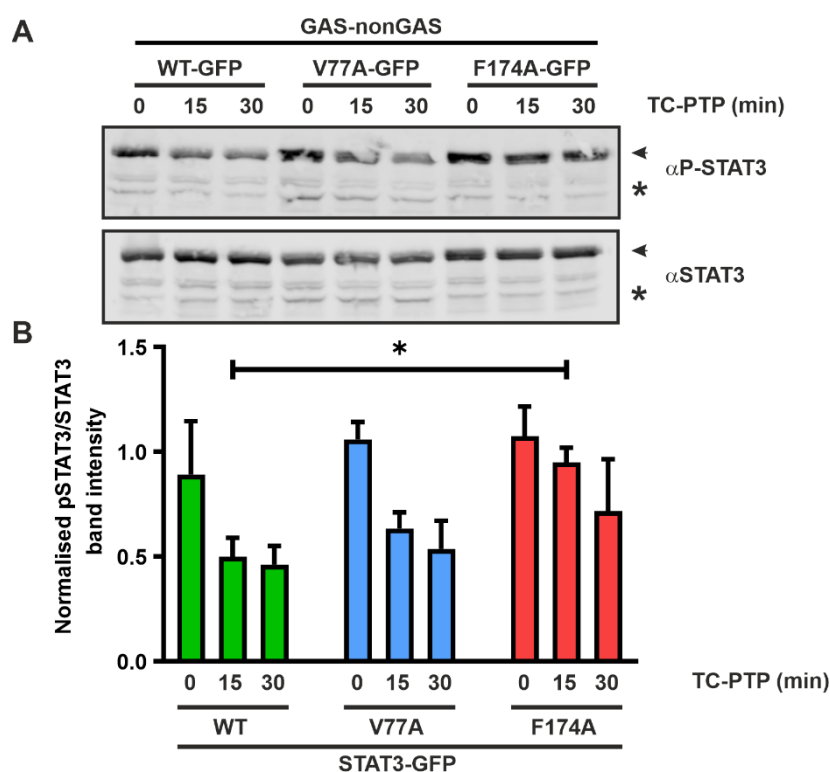


**Figure 20: STAT3 mutants are protected against the inactivating effect of TC-PTP phosphatase when bound to high-affinity GAS elements.**

Results from an *in vitro* dephosphorylation assay in the presence of GAS-nonGAS double-stranded oligonucleotides. (A) Representative immunoblot from whole cell extracts and (B) the quantitative analysis of thereof (phosphotyrosine signals divided by the pan-STAT3 signals from the same extracts). Asterisks in (B) indicate a significant difference between the WT protein and the respective mutant from three independent experiments.

The observation underscores the capacity of DNA binding to influence the dephosphorylation and subsequent conformational alterations in STAT3 dimers. Taken together, the results outline the similarities in the behaviour of STAT1 and STAT3 with respect to the importance of the parallel and anti-parallel dimeric interactions in JAK-STAT signal transduction.

---

## **3.2 The impact of unphosphorylated STAT1 on the activities of canonical JAK-STAT1 signalling**

### **3.2.1 Identification of mutations that disrupt phosphorylation and dimerization of STAT1**

As has been described in the Introduction section, the SH2 domain mediates phosphorylation of STAT proteins via docking to phosphorylated residues at the JAK-associated receptors as well as dimerization via reciprocal interactions of the critical phosphotyrosine residue to its partner molecule (Chen et al., 1998; Shuai et al., 1994). Therefore, a disruption of the SH2 domain interactions via a mutation at R602 has an impact on cytokine-stimulated phosphorylation, dimerization and nuclear import of STAT1 (McBride et al., 2002; Shuai et al., 1993).

A mutation at Y701 which is the critical site for STAT1 phosphorylation also leads to an unphosphorylated construct that cannot dimerize with other activated STAT1 and does not accumulate in the nucleus upon cytokine stimulation (Shuai et al., 1993). Therefore, the two mutations R602L and Y705F were combined in a WT STAT1-GFP expression vector, to form the dimerization-deficient mutant construct R602L/Y701F-GFP.

Based on the data from experiments involving R602L/Y701F-GFP, mutations were further introduced in the CCD and DBD of R602L/Y701F-GFP, to render a quadruple mutant (QM) STAT1. Mutations R274W and T385A in the STAT1 CCD and DBD respectively, were introduced in R602L/Y701F-GFP to generate a STAT1 species that is theoretically incapable of forming either parallel or anti-parallel dimers (Figure 21).

These two constructs, R602L/Y701F-GFP and QM-GFP, were transfected in HeLa cells or STAT1-deficient U3A cells, to perform experiments investigating the role of unphosphorylated, dimerization-deficient STAT1 in the canonical JAK-STAT pathway.

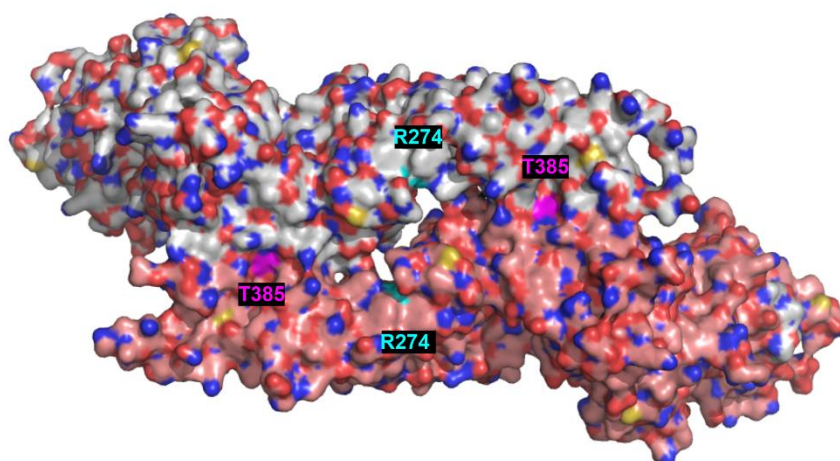


**Figure 21: Crystallographic data representing mutations in the anti-parallel dimer of STAT1.**

Anti-parallel STAT1 dimer showing the localization of residues R274 (in cyan) in the CCD and T385 (in pink) in the DBD. QM-GFP contains the above mutations in addition to R602L in the SH2 domain and Y701F in the TAD. This structure was created from the crystallographic data of an anti-parallel STAT1 dimer (PDB: 1YVL) (Mao et al., 2005).

### **3.2.2 Cytoplasmic retention and unobservable phosphorylation of co-expressed WT in IFN $\gamma$ -stimulated cells expressing R602L/Y701F-GFP**

To study the effect of unphosphorylated STAT1 on the nucleocytoplasmic distribution of phosphorylated STAT1, HeLa cells were co-transfected with a combination of expression vectors encoding R602L/Y701F-GFP and WT STAT1-Flag in equal amounts. These cells were then stimulated with IFN $\gamma$  for 45 min and subsequently stained with an anti-Flag antibody accompanied by the corresponding Cy3-labelled secondary antibody, to visualize any changes in the distribution of the STAT1-Flag resulting from cytokine stimulation. As can be seen from Figure 22, in the absence of cytokine stimulation, cells co-expressing R602L/Y701F-GFP (green) and STAT1-Flag (red) showed a predominantly cytoplasmic distribution of both STAT1 species. After stimulation with IFN $\gamma$ , the STAT1-Flag accumulated in the nucleus of the cells that selectively expressed only the Flag-tagged STAT1 construct (only red). As expected, the R602L/Y701F-GFP did not show any nuclear accumulation upon IFN $\gamma$  treatment.

However, in IFN $\gamma$ -stimulated cells co-expressing both R602L/Y701F-GFP and STAT1-Flag, the STAT1-Flag was retained in the cytoplasm along with the R602L/Y701F-GFP. This interesting phenomenon was not restricted to HeLa cells, as it was observed in similar experiments with U3A cells as well. This finding hinted at an interaction between the

unphosphorylated, dimerization-deficient mutant of STAT1 and the co-expressed WT protein, that seemed to block its nuclear import. As described in the literature characterizing the single mutants in R602L/Y701F-GFP, tyrosine phosphorylation is imperative to cytokine-dependent nuclear import (McBride et al., 2002; Shuai et al., 1993). Therefore, subsequent experiments were dedicated to investigating the impact of R602L/Y701F-GFP on the nucleocytoplasmic distribution of the phosphorylated, co-expressed WT protein.

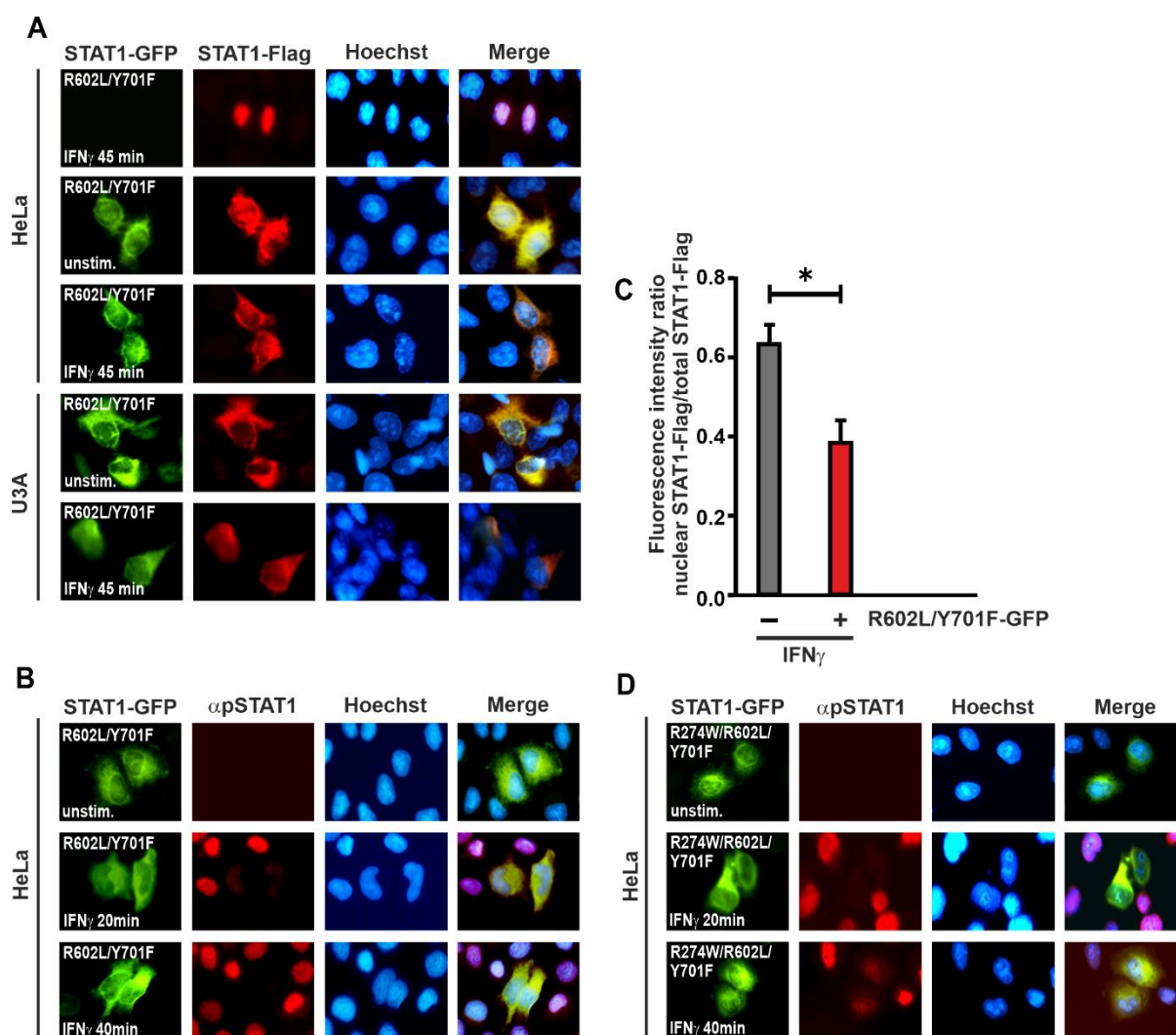


**Figure 22: Co-expressed WT protein does not accumulate in the nucleus of cytokine-stimulated cells in the presence of mutant U-STAT1**

HeLa and U3A cells were transfected with equal amounts of GFP-tagged mutant STAT1 and STAT1-Flag followed by stimulation with IFN $\gamma$  for 45 min. Cells were fixed and stained with either anti-Flag (A, B) or anti-phospho-STAT1 antibody ( $\alpha$ P-STAT1) (C, D) followed by Cy3-conjugated secondary antibodies. (A) The fluorescence micrographs show the intracellular distribution of R602L/Y701F-GFP and Flag-tagged WT STAT1 for the indicated variants as well as the localization of the corresponding Hoechst-stained nuclei (n=3 independent transfections). (B) Histogram demonstrating the nuclear STAT1-Flag distribution in IFN $\gamma$ -treated cells co-expressing R602L/Y701F-GFP, as determined by the ratio of nuclear-to-total fluorescence intensity. (C, D) HeLa



---

cells expressing mutant STAT1 variants were either left untreated or stimulated with IFN $\gamma$  and after 45 min fixed and stained with  $\alpha$ -P-STAT1 antibody followed by a Cy3-labelled secondary antibody. The fluorescence micrographs show the intracellular distribution of mutant STAT1 and WT P-STAT1 for the indicated co-expressed variants as well as the localization of the corresponding Hoechst-stained nuclei (n=3 independent transfections).

For this purpose, HeLa cells expressing R602L/Y701F-GFP were stimulated with IFN $\gamma$  and stained with an  $\alpha$ -P-STAT1 (Y701) antibody, to observe the localization of the phosphorylated endogenous STAT1 in these cells. Surprisingly, cells expressing R602L/Y701F-GFP (green) showed no or highly reduced P-STAT1 staining upon cytokine stimulation. In comparison to cells expressing R602L/Y701F-GFP, the neighbouring cells that did not express the mutant STAT1 (not green) showed normal P-STAT1 staining (Figure 22). As a control, unstimulated cells showed no P-STAT1 staining, which indicated that the primary antibody was specific to tyrosine phosphorylation. This unexpected finding led to an inference that a STAT1 construct, that could neither be phosphorylated nor could dimerize, was able to interact with other WT STAT1 proteins, hindering their nuclear import and the detection of their phosphorylation.

As described in the previous sections, STAT1 forms parallel and anti-parallel dimers, wherein interactions between the SH2 and TAD stabilize the parallel dimer, while the CCD and DBD interact to form the anti-parallel dimer. Therefore, R602L/Y701F-GFP, wherein the parallel dimer binding interfaces were already disrupted, was used as a substrate to introduce another mutation at position R274 in the CCD (Petersen et al., 2019). The hypothesis behind generating this triple mutant was to partially disrupt the anti-parallel dimeric binding interface of R602L/Y701F-GFP, in order to isolate the nature of its interaction with co-expressed WT. However, the triple mutant of STAT1 also behaved like R602L/Y701F-GFP, wherein the phosphorylation of the endogenous STAT1 molecules could not be observed in IFN $\gamma$ -stimulated HeLa cells expressing the triple mutant (Figure 22).

### **3.2.3 Disruption of parallel and anti-parallel interactions in mutant STAT1 did not rescue the invisibility of co-expressed, phosphorylated WT**

From the preceding experiments, it was clear that an unphosphorylated STAT1 construct that was incapable of binding to other STAT1 molecules via parallel or anti-parallel interactions, was able to influence the nucleocytoplasmic shuttling of phosphorylated STAT1.

By introducing the R274W mutation in the CCD of R602L/Y701F-GFP, the formation of anti-parallel interactions between the two partner protomers was disrupted. However, this generated

a hypothesis that the intact DBD of the R602L/Y701F-GFP could provide an interaction site with the CCD of a WT protein, and a single CCD mutation might not suffice to significantly weaken anti-parallel interactions in the triple mutant. Therefore, a fourth mutation was introduced in the triple mutant of STAT1, namely at residue T385 in the DBD to further weaken known binding interfaces in R602L/Y701F-GFP. This generated the STAT1 construct R274W/T385A/R602L/Y701F-GFP, which was termed here as the quadruple mutant (QM-GFP).

In principle, QM-GFP should be inert and incapable of forming either parallel or anti-parallel dimers with WT proteins, thereby not affecting their nucleocytoplasmic translocation. However, HeLa cells transfected with QM-GFP did not stain with an  $\alpha$ P-STAT1 antibody upon cytokine stimulation (Figure 23).

Interestingly, QM-GFP interfered with the cellular distribution of the phosphorylated, endogenous STAT1 of HeLa cells in a concentration-dependent manner (Figure 23B). HeLa cells expressing a high amount of QM-GFP (bright green fluorescent signal) showed a greater reduction in the intensity of P-STAT1 staining than cells which expressed the transgene at a lower concentration (faint green). The latter displayed a lesser reduction in the staining of the phosphorylated endogenous STAT1 (Figure 23 A, C).

This result led to the inference that a STAT1 protein incapable of forming parallel or anti-parallel dimers was nevertheless able to interact with other STAT1 molecules and influence their intracellular distribution.

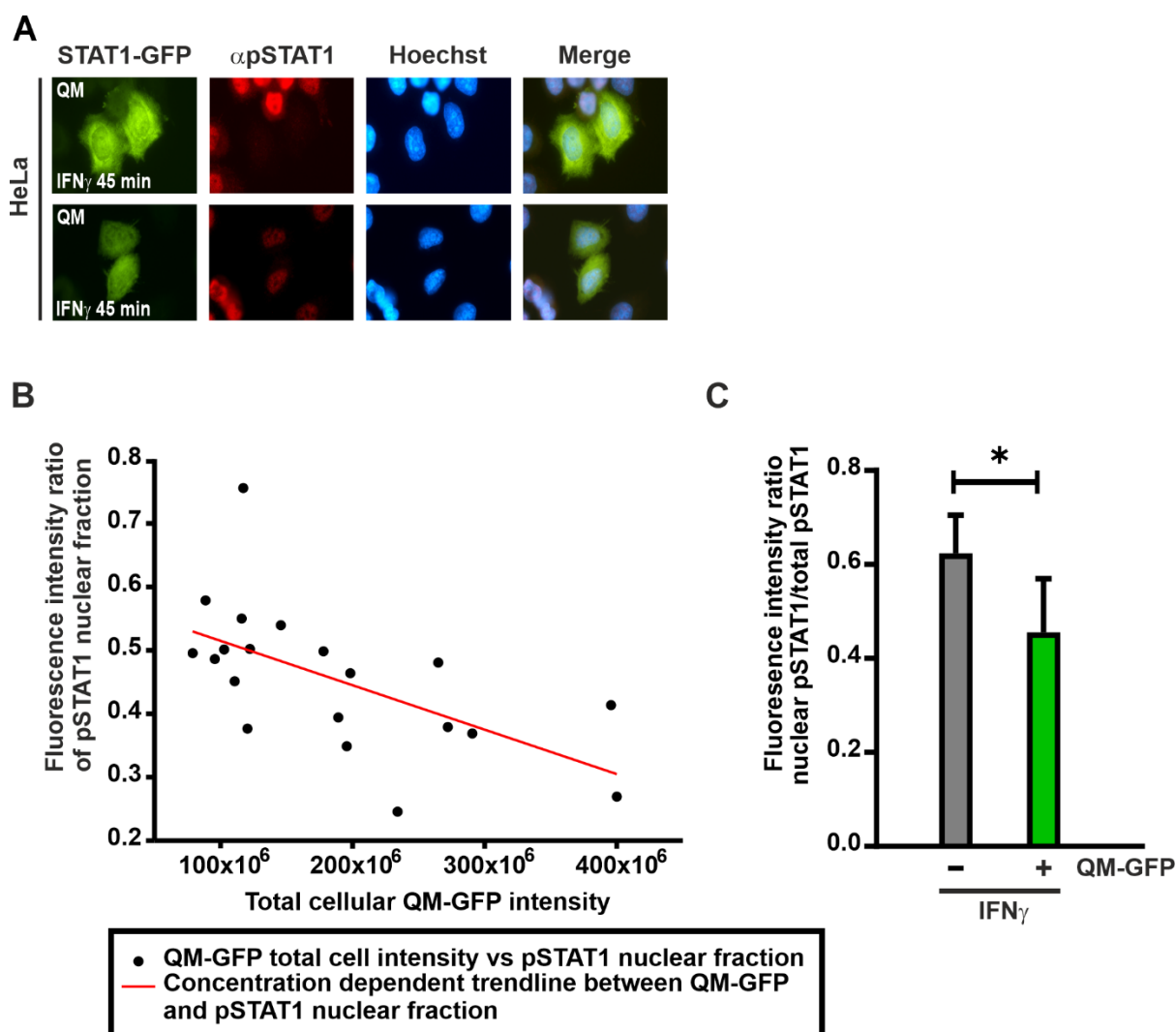


**Figure 23: Dimerization-deficient mutant U-STAT1 inhibits the detection of co-expressed WT**

HeLa cells were transfected with a plasmid coding for QM-GFP, followed by stimulation with IFN $\gamma$  on the next day. Cells were fixed 45 min after adding the cytokine and stained with  $\alpha$ P-STAT1 antibody followed by Cy3-conjugated secondary antibody. (A) The fluorescence micrographs show the intracellular distribution of QM-GFP and WT P-STAT1 as well as the localization of the corresponding Hoechst-stained nuclei (n=3 independent transfections). (B) Concentration-dependent inhibition of nuclear P-STAT1 accumulation by co-expressed QM-GFP, as shown by a linear regression graph between the intensity of nuclear P-STAT1 and cellular QM-GFP intensity. (C) Histogram demonstrating the net reduction of nuclear P-STAT1 intensity in HeLa cells expressing QM-GFP, as determined by the ratio of nuclear-to-total fluorescence intensity (n=3 independent transfections).

### 3.2.4 STAT1 mutants do not affect activation-inactivation of co-expressed WT, but impair the visibility of tyrosine-phosphorylation in cells

The subsequent experiments were designed to further investigate the diminished phosphotyrosine staining of co-expressed WT in the presence of QM-GFP. To determine whether the dimerization-deficient and unphosphorylated STAT1 mutants abolished the phosphorylation of the co-expressed WT STAT1, Western blotting experiments were

performed on whole cell lysates extracted from STAT1-deficient U3A cells expressing a combination of QM-GFP and untagged WT STAT1. Unexpectedly, lysates from U3A cells expressing both QM-GFP and the WT protein showed a clear tyrosine phosphorylation band of the WT, which was previously undetectable in immunocytochemistry experiments (Figure 24).

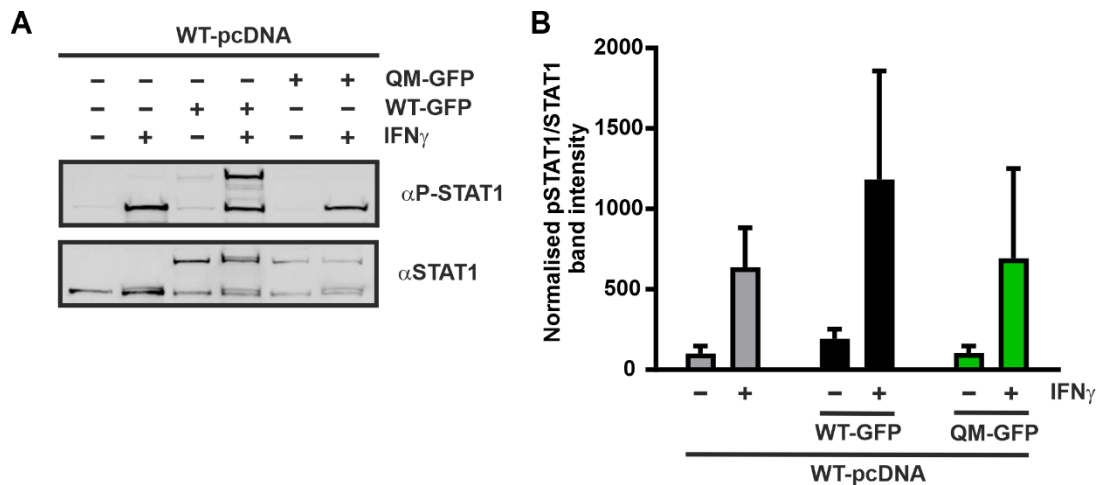


**Figure 24: Mutant U-STAT1 does not abolish tyrosine phosphorylation of WT but impairs the detection of P-STAT1 in immunofluorescence stainings**

(A) Representative immunoblot of whole cell extracts from STAT1-negative U3A cells co-expressing STAT1 and QM-GFP after treatment for 45 min with 50 ng/mL of recombinant IFN $\gamma$  and (B) the quantification of immunoblotting results from three independent transfection experiments, as shown in (A).

Additionally, the kinetics of phosphorylation and dephosphorylation of the WT protein was studied in the presence of QM-GFP. This was done to determine whether the dimerization-deficient STAT1 impaired the susceptibility of the co-expressed WT to effectively undergo JAK-catalysed phosphorylation and TC-PTP-induced dephosphorylation. However, untagged WT STAT1 co-expressed in U3A cells transfected with QM-GFP showed unaltered kinetics in *in vitro* phosphorylation and dephosphorylation assays (Figure 25). These findings hinted at a strange phenomenon occurring in these cells, that expressed high levels of a STAT1 species that could not be phosphorylated nor could bind via known dimerization interfaces but was nonetheless capable of interacting with the phosphorylated WT protein and affecting its intracellular distribution. It was inferred from the preceding experiments that the excess of unphosphorylated STAT1 molecules in the cells transfected with STAT1 mutants interfered with the import of phosphorylated WT dimers. QM-GFP and R602L/Y701F-GFP were hypothesized to bind with co-expressed phosphorylated WT dimer to form higher-order structures which could not be imported into the nucleus, thereby manifesting as a selectively cytoplasmic distribution with hidden phosphotyrosine residues.

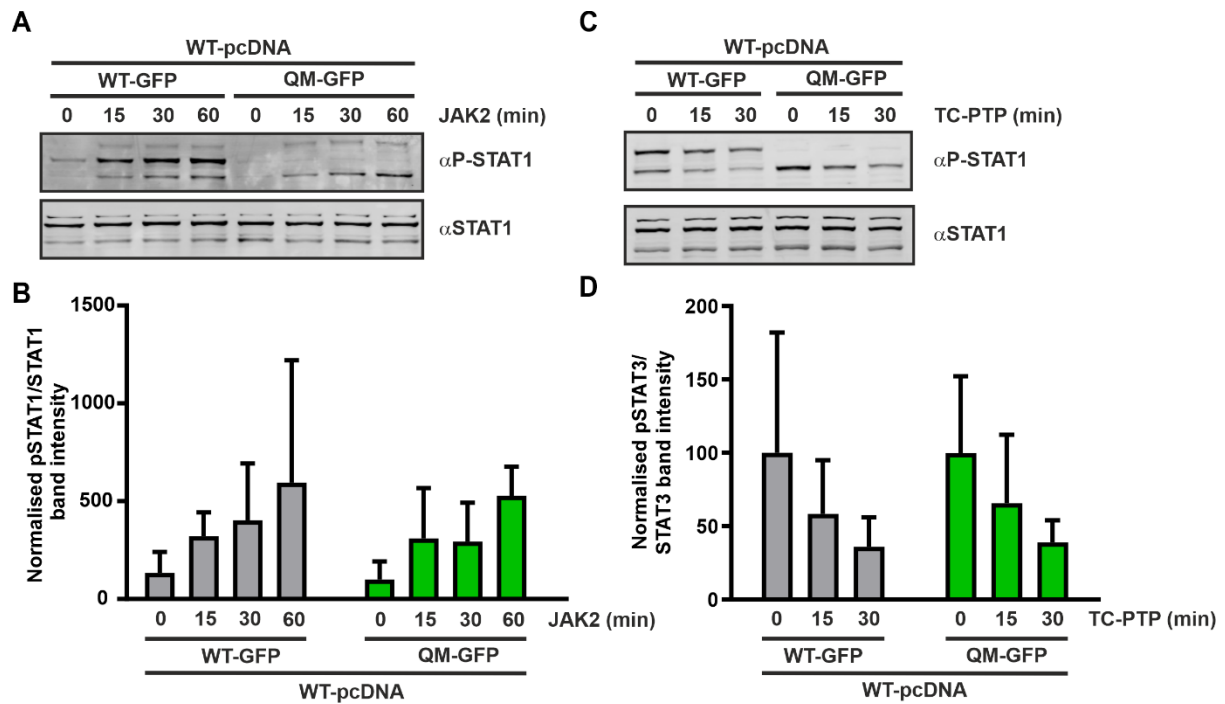


**Figure 25: Mutant U-STAT1 does not alter the *in vitro* phosphorylation and dephosphorylation of co-expressed WT**

(A) *In vitro* phosphorylation assay demonstrated no difference in tyrosine phosphorylation rates of the WT STAT1 by JAK2 with respect to the presence or absence of QM-GFP. Whole cell extracts from reconstituted U3A cells expressing both STAT1 WT and QM-GFP (10  $\mu$ l in each reaction) were incubated with 4  $\mu$ g/mL of recombinant JAK2 kinase and the levels of P-STAT1 were monitored over time by means of Western blotting (n=3). (B) Statistical analysis revealed no significant difference in the phosphorylation kinetics of the WT in the presence of either QM-GFP or WT-GFP. Results from an *in vitro* dephosphorylation assay using extracts from IFN $\gamma$ -prestimulated U3A cells expressing STAT1 WT-GFP or QM-GFP (10  $\mu$ l each) incubated for 0, 15 and 30 min with 2 U of the STAT-specific TC-PTP phosphatase (n=3). Tyrosine dephosphorylation was followed by immunoblotting (C) including a quantitative analysis of the phosphotyrosine signals divided by total amount of STAT3 signal (D).

### 3.2.5 Unphosphorylated mutant STAT1 does not impact the DNA specificity and transcriptional response of co-expressed P-STAT1

To determine whether the dimerization-deficient STAT1 mutants affected any other activities of the co-expressed WT STAT1, subsequent experiments were designed to test the kinetics of DNA binding and transcriptional induction of the WT protein in cells co-expressing both mutant and WT STAT1. Whole cell extracts from HeLa cells expressing mutant STAT1 and STAT1-deficient U3A cells expressing a combination of mutant and WT STAT1 were used to perform EMSA experiments. Despite of the presence of STAT1 mutants that were able to impact the co-expressed phosphorylated WT protein and alter its intracellular distribution, the WT protein showed normal kinetics of binding to GAS sites *in vitro*, as can be seen from Figure

26. Both QM-GFP and R602L/Y701F-GFP showed no GAS binding and did not alter the binding of the co-expressed WT to form dimers on single GAS sites or tetramers on two adjacent GAS sites. Lane 2 in Figure 26A and Lane 7 in Figure 26B show multiple bands of homo- and heterodimers of STAT1-GFP with co-expressed untagged, recombinant STAT1 (U3A) and endogenous STAT1 (HeLa). However, neither QM-STAT1 nor R602L/Y701F-GFP exhibited any interaction with the co-expressed WT protein on DNA in gelshift experiments.

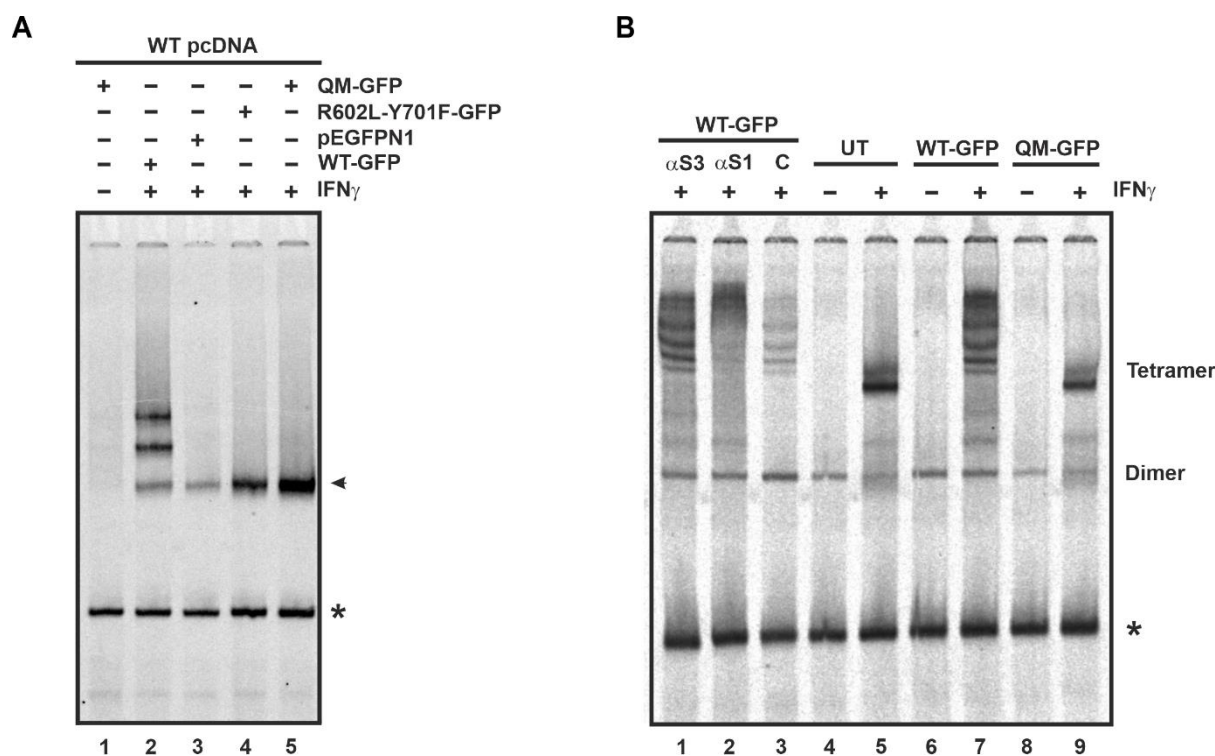


**Figure 26: Unaltered DNA binding of WT STAT1 in the presence of mutant U-STAT1**

(A) Electrophoretic mobility shift assay demonstrated unchanged binding of recombinant STAT1 WT from reconstituted U3A cell extracts to a [ $^{33}$ P]-radioactively-labelled M67 probe containing a single GAS sequence, whereas the co-expressed unphosphorylated STAT1 variants showed no DNA-binding indicated by the absence of a GFP-tagged STAT1 band in lanes 4 and 5. The presence of neither the double mutant R602L/Y701F-GFP nor the quadruple mutant R274W/T385A/R602L/Y701F-GFP hindered WT-STAT1 from binding to the probe. (B) EMSA result showing unaltered capacity of endogenous STAT1 from HeLa cell extracts to form tetramers on the labelled DNA element 2xGAS, containing two GAS sites in tandem orientation, in the presence of co-expressed QM-GFP. HeLa cells were either untransfected (UT) or transfected with the indicated expression plasmids, and on the next day treated for 45 min with IFN $\gamma$  or left untreated.

The next experiments were focussed on investigating the capacity of the phosphorylated WT STAT1 to induce luciferase reporter activity, in the presence of a STAT1 species that affected its nucleocytoplasmic distribution. HeLa cells expressing GFP fusions of the STAT1 variants and U3A cells transfected with a combination of one-part STAT1-GFP and one-part from either

of the STAT1 variants comprising of STAT1-GFP, R602L/Y701F-GFP, QM-GFP or empty vector (eGFP), were used for reporter assays.

As can be seen from Figure 27, the additional presence of R602L/Y701F-GFP or QM-GFP did not affect the induction of the luciferase reporter construct by endogenous STAT1/co-expressed WT-GFP. The STAT1 mutants showed no increase in the net reporter activity of the endogenous STAT1/co-expressed WT-GFP, which was always lesser than the combination containing twice the amount of WT STAT1, indicating that the mutant STAT1 constructs showed no reporter activity of their own.

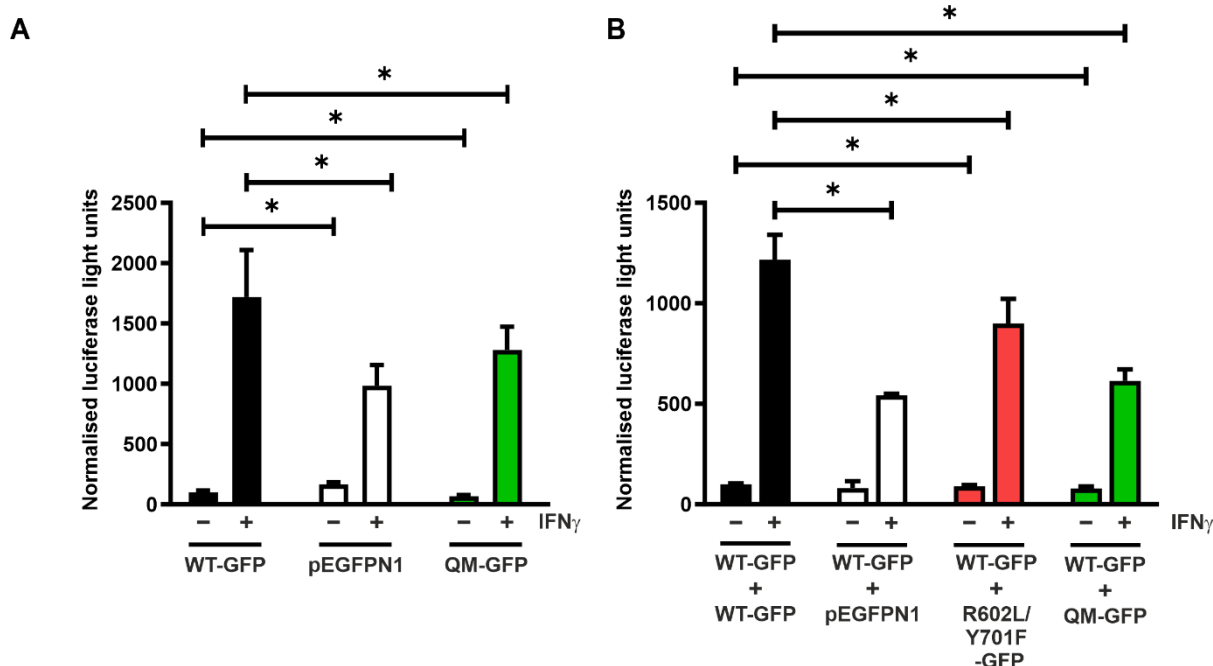


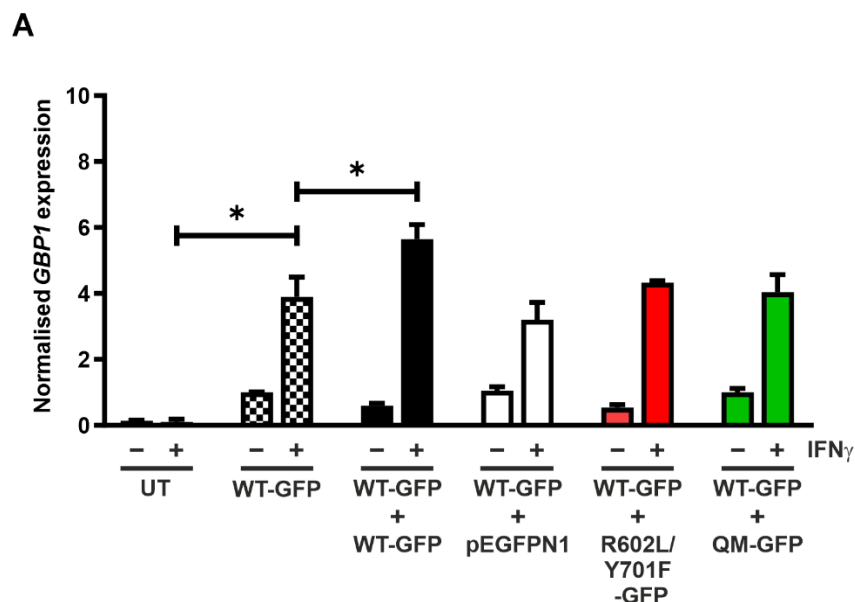
**Figure 27: Mutant U-STAT1 does not diminish the reporter activity of co-expressed WT**

(A) HeLa cells expressing WT-GFP, empty vector (pEGFPN1) or the quadruple mutant QM-GFP were left untreated or stimulated for 6 h with 50 ng/mL of IFN $\gamma$ . In whole cell extracts of these cells, luciferase luminescence of a reporter construct with a triple GAS site (3xLy6E) and the enzymatic activity of the co-expressed  $\beta$ -galactosidase were measured and represented graphically. (B) U3A cells were transfected with reporter construct,  $\beta$ -galactosidase expression vector and a combination of WT-GFP and indicated STAT1 variants, in equal amounts. These cells were either unstimulated or stimulated with 50 ng/mL of IFN $\gamma$  for 6 hours, and luciferase activity normalised to the  $\beta$ -galactosidase expression, was measured in whole cell extracts and represented graphically. The experiment was repeated in six independent transfections at least three times.

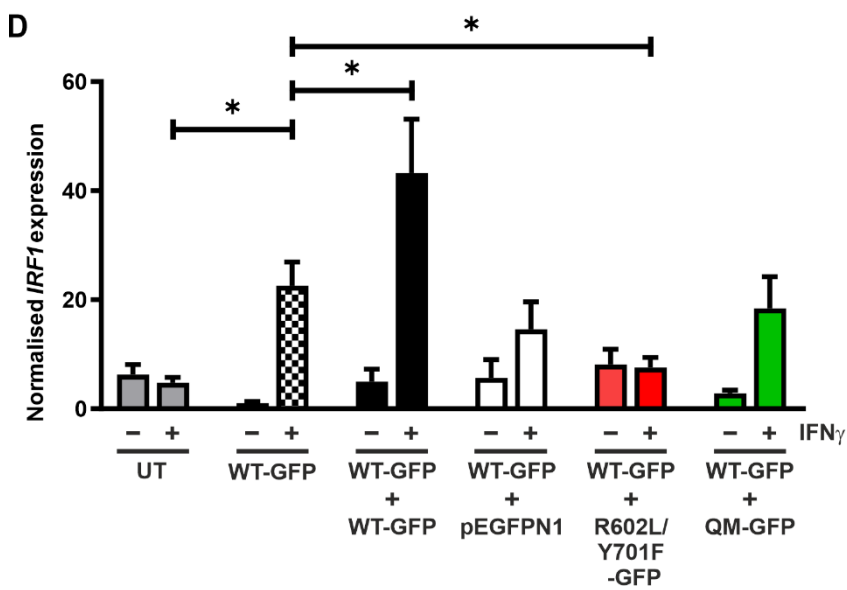
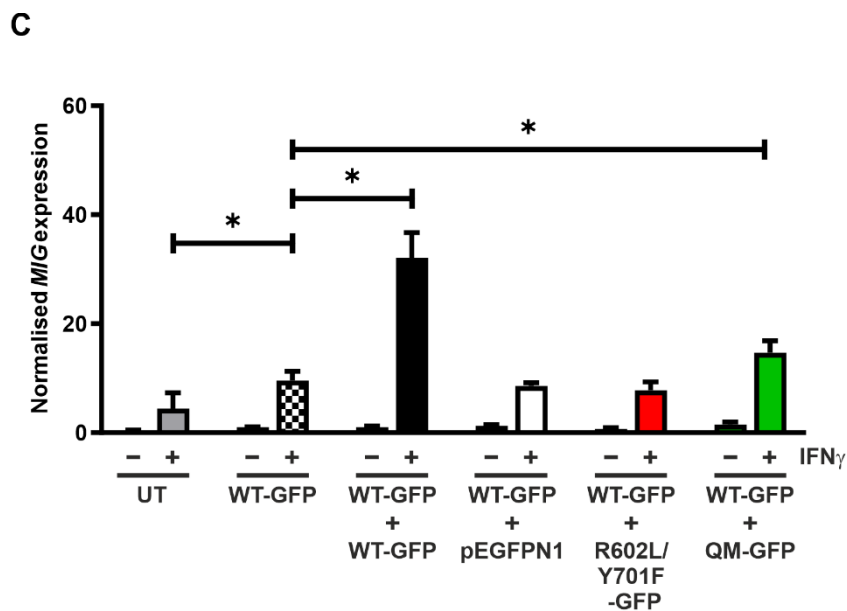
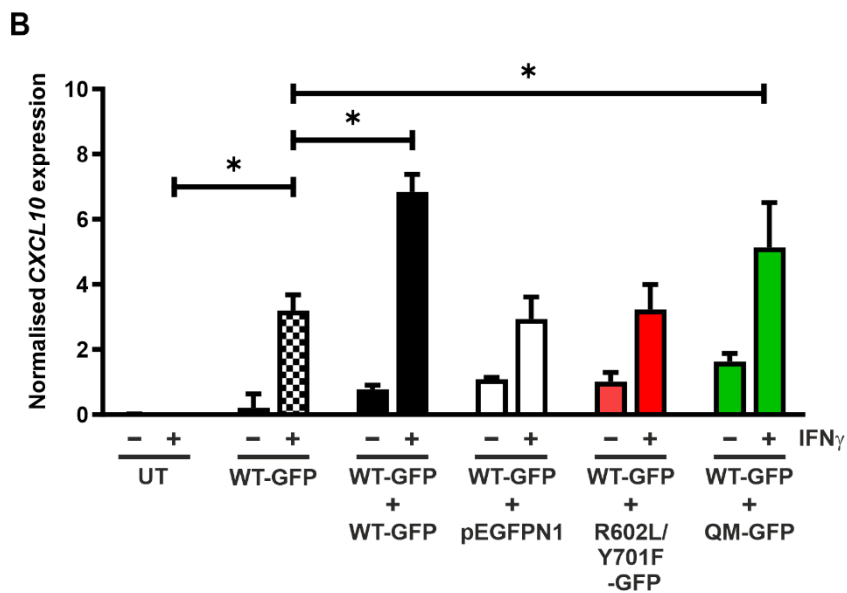
To test the impact of STAT1 mutants on the co-expressed WT-mediated transcription of STAT1 target genes, U3A cells were either left untransfected or transfected with a combination of one-part WT-GFP and one-part from either of the STAT1 variants comprising of WT-GFP, R602L/Y701F-GFP, QM-GFP or empty vector. Four STAT1 target genes, *GBP1*, *MIG*, *CXCL10* and *IRF1*, were tested by qPCR analyses. For all the genes, untransfected U3A cells

which lack endogenous STAT1 showed negligible gene expression, while cells transfected with twice the amount of WT STAT1 showed the highest fold induction (Figure 28). Cells expressing only one-part WT STAT1 or co-expressing empty vector or R602L/Y701F-GFP or QM-GFP, all showed similar gene induction patterns. These findings indicated that the additional presence of an unphosphorylated, dimerization-deficient STAT1 did not hamper the DNA binding or gene transcriptional activities of the phosphorylated STAT1 molecules present in these cells, but only affected its cellular distribution.

An interesting inference was made from these results about the transient nature of the mutant STAT1-induced blockage of nuclear import of phosphorylated WT proteins. The cytoplasmic retention or import block of the phosphorylated WT STAT1, observed in cells co-expressing R602L/Y701F-GFP or QM-GFP was not stable enough to induce any major alterations in the DNA binding or transcriptional profile of the WT protein. This observation posed a major challenge in isolating or characterizing the nature or organization of WT proteins in these hypothetical higher-order structures.







---

**Figure 28: The presence of unphosphorylated STAT1 variants does not affect the transcriptional activity of the co-expressed WT**

U3A cells were untransfected (UT), transfected with a plasmid coding for WT-GFP alone or a combination of WT-GFP and the indicated U-STAT1 variants or empty GFP vector (pEGFPN1). These cells were either untreated or stimulated with 50 ng/mL of IFN $\gamma$  for 6 h. From these cells, RNA was isolated and converted to cDNA. Histograms show the results from qPCR experiments for the following STAT1 target genes: (A) *GBP1*, (B) *CXCL10*, (C) *MIG* and (D) *IRF1*. Gene induction was normalized to the expression of the house-keeping gene *GAPDH*. Histograms show means and standard deviations wherein significant differences for IFN $\gamma$ -stimulated variant samples in comparison to the single transfection of WT protein are marked by bars and asterisks. The experiment was repeated three times with two independent transfections each.

**3.2.6 Unphosphorylated STAT1 proteins with critically impaired DNA binding do not enable the detection of co-expressed WT**

Although R602L/Y701F-GFP and QM-GFP were unable to stably bind to GAS sites *in vitro*, a hypothesis was generated that the STAT1 mutants could compete with phosphorylated WT for binding to GAS sites *in vivo*, and this could transiently knock-off WT proteins from DNA and thereby reduce nuclear retention. This approach was investigated to explain the unusual absence of nuclear retention of co-expressed, phosphorylated WT STAT1 in cells expressing the STAT1 mutants, independent of the import block hypothesis.

Here, to test if the STAT1 mutants competed with and transiently reduced the nuclear retention time of the co-expressed WT, additional mutations reducing the STAT1-DNA affinity were introduced in QM-GFP. Previously characterized as DNA<sup>minus</sup> mutations, two residues at positions V426 and T427 were mutated to aspartic acid in the QM-GFP construct and transfected in HeLa cells to be stimulated with IFN $\gamma$  (Meyer et al., 2003).

As can be seen from Figure 29, the DNA<sup>minus</sup> QM-GFP expressed in HeLa cells was unable to rescue the undetectable phosphorylation of endogenous STAT1 in immunohistochemical stainings of these cells. This disproved the hypothesis that reducing DNA affinity in the STAT1 mutants could prevent knocking-off the co-expressed, phosphorylated WT from DNA and restore nuclear P-STAT1 staining of the WT protein.

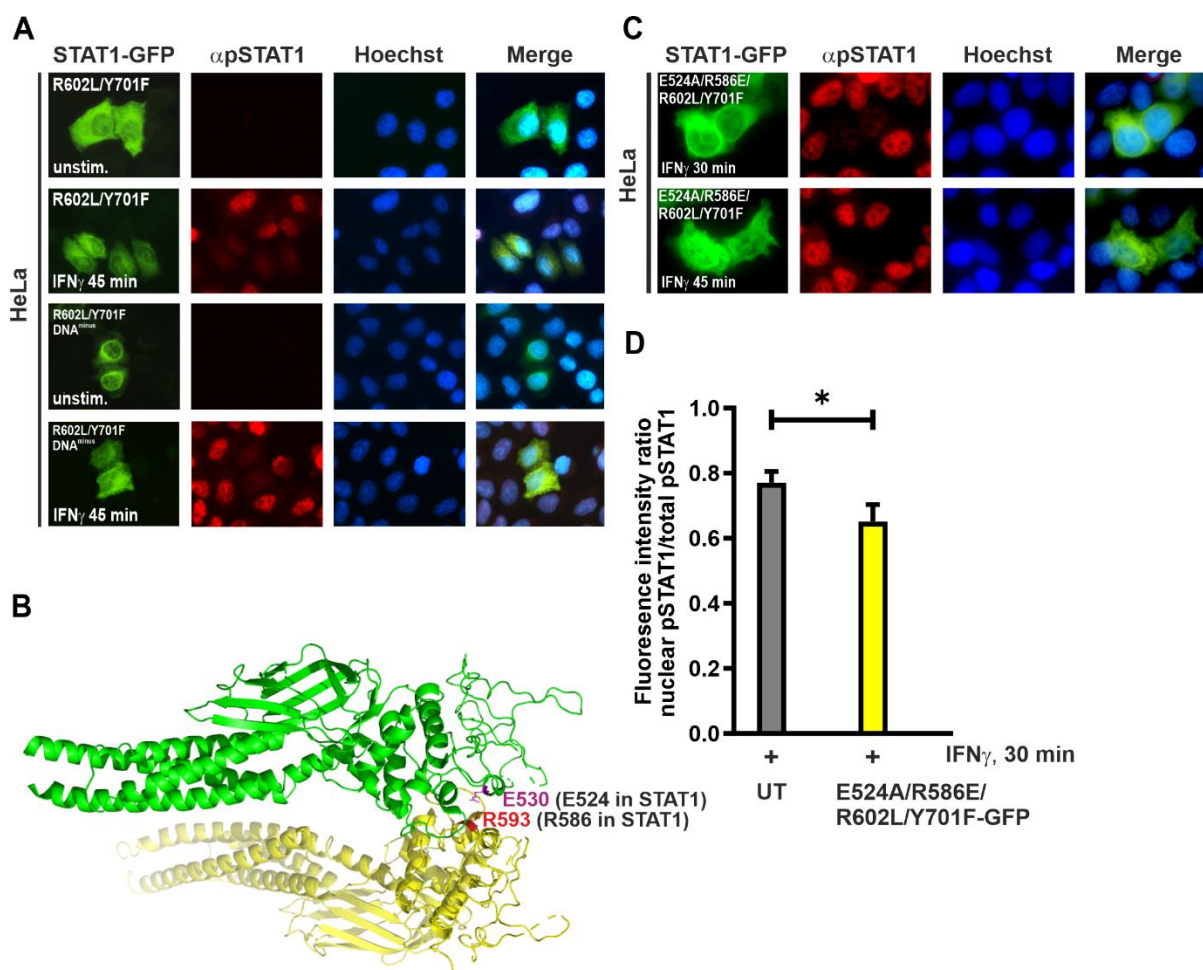


**Figure 29: Attenuating DNA affinity or disrupting the LD in mutant U-STAT1 does not restore the detection of WT P-STAT1**

(A) HeLa cells expressing R602L/Y701F-GFP with additional DNA<sup>minus</sup> mutations were either left untreated or stimulated with IFN $\gamma$  followed by staining with  $\alpha$ P-STAT1 antibody and Cy3-conjugated secondary antibody. The fluorescence micrographs show the intracellular distribution of V426D/T427D/R602L/Y701F-GFP and WT P-STAT1, as well as the localization of the corresponding Hoechst-stained nuclei (n=3 independent transfections). (B) Structure of an asymmetric unit of a crystal consisting of a STAT3 parallel dimer reported by Ren et al., 2008. Linker domain residues E530 (in pink) (homologous to E524 in STAT1) and R593 (in red) (homologous to R586 in STAT1) interacting at the binding interface in the dimer. This structure was created from the crystallographic data of a parallel unphosphorylated STAT3 dimer (PDB: 3CWG) (Ren et al., 2008) (C) HeLa cells expressing R602L/Y701F-GFP with additional mutations E524A and R586E in the STAT1 LD were stimulated and stained with  $\alpha$ P-STAT1 antibody followed by Cy3 secondary antibody. The fluorescence micrographs show the intracellular distribution of E524A/R586E/R602L/Y701F-GFP and the immunocytochemical staining pattern of WT P-STAT1, as well as the Hoechst-stained nuclei. (D) Histogram demonstrating the net reduction of nuclear P-STAT1 staining intensity in HeLa cells expressing E524A/R586E/R602L/Y701F-GFP, as determined by the ratio of nuclear-to-total fluorescence intensity (n=3 independent transfections).

In order to find interaction sites other than those involved in parallel or anti-parallel STAT1 dimer, a literature review was extended to find binding interactions discovered in other

members of the STAT family which could be examined in STAT1. An asymmetric unit of the STAT3 crystal structure studied by Ren and colleagues contained two unphosphorylated STAT3 monomers interacting with each other, forming a dimer that was widely different from the unphosphorylated dimer of STAT1 (Ren et al., 2008). The study reported a crystal structure of an unphosphorylated STAT3 dimer, wherein the participating monomeric core fragments were arranged closer to each other in a parallel orientation, forming a narrow parallel dimer. This structure was significantly different from the open, wider parallel dimer formed by phosphorylated STAT1 interacting via reciprocal SH2-phosphotyrosine interactions, wherein the core fragments pointed away from each other (Chen et al., 1998). Using the crystal structure of the STAT3 asymmetric unit from Ren et al (2008), this distinct binding interface was studied, and putative linker domain residues situated in this binding interface were recognized. For these STAT3 alternative binding LD residues, homologous STAT1 LD residues were determined by multiple sequence alignment and mutated in R602L/Y701F-GFP to determine whether the LD contained an interaction site between the unphosphorylated, dimerization-deficient STAT1 mutant and the co-expressed, phosphorylated WT protein. A hypothesis was generated that a mutation of this LD alternative binding site between two STAT monomers, if it indeed exists, would destabilize another possible interface via which the R602L/Y701F-GFP could bind to the WT protein and would rescue the absence of nuclear P-STAT1 staining from HeLa cells transfected with this mutant. For this purpose, two mutations, E524A and R586E, were introduced in the R602L/Y701F-GFP construct and transfected in HeLa cells to be stimulated with IFN $\gamma$ . As can be seen from Figure 29, a disruption of the alternative binding interface in the LD of R602L/Y701F-GFP did not rescue the absence of nuclear phosphotyrosine staining of endogenous STAT1 in HeLa cells expressing this construct. This finding undermined the relevance of this alternative binding site in the LD of STAT1 from being one of the interactions that could potentially stabilize the hypothetical transient import block structure formed by phosphorylated WT dimers by binding to the unphosphorylated, dimerization-deficient mutant STAT1.

### **3.2.7 Deletion of the N-terminus or disruption of the NLS in mutant U-STAT1 restores the visibility of co-expressed phosphorylated WT**

The NTD of STAT1 has been widely studied to play an important role in the dimerization/oligomerization of unphosphorylated STAT1 and in forming stable tetramers on adjacent GAS sites on DNA (Mao et al., 2005; Mertens et al., 2006; Meyer et al., 2004). Therefore, a hypothesis was generated that the NTD of the unphosphorylated, dimerization-

---

deficient mutant STAT1 could provide an interaction site to transiently associate with the co-expressed P-STAT1, forming higher-order structures of multiple WT P-STAT1 and mutant U-STAT1 proteins wherein the phosphotyrosine residues of the WT were undetectable. This hypothesis was first tested by mutating residues W37 and F77 in the NTD of QM-GFP. These two residues were first identified in the crystal structure of the STAT1 amino-terminal dimer to interact with each other, forming the dimer interface between the two amino termini (Chen et al., 1998; Vinkemeier et al., 1996). However, the two amino-terminal mutant constructs W37F/R274W/T385A/R602L/Y701F-GFP and F77A/R274W/T385A/R602L/Y701F-GFP displayed a similar inhibitory effect on the nuclear accumulation of co-expressed, native P-STAT1 (data not shown).

In an alternative approach, mutations R602L and Y701F were introduced in an expression vector coding for a STAT1-GFP with an amino-terminal deletion. This generated a  $\Delta$ N/R602L/Y701F-GFP construct which lacked the NTD. Immunocytochemistry was performed using HeLa cells transfected with  $\Delta$ N/R602L/Y701F-GFP and stimulated with IFN $\gamma$ . Surprisingly, cells expressing the NTD deletion construct with the double mutant R602L/Y701F did not diminish the nuclear phosphotyrosine staining of the endogenous STAT1 (Figure 30). The nuclei of IFN $\gamma$ -stimulated HeLa cells expressing  $\Delta$ N/R602L/Y701F-GFP showed a clear accumulation of endogenous P-STAT1 which was comparable to the neighbouring untransfected cells. In summary, the amino-terminal deletion completely restored the lack of nuclear accumulation and detection of P-STAT1 mediated by the presence of the double mutant. Thus,  $\Delta$ N/R602L/Y701F-GFP is inert to the action of the endogenous STAT1.

A dimer-specific NLS (dsNLS) located in a conserved motif consisting of residues L407 and L409 in the DBD of STAT1 has been reported to be responsible for its cytokine-induced nuclear import (Meyer et al., 2002). This sequence has been shown to be specific to the STAT1 dimer and when mutated, failed to undergo nuclear translocation upon activation and did not induce subsequent gene transcription despite of normal DNA-binding capability. The recognition of the STAT1 dsNLS by importin is a prerequisite for the assembly of an import complex upon cytokine stimulation. Therefore, the disruption of this sequence in U-STAT1 could possibly destabilize the import block structure formed by importin-bound P-STAT1 dimers and U-STAT1 molecules. To test this hypothesis, mutations L407A and L409A were introduced into the QM-GFP to abolish the binding of this construct to importin-bound P-STAT1 dimers.

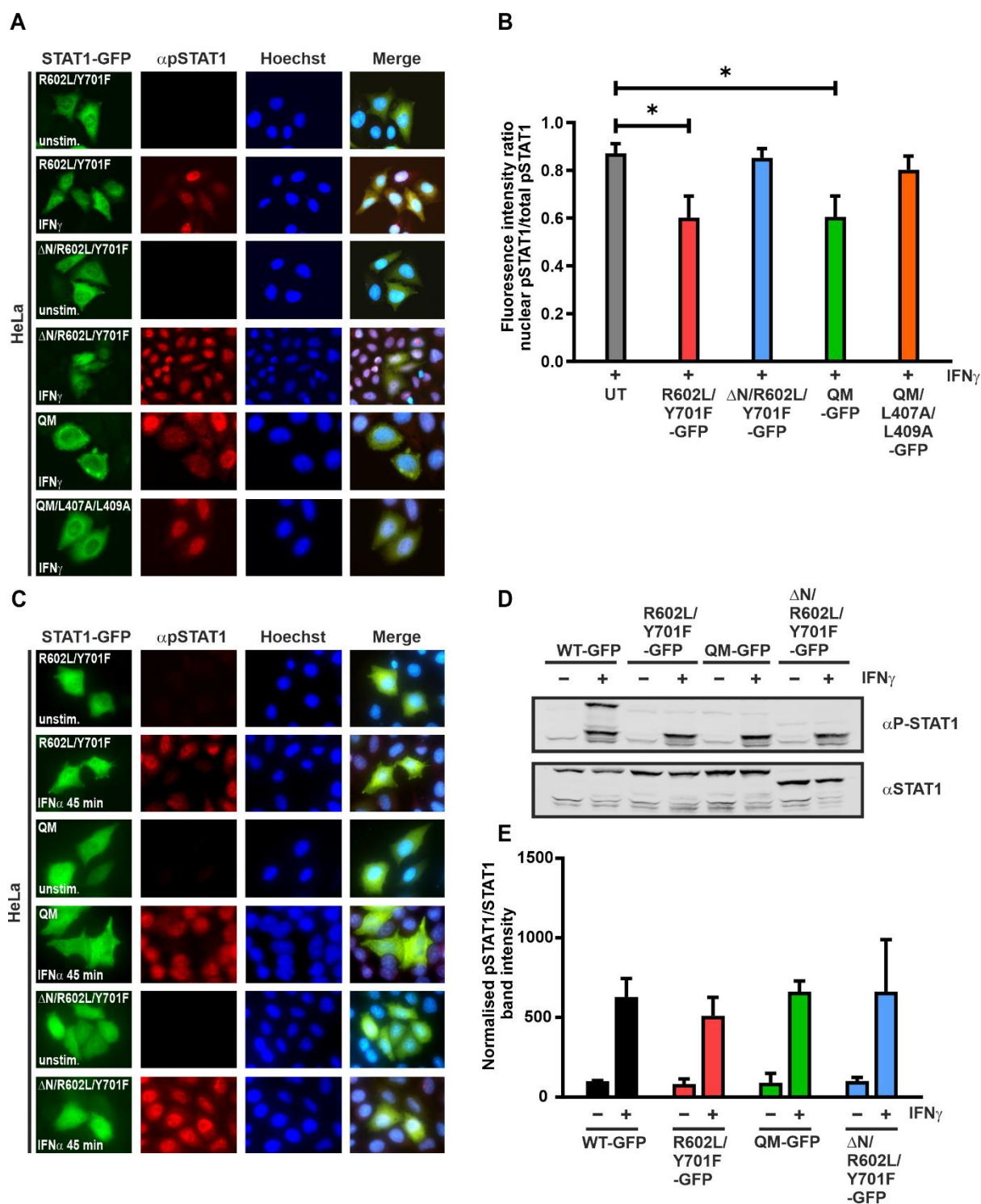


**Figure 30: Deletion of the NTD or disruption of the NLS in mutant U-STAT1 restores nuclear accumulation of co-expressed, native P-STAT1**

(A, B) HeLa cells were transfected with expression plasmids coding for R602L/Y701F-GFP,  $\Delta$ N/R602L/Y701F-GFP, QM-GFP or QM/L407A/L409A-GFP and on the next day, stimulated for 0 min or 45 min with 50 ng/mL of recombinant IFN $\gamma$ . Following stimulation, cells were fixed and stained with  $\alpha$ P-STAT1 antibody followed by Cy3-labelled secondary antibody. (A) Fluorescence micrographs show restored nuclear accumulation of endogenous P-STAT1 in cells co-expressing  $\Delta$ N/R602L/Y701F-GFP or QM/L407A/L409A-GFP and (B) the quantification thereof in comparison with untransfected HeLa cells or HeLa cells co-expressing R602L/Y701F-

---

GFP or QM-GFP from three independent experiments (n=3). (C) Fluorescence micrographs displaying the absence of nuclear endogenous P-STAT1 staining in the presence of mutant U-STAT1 constructs expressed in HeLa cells stimulated for 0 min and 45 min with recombinant IFN $\alpha$  (50 ng/mL). Note the rescue effect upon the deletion of NTD in the construct  $\Delta$ N/R602L/Y701F-GFP. (D) Representative immunoblot of whole cell extracts from HeLa cells expressing the indicated mutants, including the quadruple mutant (QM), before and after treatment for 45 min with 50 ng/mL of recombinant IFN $\gamma$  and (E) the quantification of immunoblotting results from three independent transfection experiment.

Similar to  $\Delta$ N/R602L/Y701F-GFP, the construct QM/L407A/L409A-GFP also completely restored the lack of nuclear accumulation and detection of P-STAT1 mediated by QM-GFP. These findings implied that the cytokine-induced import complex of STAT1 consists of an importin dimer bound to two STAT1 dimers, which is additionally stabilized by interactions with the amino-terminal of STAT1 proteins.

To further confirm the findings describing an absence of detectable tyrosine phosphorylation of the endogenous STAT1 in HeLa cells expressing the STAT1 mutants, immunocytochemistry experiments were performed after stimulation of transfected cells with IFN $\alpha$ , a type I interferon. As can be seen from Figure 30C, P-STAT1 staining was significantly reduced in IFN $\alpha$ -stimulated HeLa cells expressing the R602L/Y701F-GFP and QM-GFP but was rescued in cells expressing  $\Delta$ N/R602L/Y701F-GFP. This additionally validated the result that an excess of unphosphorylated, dimerization-deficient STAT1 via its NTD was able to interact with phosphorylated STAT1 proteins, causing them to form transient oligomeric structures that are retained in the cytoplasm with their phosphotyrosine residues undetectable by immunostaining.

In summary, these observations provided a significant clue about the role of the NTD in forming an interaction site via which mutant U-STAT1 could transiently block the import of WT P-STAT1. The mutant U-STAT1 construct generated in this work was able to interact via its NTD with importin- $\alpha$ 5-bound P-STAT1 dimers to transiently retain them in the cytoplasm, in a structure wherein their phosphotyrosine residues were inaccessible to the phosphotyrosine-specific antibody.

## 4. Discussion

A vast array of cytokines and growth factors influence a multitude of cellular activities, ranging from haematopoiesis, immune fitness, tissue repair and adipogenesis to inflammation, apoptosis, immune evasion and survival by utilizing the highly conserved components of the JAK-STAT pathway (Owen et al., 2019; Rawlings et al., 2004). Physiological processes like proliferation, differentiation, cell migration, immune cell development/recruitment and antigen processing, all require an active involvement of STATs. The very fact that they regulate most of the routine, developmental activities of the organism, implicates this class of proteins in several diseases. Initially identified in the study of anti-viral immunity with the discovery of STAT1, a dysfunctional JAK-STAT pathway has been extensively researched to be involved in rheumatoid arthritis, parasitic infections, dwarfism and, with the discovery of STAT3 and its oncogenic potential, in sustaining various cancers as well. While the activated full-length STATs have been most studied, the function of STAT isoforms and inactive STATs is a growing field of research. This work focusses on investigating the physiological role of unphosphorylated STATs in canonical JAK-STAT signalling. Since the anti-parallel structure seen in unphosphorylated STATs is controversial in STAT3, and an investigation into the relevance of this anti-parallel dimer interface was launched in the STAT3 protein. On the other hand, despite of having close chromatin associations and a distinct gene activation pattern, the influence of unphosphorylated STAT on its phosphorylated counterparts, if any, is unclear. Therefore, this question was studied in a model of STAT1, wherein U-STAT1 and not P-STAT1 is critically important for caspase-dependent induction of apoptosis (Yang & Stark, 2008).

### **4.1 The anti-parallel dimer interface is relevant in STAT3, the disruption of which manifests unique features that are similar yet distinct from STAT1**

The first part of this work deals with an investigation into the importance of the anti-parallel conformation seen in unphosphorylated STATs for the STAT3 protein. This conformation was first identified in STAT1, wherein the anti-parallel dimer was stabilized by reciprocal interactions between the CCD and DDB. Mutations in the CCD and DBD residues of STAT1 exhibited cytokine-induced hyper-phosphorylation, prolonged nuclear retention and conferred resistance to Tc45-catalysed dephosphorylation, together presenting a hyper-active phenotype. Furthermore, the NTD was implicated to facilitate a switch between this anti-parallel conformation of unphosphorylated STAT1 to a parallel conformation adopted by



phosphorylated STAT1. Due to a high homology with STAT1, a similar organization was expected to exist in STAT3 as well. However, the presence of contradictory data regarding mutations of critical residues in this CCD-DBD interface of STAT3, and the role of hyper-active STAT3 in driving several pathological processes made the examination of this STAT3 interface, interesting and relevant.

To study the anti-parallel dimer interface in STAT3, a phenylalanine residue at position F174 was mutated to alanine, to theoretically disrupt CCD-DBD interactions occurring around this residue. If this binding interface in STAT3 exists, the resulting mutation would significantly change the phenotype of the STAT3 construct, which was seen in subsequent experiments. Additionally, an alanine mutation was introduced at the residue V77 to study the role of the STAT3 NTD in mediating a switch between the parallel and anti-parallel forms, and this mutation also altered several characteristics of STAT3. An unphosphorylated, dimerization-deficient double mutant of STAT3, R609L/Y705F, was used as an experimental negative control.

Both point mutants of STAT3 investigated in this study showed elevated levels of cytokine-induced tyrosine phosphorylation, with the F174A being significantly phosphorylated even prior to stimulation. Both V77A and F174A showed a clear, nuclear accumulation in resting cells which slightly increased upon cytokine stimulation. The hyper-phosphorylated status of these mutants manifested as a higher occupancy on GAS sites *in vitro*. However, no change in the GAS specificity was seen, as both WT and mutant DNA-bound proteins were similarly displaced in competition experiments. The prominent nuclear localization of V77A and F174A led to a higher activation in reporter gene assays, as compared to the WT protein. Interestingly, the hyper-activating effect of these mutants on gene transcription was dependent on two distinct factors, namely: (1) the large amount of phosphorylated species in the cellular STAT3 pool and (2) the number of GAS sites in the promoter region of target genes. While the 3xLy6e luciferase reporter construct used in the reporter assay contains three tandem GAS sites, native target genes of STAT3 rarely mimic this phenomenon. Both V77A and F174A exhibited increased reporter activity, dependent on the two factors mentioned above. However, the mutants behaved differently in experiments studying STAT3 target gene transcription, wherein they increased the transcription of a gene harbouring one-and-a-half GAS site in its promoter region but virtually had no effect on target genes with a single GAS promoter.

An examination of V77A and F174A in *in vitro* phosphorylation and dephosphorylation assays revealed no differences in their susceptibility to undergo JAK2-induced phosphorylation or TC-PTP-mediated dephosphorylation. Despite of exhibiting constitutive tyrosine phosphorylation, the F174A dephosphorylated normally in the presence of TC-PTP. However, the hyper-phosphorylated mutants were insensitive to dephosphorylation induced by the pharmacological effect of staurosporine, when transfected cells were incubated with this potent kinase inhibitor. This *in vivo* observation provided a molecular explanation for the hyper-active phenotype of these mutants. Dissociation from DNA is a critical step that precedes dephosphorylation and subsequent nuclear export of STATs (Meyer et al., 2003) Therefore, a hypothesis was generated that GAS-bound mutant STAT3 molecules would be protected from dephosphorylation. This hypothesis was confirmed in an *in vitro* dephosphorylation experiment by adding double-stranded DNA oligonucleotides encoding a one-and-a-half GAS site, upon which the point mutants resisted TC-PTP-mediated-dephosphorylation.

By introducing a mutation at position F174 in the CCD, stabilizing interactions forming the STAT3 anti-parallel dimer were disrupted. This prevented the occurrence of an efficient conformational switch from a phosphorylated parallel dimer to an anti-parallel dimer, as shown in Figure 2. In STAT1, this change in conformation may occur around homotypic amino-terminal interactions within the dimer, although controversial observations have been published (Mertens et al., 2006). To study the relevance of this mechanism in STAT3, reciprocal amino-terminal interactions were disrupted by introducing the V77A mutation in the NTD. The importance of this conformational shift is to disengage the phosphotyrosine residues that are involved in reciprocal SH2-phosphotyrosine interactions that form the parallel dimer, such that it can be dephosphorylated (Mertens et al., 2006). Therefore, the hyper-phosphorylated status of the STAT3 mutants shows that the parallel/anti-parallel dimer equilibrium, as revealed for STAT1, is also relevant in STAT3. The selective ability to exist as parallel dimers is not the sole contributor to the elevated tyrosine phosphorylation of these mutants, as both mutants dephosphorylated normally in *in vitro* assays. From the response of these mutants to staurosporine treatment and the results from DNA-bound dephosphorylation experiments, it was clear that DNA binding plays a crucial role in driving the resistance of these mutants to dephosphorylation.

STATs constitutively shuttle between the nuclear and cytoplasmic compartments, wherein unphosphorylated STATs translocate via direct interactions with nucleoporins thereby not needing cytosolic carrier proteins, while tyrosine-phosphorylated STAT dimers require

importins, a Ran-GTP/GDP gradient and metabolic energy (Meyer & Vinkemeier, 2004; Martincuks et al 2016). The distribution of STAT3 within the subcellular compartments in resting cells shows a higher concentration in the cytoplasm than in the nucleus. This is the manifestation of a typical equilibrium arising from constant nuclear import and export (Bhattacharya & Schindler, 2003; Pranada et al., 2004). Since STAT3 can act as both a cytokine-inducible signal transducer and a constitutive transcriptional regulator, at a given time point both phosphorylated and unphosphorylated STAT3 can translocate to the nucleus. Unphosphorylated WT STAT3 can shuttle to the nucleus as a monomer or anti-parallel dimer, while phosphorylated WT STAT3 predominantly shuttles as a parallel dimer (Vogt et al., 2011). However, the nuclear retention displayed by the STAT3 point mutants is driven by the same two factors that are responsible for its hyper-phosphorylated status. The steady-state of V77A and F174A nuclear import and export is disrupted by the cumulative effect of two features, namely (1) the ability to selectively exist as parallel dimers, and (2) the retention of these parallel dimers at GAS sites on DNA. In the absence of a cytokine signal, mutant STAT3 shuttling into the nucleus is retained in the nucleus by its association to DNA. Therefore, the predominant nuclear localization of the STAT3 mutants is driven by a combination of the above two factors.

Despite of having unaltered affinity to GAS sites and unchanged dissociation rates from DNA, the conformational change that follows the dissociation step from DNA is disrupted in V77A and F174A. Therefore, the mutant STAT3 parallel dimers dissociating from DNA do not have the opportunity to rearrange as anti-parallel dimers as fast as the WT protein, and subsequently reassociate on DNA. As a result, the downstream activities of dephosphorylation by nuclear Tc45 phosphatase and subsequent nuclear export are abolished. A decoupling of dephosphorylation and nuclear export from nuclear import and DNA binding gives rise to the hyper-phosphorylation and predominant nuclear presence of these point mutations.

The results in this work are in line with the study conducted by Andersson and colleagues, wherein they found the hyper-phosphorylated mutation F174S in a patient with T-LGL (Andersson et al., 2016). However, this work also acknowledges the contradictory results reported with an F174W mutation by Ren et al (2008), wherein no differences were described between their mutants and WT STAT3 regarding cytokine-induced tyrosine phosphorylation and dephosphorylation elicited by an EGF receptor kinase inhibitor. Based on this evidence, the authors claimed that the reciprocal CCD-DBD anti-parallel binding interface in STAT3 does not exist or if disrupted does not affect the phosphorylation of STAT3. The results in this

work and those from Andersson et al (2016) are contradictory to those with the F174W mutation. A reasoning for this phenomenon could be that a mutation from the native phenylalanine at position 174 to the aromatic amino acid residue tryptophan would not have grossly affected the crucial reciprocal interactions involving the CCD and DBD which occur around this residue in STAT3. The similar behaviour of mutations at homologous residues in STAT1 and STAT3 has been thoroughly discussed in the Introduction section. A mutation of the hydrophobic, non-polar phenylalanine 174 to polar serine found in the T-LGL patient or to alanine as described in this work completely abolishes the interaction mediated by the insertion of the phenylalanine side chain of F174 into the hydrophobic ‘pocket’ formed by residues Q344, G388 and T412. A persistent hyperphosphorylation and hyperactivity was observed in STAT3-F174S and -F174A, but not F174W (Andersson et al., 2016; Ren et al., 2008).

Owing to its elevated level of cytokine-induced tyrosine phosphorylation, constitutive nuclear localization, resistance to dephosphorylation when bound to DNA and increased inducibility in reporter gene assays and of selected STAT3 target genes, the F174A mutation behaves as a STAT3 GOF mutation. The V77A mutation also has a hyper-phosphorylated status and shows an increased GAS-dependent gene activation, despite of its inability to bind cooperatively on DNA.

Comparing the STAT3 mutations to homologous mutations in STAT1, there are similarities and differences which underscore the homology and specificity among the different STATs. While the F174A in STAT3 and F172W in STAT1 behave similarly with respect to exhibiting a cytokine-induced tyrosine phosphorylation that is significantly increased from the WT protein, the F174A is phosphorylated even in the absence of a cytokine (Mertens et al., 2006; Staab et al., 2013; Zhong et al., 2005). Similarly, both STAT3-F174A and STAT1-F172W show persistent phosphorylation, after the inhibition of kinase activity by staurosporine. However, F174A is not resistant to TC-PTP-induced dephosphorylation *in vitro*, unless DNA is present, indicating that the persistent phosphorylation of F174A requires DNA binding. Even V77A and F77A have their own similarities and differences, wherein both mutants show a cytokine-induced hyper-phosphorylation (Meyer et al., 2004). However, a significant feature seen only in the STAT3 mutant was that both V77A and F174A display a nuclear accumulation in resting cells, while their corresponding STAT1 mutations accumulate in a cytokine-dependent manner. This deviation in their phenotype derives from the intrinsic differences between STAT1- and STAT3-mediated signal transduction. While STAT1 requires a strong cytokine signal for activation and its presence is tightly compartmentalized to achieve peak

transcriptional activity in the event of an anti-viral response, STAT3 mediates cellular processes like proliferation, migration and differentiation which are continuous and thereby require constitutive mobility.

Based on the results in the first part of this investigation and similar to STAT1, the anti-parallel dimer-binding interface exists in STAT3. A recent study characterizing MS3-6, a synthetic antibody mimetic for the inhibitory targeting of the STAT3 CCD, has described a crystal structure of an unphosphorylated STAT3 anti-parallel dimer in an asymmetric unit with their monobody (la Sala et al., 2020). The structure is quite similar to the unphosphorylated dimer of STAT1 and STAT5 $\alpha$ , wherein both monomers are arranged in an anti-parallel orientation with a close proximity between the CCD and DBD.

Some limitations of this part of the investigation include an absence of characterized STAT3 DBD residues that are homologous to the STAT1 DBD residues binding to the CCD and stabilizing the STAT1 anti-parallel dimer. This would provide additional information regarding the role of the STAT3 DBD in forming the anti-parallel STAT3 dimer. However, the characterization of GOF mutation in the STAT3 CCD not only establishes the relevance of the anti-parallel dimer interface in STAT3 but makes the STAT3 CCD and the STAT3 anti-parallel dimer a potential therapeutic target to be explored in various disease models.

#### **4.2 Unphosphorylated STAT1 affects the localization of phosphorylated STAT1 in a concentration-dependent manner**

The second part of this investigation focusses on studying the role of unphosphorylated STATs on the localization and activities of phosphorylated STAT, in the STAT1 model. Dimerization of P-STAT1 occurs via reciprocal interactions between the arginine pocket structure containing residue R602 of one protomer, and the phosphotyrosine at position 701 of the partner protein (Shuai et al., 1994). Based on this information, a double mutation at residues R602 and Y701 in STAT1 was made, such that the construct remains constitutively unphosphorylated and cannot stabilize the interactions forming a parallel dimer with phosphorylated STAT1. Due to its inability to dimerize with P-STAT1, it was expected that this construct would not have any effect on the localization of WT STAT1. However, in HeLa and U3A cells expressing R602L/Y701F-GFP, the co-expressed WT STAT1 did not accumulate in the nucleus upon cytokine stimulation. Furthermore, upon staining with a P-STAT1 antibody, it was observed that there was an absence of endogenous tyrosine-phosphorylated STAT1 in the nucleus of IFN $\gamma$ -stimulated HeLa cells expressing R602L/Y701F-GFP. This inhibitory effect on nuclear

P-STAT1 was also observed in cells expressing R602L/Y701F-GFP upon IFN $\alpha$  stimulation as well.

Upon this interesting observation, additional mutations were introduced in R602L/Y701F-GFP. The first mutation was at position R274 in the CCD of R602L/Y701F-GFP, which was followed by a mutation at T385 in the DBD, to disrupt any possible anti-parallel interactions occurring between the R602L/Y701F-GFP and WT STAT1. However, both the triple and quadruple mutant, termed QM-GFP, led to a similar disappearance of nuclear P-STAT1 in HeLa cells expressing these mutants. A note-worthy phenomenon was the observed concentration-dependent nature of the inhibitory effect of QM-GFP on nuclear P-STAT1 in HeLa cells. In cells expressing a high level of the dimerization-deficient mutant, there was a greater reduction in the nuclear P-STAT1, while a low concentration of mutant U-STAT1 inhibited the detection of nuclear P-STAT1 to a lesser degree. From these experiments, it was evident that an excess of U-STAT1 interfered with the nuclear import of P-STAT1.

To determine whether, the phosphorylation of WT STAT1 was impaired in cells expressing an excess of mutant U-STAT1, Western blotting experiments were performed in U3A cells expressing a combination of both WT STAT1 and mutant U-STAT1, and HeLa cells expressing the U-STAT1 variants alone. These experiments, in addition to unchanged kinetics of the WT in *in vitro* phosphorylation and dephosphorylation assays, showed that tyrosine phosphorylation of WT STAT1 was unaltered in the presence of large amounts of mutant U-STAT1, but the subsequent cytokine-stimulated nuclear import of STAT1 was blocked. It was hypothesized that high levels of mutant U-STAT1, interfered with the assembly of WT P-STAT1 into an importable complex that impeded its nuclear import and inhibited the detection of tyrosine phosphorylation in these structures, with the concentration of mutant U-STAT1 being the pivotal factor.

Subsequent experiments were performed to study the effect of this P-STAT1 import block on its GAS binding and transcriptional activity using U3A cells expressing a combination of both WT and mutant U-STAT1 and HeLa cells expressing the U-STAT1 mutants alone. While the U-STAT1 variants did not bind to DNA or induce transcription on their own, their additional presence did not alter WT-mediated GAS binding and IFN $\gamma$ -induced transcription of STAT1 target genes. This evidence pointed to the transient nature of the import block, wherein this inhibitory phenomenon only impaired the detection of nuclear P-STAT1, while no gross

changes occurred in the downstream signalling activities of WT P-STAT1 upon the over-expression of mutant U-STAT1.

To resolve the structure of this mutant U-STAT1-derived import block of WT P-STAT1, additional binding sites in the STAT1 structure were identified and mutated. The first of these mutagenesis approaches included reducing the DNA affinity in mutant U-STAT1 by replacing critical residues identified to render DNA affinity with negatively charged residues, in a mutation V426D/T427D in the DBD. This mutant called QM/DNA<sup>minus</sup>-GFP did not rescue the undetectability of P-STAT1 in HeLa cells stimulated with IFN $\gamma$ , thereby disproving the hypothesis that mutant U-STAT1 through its affinity to temporarily associate with DNA could knock off WT P-STAT1 and impair its nuclear retention.

The second approach was to determine the relevance of a hypothetical dimerization site identified in a crystal structure of an unphosphorylated STAT3 dimer in the mutant U-STAT1 construct. The asymmetric unit of the unphosphorylated STAT3 core fragment reported by Ren et al (2008) contained two monomers of STAT3 arranged in a parallel orientation, binding to each other via possible interactions at the STAT3 LD. Based on this structure, two STAT1 residues, namely E524A and R586E homologous to the STAT3 LD residues involved in this interaction, were mutated in R602L/Y701F-GFP to determine whether this hypothetical LD interaction site existed and stabilized the binding of mutant U-STAT1 and WT P-STAT1. However, the nuclear accumulation of tyrosine-phosphorylated, endogenous STAT1 could still not be detected in IFN $\gamma$ -stimulated HeLa cells expressing the GFP-fusion protein of E524A/R586E/R602L/Y701F.

Since the NTD has been implicated in driving the dimerization and oligomerization of STATs, a deletion of the NTD was done in R602L/Y701F-GFP. This construct, termed  $\Delta$ N/R602L/Y701F-GFP, showed no inhibition of the nuclear P-STAT1 detection upon stimulation of cells with IFN $\gamma$ . The transient import block induced by a high concentration of mutant U-STAT1 was relieved upon disruption of amino-terminal interactions in this variant via the complete deletion of the NTD. This finding also underscores the unique novel function of the STAT1 NTD in impacting the nucleocytoplasmic shuttling of the STAT1. The NTD of STAT1 is required for associations with importin  $\alpha$ 5 upon stimulation with IFN $\gamma$  (Meissner et al., 2004). Therefore, P-STAT1 molecules bound to importins via NLS recognition could possibly be stabilized by additional interactions with the NTD. In addition to the deletion of the NTD, disrupting NLS recognition in mutant U-STAT1 also relieved the block on cytokine-

induced nuclear import of importin-bound P-STAT1 molecules, indicating that the assembly of a STAT1 import complex requires both NLS recognition and a functional amino-terminus for stabilization.

This is in accordance with the contribution of homotypic NTD interactions in the dimerization of STAT1. Apart from the mutation F77A that leads to a loss of tetramerization and cooperative DNA binding, there are other residues like M28 and L78 implicated in the STAT1 NTD interface to interfere with dimer formation in STAT1 (Chen, 2003). Therefore, a complete deletion of the NTD in the R602L/Y701F-GFP protein led to the loss of several binding interactions in this interface and significantly weakened the interaction between the amino-terminal deletion mutant and the co-expressed P-STAT1.

Also, IFN-induced association with importin  $\alpha 5$  requires the NTD, as the  $\Delta N$  mutant of STAT1-GFP does not accumulate in the nucleus upon cytokine stimulation, suggesting that the NTD of STAT1 could possibly contribute to importin binding (Meissner et al., 2004). The STAT1 NTD could potentially stabilize several importin-bound P-STAT1 molecules and a high concentration of mutant U-STAT1 could interfere with this process. Cytoplasmic retention of WT STAT1 and the absence of nuclear P-STAT1 seen in the preceding experiments could be mediated via interactions with the mutant U-STAT1 NTD and importins. This interaction is although transient as it does not alter the phosphorylation or GAS binding and subsequent transcription of the WT P-STAT1. However, the relevance of this transient cytoplasmic retention of the co-expressed WT P-STAT1 in the presence of an excess of mutant U-STAT1 can be seen from the priming effect of IFN $\gamma$  stimulation on immune cells, wherein lower concentrations of IFN $\gamma$  do not elicit an actual immune response, but instead prepare cells to strongly respond to a subsequent viral or parasitic load. A transient retention or block of P-STAT1 detected in the preceding experiments could serve as a mechanism that impedes the signal transduction cascade unless signal saturation has been reached.

Based on the results from the second part of this work, a proposed model illustrating the effects of U-STAT1 (corresponding to STAT1 mutants R602L/Y701F-GFP, QM-GFP, QM/DNA<sup>minus</sup>-GFP and E524A/R586E/R602L/Y701F-GFP) on the nucleocytoplasmic translocation of P-STAT1 is shown in Figure 31. The left panel describes a condition under low levels of STAT1, such as a cell not expressing the U-STAT1 variants. Here, in response to cytokine stimulation, tyrosine-phosphorylated STAT1 proteins associate to form P-STAT1 parallel dimers, which bind to importins and are translocated to the nucleus as shown. In the



presence of low concentrations of U-STAT1, most of the P-STAT1 proteins form the importable complex and are rapidly translocated to the nucleus upon cytokine stimulation. Under IFN $\gamma$  stimulation, most of the cytosolic STAT1 undergoes tyrosine phosphorylation and forms stable high affinity dimers, which faces little resistance from the low concentration of U-STAT1 in the cell. While a study suggests that an importin molecule binds to a P-STAT1 dimer in a 2:1 ratio wherein two STAT proteins are bound to a single importin  $\alpha 5$ , another report argues that two  $\alpha 5$  importins can bind to the two STAT1 protomers in a dimer (Fagerlund et al., 2002; Melén et al., 2003; Nardozzi et al., 2010). Additionally, it is known that rapid translocation of larger cargoes requires more than one transport molecules for import (Ribbeck & Görlich, 2002) and that the nuclear import factor karyopherin  $\alpha$  forms a dimer (Conti et al., 1998). Taking these observations together, the hypothesis of a higher-order import complex comprising of a dimer of importins bound to two P-STAT1 dimers stabilized via STAT1-NTD interactions is illustrated in the left panel of Figure 31. For the stability of this complex, it can be hypothesized that one out of the STAT1 molecules forming each dimer binds via to its NTD to the other importin molecule. A cross-over assembly is most stable, wherein each STAT1 dimer binds to both components of the importin dimer via the NLS localized in the DBD to one importin molecule, and through the NTD to the other.

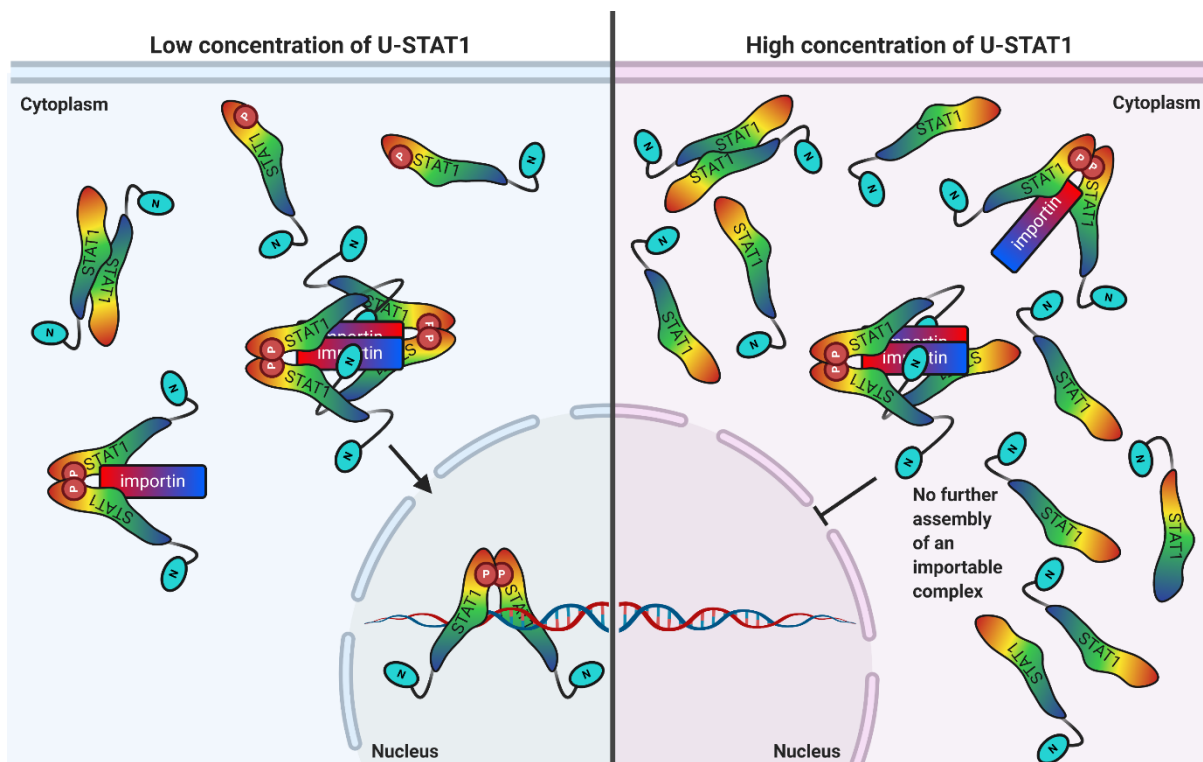


**Figure 31: Proposed model of U-STAT1-dependent transient import block of P-STAT1**

The left panel describes a condition of low-level cellular U-STAT1, wherein higher-order importable structures of P-STAT1 are formed, which undergo nuclear import leading to nuclear accumulation in cytokine-stimulated cells. The right panel describes a high-concentration of U-STAT1, wherein U-STAT1 interacts via its NTD with one importin molecule and the NLS in the DBD to the other component of the importin dimer. Further assembly towards an importable STAT1 tetrameric complex bound to an importin dimer is hindered by the missing phosphorylated tyrosine residue of U-STAT1 dimer.

In the right panel of Fig 31, a premise of high levels of U-STAT1 in a cell, such as IFN-primed HeLa cells or U3A cells transfected with U-STAT1 variants, is described. Upon IFN $\gamma$  stimulation, while most of the endogenous STAT1 molecules in HeLa cells or recombinant WT STAT1 in transfected U3A cells are tyrosine phosphorylated, these cells express high levels of U-STAT1. Therefore, the assembly of P-STAT1 molecules into importable structures is halted due to a high number of U-STAT1 proteins which interact via their NTDs and DBD with the importin  $\alpha$ 5-bound P-STAT1 dimers and cease further assembly into a fully importable complex. A large number of U-STAT1 proteins in this condition can transiently block several P-STAT1 dimers bound to importins, which manifests as a cytoplasmic retention of P-STAT1. The formation of higher-order aggregates of STAT1 and importins are disrupted, which increases the solubility of P-STAT1, thereby affecting detection by an anti-phosphotyrosine antibody.

The physiological relevance of this temporary nuclear import block can be seen from the impact of IFN priming on macrophages and monocytes (da Silva et al., 2015; Green et al., 2017; Schroder et al., 2006). Antigen-presenting cells (APCs) like dendritic cells and macrophages are tightly regulated by cytokines such as IFN $\gamma$  to rapidly respond to infections but are also under modulation to avoid the undesirable effects of excessive activation. IFN $\gamma$  at suboptimal concentrations does not actually activate these cells but prepares them for a subsequent response to stimuli, in a process called IFN $\gamma$  priming. This priming effect of IFN $\gamma$  can be seen in the augmentation of lipopolysaccharide (LPS)-induced tumour necrosis factor  $\alpha$  (TNF $\alpha$ ) expression and subsequent induction of a pro-inflammatory repertoire via nuclear factor kappa B (NF- $\kappa$ B) in macrophages and monocytes (Hayes et al., 1995; Schroder et al., 2006). A pre-exposure to low, sub-activating concentrations of IFN $\gamma$  sensitizes these cells to produce enhanced responses to strong extracellular inflammatory stimuli that includes IFNs themselves, as well as other cytokines such as TNF $\alpha$ /LPS (Green et al., 2017). Apart from

inducing post-transcriptional modifications and epigenetic remodelling that enhances the LPS-induced response, pre-stimulation with IFN $\gamma$  mainly leads to an upregulation of STAT1 in these cells. IFN $\gamma$  priming in the early stages of immune activation does not illicit a complete IFN $\gamma$  response, as the cytokine concentration is not strong enough to phosphorylate most of the STAT1 in the cell. Instead, priming increases the transcription of STAT1 within the cell. High levels of STAT1 in IFN $\gamma$ -primed cells is represented in Fig 31 (right panel). The large amount of STAT1 induces a transient refractory period, until a strong, activating signal is received such that most of the STAT1 in the cell is phosphorylated in response to it. The transient import block caused by a high number of cytoplasmic circulating STAT1 does not abolish DNA binding or transcriptional activity, as can be seen from the results in the preceding section. Therefore, it is in accordance with priming activity of IFN $\gamma$ , as STAT1-mediated transcription is required to further upregulate STAT1. However, an inhibitory mechanism is essential to prevent hyper-responsiveness to small amounts of IFN $\gamma$  stimulation.

SUMOylation is an elegant example of a congenital inhibitory mechanism of STAT1, wherein small ubiquitin-like modifier (SUMO) conjugation close to the tyrosine residue 701 constitutively inhibits tyrosine phosphorylation, serving as a mechanism to permanently attenuate the IFN $\gamma$  sensitivity of cells, thereby preventing hyperresponsiveness to IFN $\gamma$  and its potentially deleterious consequences (Begitt et al., 2011). However, SUMO conjugation has a direct effect on IFN $\gamma$ -induced tyrosine phosphorylation and target gene transcription, which cannot explain the priming effect of IFN $\gamma$ . On the other hand, the transient import block model proposed in this work is intrinsic to STAT1, mediated via temporary interactions between the STAT1 import complex and U-STAT1 NTD, is concentration-dependent but does not impair transcription, and therefore could serve as a mechanism by which IFN $\gamma$  primes immune cells.

Cell death via apoptosis poses another scenario wherein the STAT1 intrinsic import block plays a physiological role. STAT1 is required for the efficient, constitutive expression of caspases and *Fas* genes known to drive apoptosis, wherein STAT1-deficient cells were resistant to the apoptotic effects of TNF $\alpha$  (Kumar et al., 1997). However, a reconstitution with the U-STAT1 mutants Y701F or R602L restored sensitivity to apoptosis, indicating that STAT1 contributed to regulating cell death, irrespective of cytokine stimulation. Several studies report the role of STAT1 in inducing apoptosis via the upregulation of caspases upon stimulation with IFN $\gamma$ , thereby serving as the mechanism by which IFN $\gamma$  sensitizes cells to undergo cell death (Chin et al., 1997; Fulda & Debatin, 2002; Kim & Lee, 2007; Sironi & Ouchi, 2004; Stephanou &

Latchman, 2003). However, the heightened sensitivity to apoptosis in IFN $\gamma$ -primed cells, expressing high levels of STAT1 can be severely detrimental in the absence of a negative feedback loop. To counter this phenomenon, there is increasing evidence of STAT1 being a substrate for cleavage via caspases, in response to dsRNA and other inducers of apoptosis (King & Goodbourn, 1998). Histone deacetylase inhibitor (HDACi) treatment of transformed haematopoietic cells expressing high STAT1, but not in primary and differentiated cells, showed a caspase-mediated cleavage of STAT1 that induces apoptosis (Licht et al., 2014). Therefore, the role of STAT1 in inducing apoptosis is ambivalent, in the sense that, depending on the cell type and its concentration, STAT1 can induce and inhibit apoptosis. In an apoptotic cell, proteolytic cleavage by caspases renders STAT1 unable to participate in IFN $\gamma$ -induced signal transduction. Therefore, in the event of apoptosis induced by factors such as dsRNA, the cellular STAT1 may participate in two processes, namely (1) pause in the cytosol and commit to cell death via caspase-mediated proteolysis, or (2) translocate to the nucleus and participate in cytokine signalling, in order to respond to its extracellular environment and also warn neighbouring cells in the premise of a pathogenic attack or inflammation. A transient cessation of STAT1 in the cytoplasm can possibly serve as a buffer between the two antagonistic cell fates, namely that of cell death or survival and subsequent cytokine-mediated cellular response. While a lack of STAT1 confers resistance to apoptosis, in the event of an infection, the cell can decide to undergo apoptosis or, alternatively, survive and promote inflammatory responses depending on the concentration and localization of STAT1.

In cells expressing high levels of STAT1 (Fig 31, right panel), a transient retention of STAT1 in the cytosol provides an opportunity for the cell to choose between triggering cell death or transduce extracellular signals to the nucleus. The interesting aspect of the transient import block model induced by high levels of unphosphorylated STAT1 described by the results in this work, is the unaltered signal transduction of P-STAT1. This mechanism can effectively explain the participation of activated macrophages or IFN $\gamma$ -primed cells in inflammatory responses, while simultaneously the high concentration of STAT1 in these cells renders them highly sensitive to apoptosis. Although activated macrophages are a crucial component of host defence, when uncontrolled they are capable of causing extensive local damage by causing septic shock, a severe systemic inflammatory response triggered by the interaction of LPS and some bacterial components with macrophages and other host cells (Kim & Lee, 2005). Therefore, promoting inflammation via cytokine signalling or inducing death and thereby controlling inflammation can be a cellular decision depending on the concentration and

compartmentalization of STAT1 in the cell. The hypothesis that STAT1 may contain an intrinsic self-inhibitory mechanism that does not drastically impact its activities, but merely helps the cell to make more informed decision depending on its microenvironment, not only makes for a logical accessory to STAT1 signalling that is implicated in several processes of immunomodulation, but also contributes to its versatility.

In summary, this work involves the study of binding interfaces and functional relevance of unphosphorylated STAT in JAK-STAT signalling. In addition to providing evidence of an anti-parallel dimer interface in STAT3 with the capacity to impair its dephosphorylation and induce nuclear retention, a novel role of unphosphorylated STAT1 in the nucleocytoplasmic distribution of P-STAT1 was explored through the experiments described in this work. While the examination of the anti-parallel dimer interface of STAT3 assisted in characterizing a GOF mutation at position F174 and elucidating similarities and differences in the regulation of STAT1 and STAT3, the study of a dimerization-deficient mutant of unphosphorylated STAT1 identified its inhibitory function on the nuclear import of phosphorylated STAT1 that did not significantly hamper  $\text{IFN}\gamma$  signal transduction. These findings emphasize the role of unphosphorylated STATs, independent of their phosphorylated species in mediating cytokine responses via the JAK-STAT pathway.

---

## 5. References

- Andersson, E., Kuusanmäki, H., Bortoluzzi, S., Lagström, S., Parsons, A., Rajala, H., van Adrichem, A., Eldfors, S., Olson, T., Clemente, M. J., Laasonen, A., Ellonen, P., Heckman, C., Loughran, T. P., Maciejewski, J. P., & Mustjoki, S. (2016). Activating somatic mutations outside the SH2-domain of STAT3 in LGL leukemia. *Leukemia* **30**(5), 1204–1208.
- Arpino, J. A. J., Rizkallah, P. J., & Jones, D. D. (2012). Crystal structure of enhanced green fluorescent protein to 1.35 Å resolution reveals alternative conformations for glu222. *PLoS ONE*. **7**(10), 47132.
- Avalle, L., Pensa, S., Regis, G., Novelli, F., & Poli, V. (2012). STAT1 and STAT3 in tumorigenesis. *JAK-STAT*. **1**(2), 65–72.
- Azam, M., Erdjument-Bromage, H., Kreider, B. L., Xia, M., Quelle, F., Basu, R., Saris, C., Tempst, P., Ihle, J. N., & Schindler, C. (1995). Interleukin-3 signals through multiple isoforms of Stat5. *EMBO Journal*, **14**(7), 1402–1411.
- Bacon, C. M., Petricoin, E. F., Ortaldo, J. R., Rees, R. C., Larner, A. C., Johnston, J. A., & O’Shea, J. J. (1995). Interleukin 12 induces tyrosine phosphorylation and activation of STAT4 in human lymphocytes. *Proceedings of the National Academy of Sciences of the United States of America*, **92**(16), 7307–7311.
- Becker, S., Groner, B., & Müller, C. W. (1998). Three-dimensional structure of the Stat3 $\beta$  homodimer bound to DNA. *Nature* **394**(6689), 145–151.
- Begitt, A, Meyer, T., van Rossum, M., & Vinkemeier, U. (2000). Nucleocytoplasmic translocation of Stat1 is regulated by a leucine-rich export signal in the coiled-coil domain. *Proceedings of the National Academy of Sciences of the United States of America*, **97**(19), 10418–10423.

- Begitt, A., Droescher, M., Knobloch, K. P., & Vinkemeier, U. (2011).** SUMO conjugation of STAT1 protects cells from hyperresponsiveness to IFN $\gamma$ . *Blood*, **118(4)**, 1002–1007.
- Bhattacharya, S., & Schindler, C. (2003).** Regulation of Stat3 nuclear export. *Journal of Clinical Investigation*, **111(4)**, 553–559.
- Bromberg, J., & Darnell, J. E. (2000).** The role of STATs in transcriptional control and their impact on cellular function. *Oncogene* **19 (21)**, 2468–2473.
- Bromberg, J. F., Wrzeszczynska, M. H., Devgan, G., Zhao, Y., Pestell, R. G., Albanese, C., & Darnell, J. E. (1999).** Stat3 as an oncogene. *Cell*, **98(3)**, 295–303.
- Brown, S., & Zeidler, M. P. (2008).** Unphosphorylated STATs go nuclear. *Current Opinion in Genetics and Development* **18(5)**, 455–460.
- Caldenhoven, E., van Dijk, T. B., Solari, R., Armstrong, J., Raaijmakers, J. A. M., Lammers, J. W. J., Koenderman, L., & de Groot, R. P. (1996).** STAT3 $\beta$ , a splice variant of transcription factor STAT3, is a dominant negative regulator of transcription. *Journal of Biological Chemistry*, **271(22)**, 13221–13227.
- Carpenter, R. L., & Lo, H. W. (2014).** STAT3 target genes relevant to human cancers. *Cancers*. **6(2)**, 897–925.
- Cartwright, P., McLean, C., Sheppard, A., Rivett, D., Jones, K., & Dalton, S. (2005).** LIF/STAT3 controls ES cell self-renewal and pluripotency by a Myc-dependent mechanism. *Development*. **132(5)**, 885–896.
- Chen, X., Bhandari, R., Vinkemeier, U., Van Den Akker, F., Darnell, J. E., Jr, & Kuriyan, J. (2003).** A reinterpretation of the dimerization interface of the N-terminal Domains of STATs. *Protein Science*. **12(2)**, 361–365.
- Chen, X., Vinkemeier, U., Zhao, Y., Jeruzalmi, D., Darnell, J. E., & Kuriyan, J. (1998).** Crystal structure of a tyrosine phosphorylated STAT-1 dimer bound to DNA. *Cell*. **93(5)**, 827–839.

- Cheon, H. J., & Stark, G. R. (2009).** Unphosphorylated STAT1 prolongs the expression of interferon-induced immune regulatory genes. *Proceedings of the National Academy of Sciences of the United States of America*. **106(23)**, 9373–9378.
- Chin, Y. E., Kitagawa, M., Kuida, K., Flavell, R. A., & Fu, X. Y. (1997).** Activation of the STAT signaling pathway can cause expression of caspase 1 and apoptosis. *Molecular and Cellular Biology*. **17(9)**, 5328–5337.
- Cho, S. S., Bacon, C. M., Sudarshan, C., Rees, R. C., Finbloom, D., Pine, R., & O’Shea, J. J. (1996).** Activation of STAT4 by IL-12 and IFN- $\alpha$ : evidence for the involvement of ligand-induced tyrosine and serine phosphorylation. *The Journal of Immunology*. **157(11)**, 4781-9.
- Cohen, S. N., Chang, A. C., & Hsu, L. (1972).** Nonchromosomal antibiotic resistance in bacteria: genetic transformation of *Escherichia coli* by R-factor DNA. *Proceedings of the National Academy of Sciences of the United States of America*. **69(8)**, 2110–2114.
- Conti, E., Uy, M., Leighton, L., Blobel, G., & Kuriyan, J. (1998).** Crystallographic analysis of the recognition of a nuclear localization signal by the nuclear import factor karyopherin alpha. *Cell*. **94(2)**, 193–204.
- da Silva, H. B., Fonseca, R., Alvarez, J. M., & Lima, M. R. D. I. (2015).** IFN- $\gamma$  priming effects on the maintenance of effector memory CD4<sup>+</sup> T cells and on phagocyte function: evidences from infectious diseases. *Journal of Immunology Research* **2015**.
- Darnell, J. E. (1997).** STATs and gene regulation. *Science*. **277(5332)**, 1630–1635.
- Darnell, J. E., Kerr, I. M., & Stark, G. R. (1994).** Jak-STAT pathways and transcriptional activation in response to IFNs and other extracellular signaling proteins. *Science*. **264(5164)**, 1415–1421.
- David, M., Wongi, L., Flavell, R., Thompson, S. A., Wells, A., Lerner, A. C., & Johnson, G. R. (1996).** STAT activation by epidermal growth factor (EGF) and amphiregulin:



- requirement for the EGF receptor kinase but not for tyrosine phosphorylation sites or JAK1. *Journal of Biological Chemistry*. **271(16)**, 9185–9188.
- de Araujo, E. D., Orlova, A., Neubauer, H. A., Bajusz, D., Seo, H. S., Dhe-Paganon, S., Keserú, G. M., Moriggl, R., & Gunning, P. T. (2019).** Structural implications of STAT3 and STAT5 SH2 domain mutations. *Cancers*. **11(11)**, 1757
- Decker, T., & Kovarik, P. (2000).** Serine phosphorylation of STATs. *Oncogene* **19(21)**, 2628–2637.
- Decker, T., Kovarik, P., & Meinke, A. (1997).** GAS elements: A few nucleotides with a major impact on cytokine-induced gene expression. *Journal of Interferon and Cytokine Research*. **17(3)**, 121–134.
- Decker, T., & Müller, M. (2012).** Jak-stat signaling: From basics to disease. *Jak-Stat Signaling: From Basics to Disease*.
- Delgoffe, G. M., & Vignali, D. A. A. (2013).** STAT heterodimers in immunity. *JAK-STAT*. **2(1)**, 23060
- Domoszlai, T., Martincuks, A., Fahrenkamp, D., de Leur, H. S. van, Küster, A., & Müller-Newen, G. (2014).** Consequences of the disease-related I78R mutation for dimerization and activity of STAT3. *Journal of Cell Science*. **127(9)**, 1899–1910.
- Dutta, P., Zhang, L., Zhang, H., Peng, Q., Montgrain, P. R., Wang, Y., Song, Y., Li, J., & Li, W. X. (2020).** Unphosphorylated STAT3 in heterochromatin formation and tumor suppression in lung cancer. *BMC Cancer*. **20(1)**, 145.
- Fagerlund, R., Mélen, K., Kinnunen, L., & Julkunen, I. (2002).** Arginine/lysine-rich nuclear localization signals mediate interactions between dimeric STATs and importin alpha 5. *The Journal of Biological Chemistry*. **277(33)**, 30072–30078.
- Fornerod, M., Ohno, M., Yoshida, M., & Mattaj, I. W. (1997).** CRM1 is an export receptor for leucine-rich nuclear export signals. *Cell*. **90(6)**, 1051–1060.

- Fu, X. Y., Schindler, C., Imbrota, T., Aebersold, R., & Darnell, J. E. (1992).** The proteins of ISGF-3, the interferon  $\alpha$ -induced transcriptional activator, define a gene family involved in signal transduction. *Proceedings of the National Academy of Sciences of the United States of America*. **89(16)**, 7840–7843.
- Fulda, S., & Debatin, K. M. (2002).** IFN $\gamma$  sensitizes for apoptosis by upregulating caspase-8 expression through the Stat1 pathway. *Oncogene*. **21(15)**, 2295–2308.
- Gouilleux, F., Wakao, H., Mundt, M., & Groner, B. (1994).** Prolactin induces phosphorylation of Tyr694 of Stat5 (MGF), a prerequisite for DNA binding and induction of transcription. *EMBO Journal*. **13(18)**, 4361–4369.
- Green, D. S., Young H. A., Valencia, J. C., & Young, H. A. (2017).** Current prospects of type II interferon gamma signaling and autoimmunity. *Journal of Biological Chemistry*. **292(34)**, 13925-13933.
- Haan, S., Keller, J. F., Behrmann, I., Heinrich, P. C., & Haan, C. (2005).** Multiple reasons for an inefficient STAT1 response upon IL-6-type cytokine stimulation. *Cellular Signalling*. **17(12)**, 1542–1550.
- Haan, S., Kortylewski, M., Behrmann, I., Müller-Esterl, W., Heinrich, P. C., & Schaper, F. (2000).** Cytoplasmic STAT proteins associate prior to activation. *Biochem. J.* **345**.
- Haspel, R. L., & Darnell, J. E. (1999).** A nuclear protein tyrosine phosphatase is required for the inactivation of Stat1. *Proceedings of the National Academy of Sciences of the United States of America*. **96(18)**, 10188–10193.
- Haspel, R. L., Salditt-Georgieff, M., & Darnell, J. E. (1996).** The rapid inactivation of nuclear tyrosine phosphorylated Stat1 depends upon a protein tyrosine phosphatase. *EMBO Journal*. **15(22)**, 6262–6268.

- 
- Hayes, M. P., Freeman, S. L., & Donnelly, R. P. (1995).** IFN- $\gamma$  priming of monocytes enhances LPS-induced TNF production by augmenting both transcription and mRNA stability. *Cytokine*. **7(5)**, 427–435.
- Ho, H. H., & Ivashkiv, L. B. (2006).** Role of STAT3 in type I interferon responses: Negative regulation of STAT1-dependent inflammatory gene activation. *Journal of Biological Chemistry*. **281(20)**, 14111–14118.
- Holland, S. M., DeLeo, F. R., Elloumi, H. Z., Hsu, A. P., Uzel, G., Brodsky, N., Freeman, A. F., Demidowich, A., Davis, J., Turner, M. L., Anderson, V. L., Darnell, D. N., Welch, P. A., Kuhns, D. B., Frucht, D. M., Malech, H. L., Gallin, J. I., Kobayashi, S. D., Whitney, A. R., Voyich, J.M., Musser, J.M., Woellner, C., Schäffer, A.A., Puck, J.M., & Grimbacher, B. (2007).** STAT3 mutations in the hyper-IgE syndrome. *New England Journal of Medicine*. **357(16)**, 1608–1619.
- Horvath, C. M., Wen, Z., & Darnell, J. E. (1995).** A STAT protein domain that determines DNA sequence recognition suggests a novel DNA-binding domain. *Genes and Development*. **9(8)**, 984–994.
- Hou, J., Schindler, U., Henzel, W. J., Ho, T. C., Brasseur, M., & McKnight, S. L. (1994).** An interleukin-4-induced transcription factor: IL-4 Stat. *Science*. **265(5179)**, 1701–1706.
- Hu, T., Yeh, J. E., Pinello, L., Jacob, J., Chakravarthy, S., Yuan, G.-C., Chopra, R., & Frank, D. A. (2015).** Impact of the N-terminal domain of STAT3 in STAT3-dependent transcriptional activity. *Molecular and Cellular Biology*. **35(19)**, 3284–3300.
- Huang, S., Bucana, C. D., van Arsdall, M., & Fidler, I. J. (2002).** Stat1 negatively regulates angiogenesis, tumorigenicity and metastasis of tumor cells. *Oncogene*. **21(16)**, 2504–2512.
- Hüntelmann, B., Staab, J., Herrmann-Lingen, C., & Meyer, T. (2014).** A conserved motif in the linker domain of STAT1 transcription factor is required for both recognition and release from high-affinity DNA-binding sites. *PLoS ONE*. **9(5)**, 97633.
-

- Improta, T., Schindler, C., Horvath, C. M., Kerr, I. M., Stark, G. R., & Darnell, J. E. (1994a).** Transcription factor ISGF-3 formation requires phosphorylated Stat91 protein, but Stat113 protein is phosphorylated independently of Stat91 protein. *Proceedings of the National Academy of Sciences of the United States of America*. **91(11)**, 4776–4780.
- John, S., Vinkemeier, U., Soldaini, E., Darnell, J. E., & Leonard, W. J. (1999).** The significance of tetramerization in promoter recruitment by stat5. *Molecular and Cellular Biology*. **19(3)**, 1910–1918.
- Kaplan, D. H., Shankaran, V., Dighe, A. S., Stockert, E., Aguet, M., Old, L. J., & Schreiber, R. D. (1998).** Demonstration of an interferon  $\gamma$ -dependent tumor surveillance system in immunocompetent mice. *Proceedings of the National Academy of Sciences of the United States of America*. **95(13)**, 7556–7561.
- Kaptein, A., Paillard, V., & Saunders, M. (1996).** Dominant negative Stat3 mutant inhibits interleukin-6-induced Jak-STAT signal transduction. *Journal of Biological Chemistry*. **271(11)**, 5961–5964.
- Keppler, A., Kindermann, M., Gendreizig, S., Pick, H., Vogel, H., & Johnsson, K. (2004).** Labeling of fusion proteins of O6-alkylguanine-DNA alkyltransferase with small molecules in vivo and in vitro. *Methods*. **32(4)**, 437–444.
- Khan, K.D. Shuai, K., Lindwall, G., Maher, S. E., Darnell, J. E., & Bothwell, A. L. M. (1993).** Induction of the Ly-6A/E gene by interferon  $\alpha/\beta$  and  $\gamma$  requires a DNA element to which a tyrosine-phosphorylated 91-kDa protein binds. *Proceedings of the National Academy of Sciences of the United States of America*. **90(14)**, 6806–6810.
- Kim, H. S., & Lee, M. S. (2007).** STAT1 as a key modulator of cell death. *Cellular Signalling*. **19(3)**, 454–465.
- Kim, H. S., & Lee, M.-S. (2005).** Essential role of stat1 in caspase-independent cell death of activated macrophages through the p38 mitogen-activated protein kinase/STAT1/reactive oxygen species pathway. *Molecular and Cellular Biology*. **25(15)**, 6821–6833.

- King, P., & Goodbourn, S. (1998).** STAT1 is inactivated by a caspase. *Journal of Biological Chemistry*. **273(15)**, 8699–8704.
- Koch, V., Staab, J., Ruppert, V., & Meyer, T. (2012).** Two glutamic acid residues in the DNA-binding domain are engaged in the release of STAT1 dimers from DNA. *BMC Cell Biology*. **13(22)**.
- Kojima, H., Nakajima, K., & Hirano, T. (1996).** IL-6-inducible complexes on an IL-6 response element of the junB promoter contain Stat3 and 36 kDa CRE-like site binding protein(s). *Oncogene*. **12(3)**, 547–554.
- Kotanides, H., & Reich, N. C. (1993).** Requirement of tyrosine phosphorylation for rapid activation of a DNA binding factor by IL-4. *Science*. **262(5137)**, 1265–1267.
- Kretzschmar, A. K., Dinger, M. C., Henze, C., Brocke-Heidrich, K., & Horn, F. (2004).** Analysis of Stat3 (signal transducer and activator of transcription 3) dimerization by fluorescence resonance energy transfer in living cells. *Biochem. J.* **377(Pt 2)**, 289–297.
- Kudo, N., Matsumori, N., Taoka, H., Fujiwara, D., Schreiner, E. P., Wolff, B., Yoshida, M., & Horinouchi, S. (1999).** Leptomycin B inactivates CRM1/exportin 1 by covalent modification at a cysteine residue in the central conserved region. *Proceedings of the National Academy of Sciences*. **96(16)**, 9112–9117.
- Kumar, A., Commane, M., Flickinger, T. W., Horvath, C. M., & Stark, G. R. (1997).** Defective TNF- $\alpha$ -induced apoptosis in STAT1-null cells due to low constitutive levels of caspases. *Science*. **278(5343)**, 1630–1632.
- la Sala, G., Michiels, C., Kükenshöner, T., Brandstoetter, T., Maurer, B., Koide, A., Lau, K., Pojer, F., Koide, S., Sexl, V., Dumoutier, L., & Hantschel, O. (2020).** Selective inhibition of STAT3 signaling using monobodies targeting the coiled-coil and N-terminal domains. *Nature Communications*. **11(1)**, 4115.
- Leonard, W. J., & O’Shea, J. J. (1998).** JAKS AND STATS: Biological Implications. *Annual Review of Immunology*. **16(1)**, 293–322.

- Leung, S., Qureshi, S. A., Kerr, I. M., Darnell, J. E., & Stark, G. R. (1995).** Role of STAT2 in the alpha interferon signaling pathway. *Molecular and Cellular Biology*. **15(3)**, 1312–1317.
- Levy, D. E., Kessler, D. S., Pine, R., Reich, N., & Darnell, J. E. (1988).** Interferon-induced nuclear factors that bind a shared promoter element correlate with positive and negative transcriptional control. *Genes & Development*. **2(4)**, 383–393.
- Levy, D. E., & Darnell, J. (2002).** STATs: Transcriptional control and biological impact. *Nature Reviews Molecular Cell Biology*. **3(9)**, 651–662.
- Levy, D. E., & Lee, C. (2002).** What does Stat3 do? *Journal of Clinical Investigation*. **109(9)**, 1143–1148.
- Li, W. X. (2008).** Canonical and non-canonical JAK-STAT signaling. *Trends in Cell Biology*. **18(11)**, 545–551.
- Licht, V., Noack, K., Schlott, B., Förster, M., Schlenker, Y., Licht, A., Krämer, O. H., & Heinzl, T. (2014).** Caspase-3 and caspase-6 cleave STAT1 in leukemic cells. *Oncotarget*. **5(8)**, 2305–2317.
- Lütticken, C., Wegenka, U. M., Yuan, J., Buschmann, J., Schindler, C., Ziemiecki, A., Harpur, A. G., Wilks, A. F., Yasukawa, K., Taga, T., Kishimoto, T., Barbieri, G., Pellegrini, S., Sendtner, M., Heinrich, P. C., & Horn, F. (1994).** Association of transcription factor APRF and protein kinase Jak1 with the interleukin-6 signal transducer gp130. *Science*. **263(5143)**, 89–92.
- Ma, J., Zhang, T., Novotny-Diermayr, V., Tan, A. L. C., & Cao, X. (2003).** A novel sequence in the coiled-coil domain of Stat3 essential for its nuclear translocation. *Journal of Biological Chemistry*. **278(31)**, 29252–29260.

- Majoros, A., Platanitis, E., Kernbauer-Hölzl, E., Rosebrock, F., Müller, M., & Decker, T. (2017).** Canonical and non-canonical aspects of JAK-STAT signaling: Lessons from interferons for cytokine responses. *Frontiers in Immunology*. **8**, 29.
- Mao, X., Ren, Z., Parker, G. N., Sonderrmann, H., Pastorello, M. A., Wang, W., McMurray, J. S., Demeler, B., Darnell, J. E., & Chen, X. (2005).** Structural bases of unphosphorylated STAT1 association and receptor binding. *Molecular Cell*. **17(6)**, 761–771.
- Marg, A., Shan, Y., Meyer, T., Meissner, T., Brandenburg, M., & Vinkemeier, U. (2004).** Nucleocytoplasmic shuttling by nucleoporins Nup153 and Nup214 and CRM1-dependent nuclear export control the subcellular distribution of latent Stat1. *Journal of Cell Biology*. **165(6)**, 823–833.
- Martincuks, A., Fahrenkamp, D., Haan, S., Herrmann, A., Küster, A., & Müller-Newen G. (2016)** Dissecting functions of the N-terminal domain and GAS-site recognition in STAT3 nuclear trafficking. *Cell Signal*. **28(8)**, 810–825.
- McBride, K. M., McDonald, C., & Reich, N.C. (2000).** Nuclear export signal located within the DNA-binding domain of the STAT1 transcription factor. *The EMBO Journal*. **19(22)**, 6196–6206.
- McBride, K. M., Banninger, G., McDonald, C., & Reich, N. C. (2002).** Regulated nuclear import of the STAT1 transcription factor by direct binding of importin- $\alpha$ . *EMBO Journal*. **21(7)**, 1754–1763.
- McKendry, R., John, J., Flavell, D., Muller, M., Kerr, I. M., & Stark, G. R. (1991).** High-frequency mutagenesis of human cells and characterization of a mutant unresponsive to both  $\alpha$  and  $\gamma$  interferons. *Proceedings of the National Academy of Sciences of the United States of America*. **88(24)**, 11455–11459.
- Meissner, T., Krause, E., Lödige, I., & Vinkemeier, U. (2004).** Arginine methylation of STAT1: A reassessment. *Cell*. **119(5)**, 587–589.

- Melén, K., Fagerlund, R., Franke, J., Köhler, M., Kinnunen, L., & Julkunen, I. (2003).** Importin  $\alpha$  nuclear localization signal binding sites for STAT1, STAT2, and influenza A virus nucleoprotein. *Journal of Biological Chemistry*. **278(30)**, 28193–28200.
- Melén, K., Kinnunen, L., & Julkunen, I. (2001).** Arginine/lysine-rich structural element is involved in interferon-induced nuclear import of stats. *Journal of Biological Chemistry*. **276(19)**, 16447–16455.
- Mertens, C., Haripal, B., Klinge, S., & Darnell, J. E. (2015).** Mutations in the linker domain affect phospho-STAT3 function and suggest targets for interrupting STAT3 activity. *Proceedings of the National Academy of Sciences of the United States of America*. **112(48)**, 14811–14816.
- Mertens, C., Zhong, M., Krishnaraj, R., Zou, W., Chen, X., & Darnell, J. E. (2006).** Dephosphorylation of phosphotyrosine on STAT1 dimers requires extensive spatial reorientation of the monomers facilitated by the N-terminal domain. *Genes and Development*. **20(24)**, 3372–3381.
- Meyer, T., Begitt, A., Lödige, I., van Rossum, M., & Vinkemeier, U. (2002).** Constitutive and IFN- $\gamma$ -induced nuclear import of STAT1 proceed through independent pathways. *EMBO Journal*. **21(3)**, 344–354.
- Meyer, T., Hendry, L., Begitt, A., John, S., & Vinkemeier, U. (2004).** A single residue modulates tyrosine dephosphorylation, oligomerization, and nuclear accumulation of stat transcription factors. *Journal of Biological Chemistry*. **279(18)**, 18998–19007.
- Meyer, T., Marg, A., Lemke, P., Wiesner, B., & Vinkemeier, U. (2003).** DNA binding controls inactivation and nuclear accumulation of the transcription factor Stat1. *Genes and Development*. **17(16)**, 1992–2005.
- Meyer, T., & Vinkemeier, U. (2004).** Nucleocytoplasmic shuttling of STAT transcription factors. *European Journal of Biochemistry*. **271(23-24)**, 4606–4612.



- 
- Miklossy, G., Hilliard, T. S., & Turkson, J. (2013).** Therapeutic modulators of STAT signalling for human diseases. *Nature Reviews Drug Discovery*. 12(8), 611–629.
- Mössner, R., Diering, N., Bader, O., Forkel, S., Overbeck, T., Groß, U., Grimbacher, B., Schön, M., & Buhl, T. (2016).** Ruxolitinib induces interleukin 17 and ameliorates chronic mucocutaneous candidiasis caused by stat1 gain-of-function mutation. *Clinical Infectious Diseases*. 62(7), 951–953.
- Mui, A. L. F., Wakao, H., O’Farrell, A. M., Harada, N., & Miyajima, A. (1995).** Interleukin-3, granulocyte-macrophage colony stimulating factor and interleukin-5 transduce signals through two STAT5 homologs. *EMBO Journal*. 14(6), 1166–1175.
- Najjar, I., & Fagard, R. (2010).** STAT1 and pathogens, not a friendly relationship. *Biochimie*. 92(5), 425–444.
- Nardozi, J., Wenta, N., Yasuhara, N., Vinkemeier, U., & Cingolani, G. (2010).** Molecular basis for the recognition of phosphorylated stat1 by importin  $\alpha 5$ . *Journal of Molecular Biology*. 402(1), 83–100.
- Ndubuisi, M. I., Guo, G. G., Fried, V. A., Etlinger, J. D., & Sehgal, P. B. (1999).** Cellular physiology of STAT3: Where’s the cytoplasmic monomer? *Journal of Biological Chemistry*. 274(36), 25499–25509.
- Neculai, D., Neculai, A. M., Verrier, S., Straub, K., Klumpp, K., Pfitzner, E., & Becker, S. (2005).** Structure of the unphosphorylated STAT5a dimer. *Journal of Biological Chemistry*. 280(49), 40782–40787.
- Nkansah, E., Shah, R., Collie, G. W., Parkinson, G. N., Palmer, J., Rahman, K. M., Bui, T. T., Drake, A. F., Husby, J., Neidle, S., Zinzalla, G., Thurston, D. E., & Wilderspin, A. F. (2013).** Observation of unphosphorylated STAT3 core protein binding to target *ds* DNA by PEMSAs and X-ray crystallography. *FEBS Letters*. 587(7), 833–839.
- O’Shea, J. J., Holland, S. M., & Staudt, L. M. (2013).** JAKs and STATs in immunity, immunodeficiency, and cancer. *New England Journal of Medicine*. 368(2), 161–170.
-

- O'Shea, J. J., Schwartz, D. M., Villarino, A. v., Gadina, M., McInnes, I. B., & Laurence, A. (2015).** The JAK-STAT pathway: Impact on human disease and therapeutic intervention. *Annual Review of Medicine*. **66**, 311–328.
- Ota, N., Brett, T. J., Murphy, T. L., Fremont, D. H., & Murphy, K. M. (2004).** N-domain-dependent nonphosphorylated STAT4 dimers required for cytokine-driven activation. *Nature Immunology*. **5(2)**, 208–215.
- Owen, K. L., Brockwell, N. K., & Parker, B. S. (2019).** Jak-stat signaling: A double-edged sword of immune regulation and cancer progression. *Cancers*. **11(12)**
- Parrini, M., Meissl, K., Ola, M. J., Lederer, T., Puga, A., Wienerroither, S., Kovarik, P., Decker, T., Müller, M., & Strobl, B. (2018).** The C-terminal transactivation domain of stat1 has a gene-specific role in transactivation and cofactor recruitment. *Frontiers in Immunology*. **9**, 2879.
- Paulson, M., Pisharody, S., Pan, L., Guadagno, S., Mui, A. L., & Levy, D. E. (1999).** STAT protein transactivation domains recruit p300/CBP through widely divergent sequences. *Journal of Biological Chemistry*. **274(36)**, 25343–25349.
- Petersen, J., Staab, J., Bader, O., Buhl, T., Ivetic, A., & Meyer, T. (2019).** Identification of a distinct subset of disease-associated gain-of-function missense mutations in the STAT1 coiled-coil domain as system mutants. *Molecular Immunology*. **114**, 30–40.
- Pranada, A. L., Metz, S., Herrmann, A., Heinrich, P. C., & Müller-Newen, G. (2004).** Real time analysis of STAT3 nucleocytoplasmic shuttling. *Journal of Biological Chemistry*. **279(15)**, 15114–15123.
- Ramana, C. V., Grammatikakis, N., Chernov, M., Nguyen, H., Goh, K. C., Williams, B. R. G., & Stark, G. R. (2000).** Regulation of *c-myc* expression by IFN- $\gamma$  through Stat1-dependent and -independent pathways. *EMBO Journal*. **19(2)**, 263–272.

- Rawlings, J. S., Rosler, K. M., & Harrison, D. A. (2004).** The JAK/STAT signaling pathway. *Journal of Cell Science.* **117(8)**, 1281–1283.
- Raz, R., Durbin, J. E., & Levy, D. E. (1994).** Acute phase response factor and additional members of the interferon-stimulated gene factor 3 family integrate diverse signals from cytokines, interferons, and growth factors. *Journal of Biological Chemistry.* **269(39)**, 24391–24395.
- Regis, G., Pensa, S., Boselli, D., Novelli, F., & Poli, V. (2008).** Ups and downs: The STAT1:STAT3 seesaw of interferon and gp130 receptor signalling. *Seminars in Cell and Developmental Biology.* **19(4)**, 351–359.
- Ren, Z., Mao, X., Mertens, C., Krishnaraj, R., Qin, J., Mandal, P. K., Romanowski, M. J., McMurray, J. S., & Chen, X. (2008).** Crystal structure of unphosphorylated STAT3 core fragment. *Biochemical and Biophysical Research Communications.* **374(1)**, 1–5.
- Ribbeck, K., & Görlich, D. (2002).** The permeability barrier of nuclear pore complexes appears to operate via hydrophobic exclusion. *EMBO Journal.* **21(11)**, 2664–2671.
- Riebeling, T., Staab, J., Herrmann-Lingen, C., & Meyer, T. (2014).** DNA binding reduces the dissociation rate of STAT1 dimers and impairs the interdimeric exchange of protomers. *BMC Biochemistry.* **15(1)**.
- Scherer, W. F., Syverton, J. T., & Gey, G. O. (1953).** Studies on the propagation in vitro of poliomyelitis viruses: IV. Viral multiplication in a stable strain of human malignant epithelial cells (strain HeLa) derived from an epidermoid carcinoma of the cervix. *Journal of Experimental Medicine.* **97(5)**, 695–710.
- Schindler, C., Kashleva, H., Pernis, A., Pine, R., & Rothman, P. (1994).** STF-IL-4: a novel IL-4-induced signal transducing factor. *EMBO Journal.* **13(6)**, 1350–1356.
- Schindler, C., Fu, X. Y., Improta, T., Aebersold, R., & Darnell, J. E. (1992).** Proteins of transcription factor ISGF-3: One gene encodes the 91- and 84-kDa ISGF-3 proteins that

---

are activated by interferon  $\alpha$ . *Proceedings of the National Academy of Sciences of the United States of America*. **89(16)**, 7836–7839.

**Schroder, K., Sweet, M. J., & Hume, D. A. (2006)**. Signal integration between IFN $\gamma$  and TLR signalling pathways in macrophages. *Immunobiology*. **211(6–8)**, 511–524.

**Semper, C., Leitner, N. R., Lassnig, C., Parrini, M., Mahlakoiv, T., Rammerstorfer, M., Lorenz, K., Rigler, D., Muller, S., Kolbe, T., Vogl, C., Rulicke, T., Staeheli, P., Decker, T., Muller, M., & Strobl, B. (2014)**. STAT1 is not dominant negative and is capable of contributing to gamma interferon-dependent innate immunity. *Molecular and Cellular Biology*. **34(12)**, 2235–2248.

**Shuai, K., Horvath, C. M., Huang, L. H. T., Qureshi, S. A., Cowburn, D., & Darnell, J. E. (1994)**. Interferon activation of the transcription factor Stat91 involves dimerization through SH2-phosphotyrosyl peptide interactions. *Cell*. **76(5)**, 821–828.

**Shuai, K., Schindler, C., Prezioso, V. R., & Darnell, J. E. (1992)**. Activation of transcription by IFN- $\gamma$ : Tyrosine phosphorylation of a 91-kD DNA binding protein. *Science*. **258(5089)**, 1808–1812.

**Shuai, K., Stark, G. R., Kerr, I. M., & Darnell, J. E. (1993)**. A single phosphotyrosine residue of Stat91 required for gene activation by interferon- $\gamma$ . *Science*. **261(5129)**, 1744–1746.

**Shuai, K., Ziemiecki, A., Wilks, A. F., Harpur, A. G., Sadowski, H. B., Gilman, M. Z., & Darnell, J. E. (1993)**. Polypeptide signalling to the nucleus through tyrosine phosphorylation of JAK and STAT proteins. *Nature*. **366(6455)**, 580–583.

**Sironi, J. J., & Ouchi, T. (2004)**. STAT1-induced apoptosis is mediated by caspases 2, 3, and 7. *Journal of Biological Chemistry*. **279(6)**, 4066–4074.

**Staab, J., Herrmann-Lingen, C., & Meyer, T. (2013)**. Clinically relevant dimer interface mutants of stat1 transcription factor exhibit differential gene expression. *PLoS ONE*. **8(7)**, 69903.

- Stark, G. R., & Darnell, J. E. (2012).** The JAK-STAT Pathway at Twenty. *Immunity*. **36(4)**, 503–514.
- Starr, R., & Hilton, D. J. (1999).** Negative regulation of the JAK/STAT pathway. *BioEssays* **21(1)**, 47–52.
- Stephanou, A., & Latchman, D. S. (2003).** STAT-1: A novel regulator of apoptosis. *International Journal of Experimental Pathology*. **84(6)**, 239–244.
- Stephanou, A., & Latchman, D. S. (2005).** Opposing actions of STAT-1 and STAT-3. *Growth Factors*. **23(3)**, 177–182.
- Valente, A. J., Xie, J. F., Abramova, M. A., Wenzel, U. O., Abboud, H. E., & Graves, D. T. (1998).** A complex element regulates IFN- $\gamma$ -stimulated monocyte chemoattractant protein-1 gene transcription. *Journal of Immunology*. **161(7)**, 3719–3728.
- Villarino, A. v., Kanno, Y., Ferdinand, J. R., & O’Shea, J. J. (2015).** Mechanisms of Jak/STAT signaling in immunity and disease. *Journal of Immunology*. **194(1)**, 21–27.
- Vinkemeier, U., Cohen, S.L., Moarefi, I., Chait, B.T., Kuriyan, J., & Darnell J.E.(1996).** DNA binding of in vitro activated Stat1 $\alpha$ , Stat1 $\beta$  and truncated Stat1: interaction between NH2-terminal domains stabilizes binding of two dimers to tandem DNA sites. *EMBO J*. **15(20)**, 5616–5626.
- Vogt, M., Domszlai, T., Kleshchanok, D., Lehmann, S., Schmitt, A., Poli, V., Richtering, W., & Müller-Newen, G. (2011).** The role of the N-terminal domain in dimerization and nucleocytoplasmic shuttling of latent STAT3. *Journal of Cell Science*. **124(6)**, 900–909.
- Wegenka, U. M., Lütticken, C., Buschmann, J., Yuan, J., Lottspeich, F., Müller-Esterl, W., Schindler, C., Roeb, E., Heinrich, P. C., & Horn, F. (1994).** The interleukin-6-activated acute-phase response factor is antigenically and functionally related to members of the signal transducer and activator of transcription (STAT) family. *Molecular and Cellular Biology*. **14(5)**, 3186–3196.

- Wen, Z., Zhong, Z., & Darnell, J. E. (1995).** Maximal activation of transcription by Stat1 and stat3 requires both tyrosine and serine phosphorylation. *Cell*. **82(2)**, 241–250.
- Wenta, N., Strauss, H., Meyer, S., & Vinkemeier, U. (2008).** Tyrosine phosphorylation regulates the partitioning of STAT1 between different dimer conformations. *Proceedings of the National Academy of Sciences of the United States of America*. **105(27)**, 9238–9243.
- Yamamoto, K., Quelle, F. W., Thierfelder, W. E., Kreider, B. L., Gilbert, D. J., Jenkins, N. A., Copeland, N. G., Silvennoinen, O., & Ihle, J. N. (1994).** Stat4, a novel gamma interferon activation site-binding protein expressed in early myeloid differentiation. *Molecular and Cellular Biology*. **14(7)**, 4342–4349.
- Yang, E., Henriksen, M. A., Schaefer, O., Zakharova, N., & Darnell, J. E. (2002).** Dissociation time from DNA determines transcriptional function in a STAT1 linker mutant. *Journal of Biological Chemistry*. **277(16)**, 13455–62.
- Yang, E., Wen, Z., Haspel, R. L., Zhang, J. J., & Darnell, J. E. (1999).** The linker domain of stat1 is required for gamma interferon-driven transcription. *Molecular and Cellular Biology*. **19(7)**, 5106–5112.
- Yang, J., Liao, X., Agarwal, M. K., Barnes, L., Auron, P. E., & Stark, G. R. (2007).** Unphosphorylated STAT3 accumulates in response to IL-6 and activates transcription by binding to NF $\kappa$ B. *Genes and Development*. **21(11)**, 1396–1408.
- Yang, J., & Stark, G. R. (2008).** Roles of unphosphorylated STATs in signaling. *Cell Research*. **18(4)**, 443–451.
- Yue, H., Li, W., Desnoyer, R., & Karnik, S. S. (2010).** Role of nuclear unphosphorylated STAT3 in angiotensin II type 1 receptor-induced cardiac hypertrophy. *Cardiovascular Research*. **85(1)**, 90–99.
- Zhang, H. X., Yang, P. L., Li, E. M., & Xu, L. Y. (2019).** STAT3 $\beta$ , a distinct isoform from STAT3. *International Journal of Biochemistry and Cell Biology*. **110**, 130–139.

**Zhong, M., Henriksen, M. A., Takeuchi, K., Schaefer, O., Liu, B., ten Hoeve, J., Ren, Z., Mao, X., Chen, X., Shuai, K., & Darnell, J. E. (2005).** Implications of an antiparallel dimeric structure of nonphosphorylated STAT1 for the activation-inactivation cycle. *Proceedings of the National Academy of Sciences of the United States of America*. **102(11)**, 3966–3971.

**Zhong, Z., Wen, Z., & Darnell, J. E. (1994a).** Stat3: A STAT family member activated by tyrosine phosphorylation in response to epidermal growth factor and interleukin-6. *Science*. **264(5155)**, 95–98.

**Zhong, Z., Wen, Z., & Darnell, J. E. (1994b).** Stat3 and Stat4: Members of the family of signal transducers and activators of transcription. *Proceedings of the National Academy of Sciences of the United States of America*. **91(11)**, 4806–4810.

## Curriculum vitae

Name: Priyanka Rajeev Menon  
Date of Birth: 30 March 1992  
Place of Birth: Vadodara, India  
Nationality: Indian

### Education:

- 12/2017 – present     Doctoral student, Laboratory for Molecular Psychocardiology,  
Department of Psychosomatic Medicine and Psychotherapy,  
University Medical Center Göttingen, Germany,  
PhD program: Molecular Medicine
- 10/2015 – 09/2017    Master of Science – Cardiovascular Science  
Georg-August-University Göttingen, Germany  
Master thesis: Effects of external stressors and reduced plakoglobin  
expression on disease development in arrhythmogenic right  
ventricular cardiomyopathy  
Master thesis done at Institute of Cardiovascular Sciences,  
University of Birmingham, United Kingdom
- 08/2011 – 05/2015    Bachelor of Technology – Genetic Engineering  
SRM Institute of Science and Technology, Chennai, India  
Bachelor thesis: Overcoming adaptive resistance in cancer cells by  
inhibition of heat shock protein 90  
Bachelor thesis done at Brigham and Women’s Hospital,  
Harvard Medical School, United States
- 05/2008 – 05/2010    Delhi Public School, Vadodara, India (Class 10–12)

### Publications:

**Menon, P.R., Petersen, J, Mumtaz, S., Ivetic, A., Meyer, T.** Characterization of two STAT1 gain-of-function mutants resulting in premature cytokine-induced nuclear accumulation, **Cytokines 2019: 7th Annual Meeting of the International Cytokine & Interferon Society (ICIS)**, Vienna, Austria

**Menon, P.R., Doudin, A., Gregus, A., Staab, J., Wirths, O., Meyer, T.** The anti-parallel dimer conformation of STAT3 is required for the inactivation of cytokine signal transduction. (submitted)

**Menon, P.R. et al.** An inhibitory effect on the nuclear import of phospho-STAT1 by its unphosphorylated form. (under preparation)